

January 2022

## Novel Interaction Of Cxcr4 And Pi4kiii $\alpha$ In Prostate Cancer

Barani Govindarajan  
*Wayne State University*

Follow this and additional works at: [https://digitalcommons.wayne.edu/oa\\_dissertations](https://digitalcommons.wayne.edu/oa_dissertations)

 Part of the [Medicine and Health Sciences Commons](#)

---

### Recommended Citation

Govindarajan, Barani, "Novel Interaction Of Cxcr4 And Pi4kiii $\alpha$  In Prostate Cancer" (2022). *Wayne State University Dissertations*. 3669.

[https://digitalcommons.wayne.edu/oa\\_dissertations/3669](https://digitalcommons.wayne.edu/oa_dissertations/3669)

This Open Access Dissertation is brought to you for free and open access by DigitalCommons@WayneState. It has been accepted for inclusion in Wayne State University Dissertations by an authorized administrator of DigitalCommons@WayneState.

**NOVEL INTERACTION OF CXCR4 AND PI4KIII $\alpha$  IN PROSTATE CANCER**

by

**BARANI GOVINDARAJAN**

**DISSERTATION**

Submitted to the Graduate School

of Wayne State University,

Detroit, Michigan

in partial fulfillment of the requirements

for the degree of

**DOCTOR OF PHILOSOPHY**

2022

MAJOR: PATHOLOGY

Approved By:

---

Advisor

Date

---

---

---

---

## DEDICATION

*I would like to dedicate this work to my ever-supporting family. All my success and happiness are a testament to their constant love, support, prayers and faith.*

## ACKNOWLEDGMENTS

I would like to thank my advisor Dr.Sreenivasa Chinni, for all the support and encouragement. For always being there and constantly being a warm guiding force. I have learnt to be a diligent and persistent scientist, and you have always provided a nourishing environment for me to grow.

I would also like to thank my committee members Dr.Hyeong-Reh Kim, Dr.Todd Leff, Dr.Kaladhar Reddy and Dr.Michael Cher whose constant guidance and wisdom are something I'll cherish forever.

Finally, I would like to thank my colleagues Diego, Abdo, and Tri who have supported me in this journey, encouraged me throughout and for all the kindness you have showed.

## TABLE OF CONTENTS

DEDICATION .....	ii
ACKNOWLEDGMENTS .....	iii
TABLE OF CONTENTS .....	iv
LIST OF TABLES .....	viii
LIST OF FIGURES .....	ix
CHAPTER 1- INTRODUCTION.....	1
<i>1.1 Prostate Cancer.....</i>	<i>1</i>
<i>1.2 Phosphatidylinositol metabolism. ....</i>	<i>4</i>
<i>1.3 Phosphatidylinositol kinases in Cancer.....</i>	<i>9</i>
<i>1.4 Biological Functions of CXCR4. ....</i>	<i>11</i>
<i>1.5 CXCR4 function in tumor microenvironment and cancer metastasis. ....</i>	<i>12</i>
CHAPTER 2- HYPOTHESIS & RATIONALE .....	16
CHAPTER 3- DETERMINE THE MECHANISMS OF PI4KIII $\alpha$ INTERACTION WITH CXCR4 IN PROSTATE CANCER.....	22
<i>3.0 Introduction. ....</i>	<i>22</i>
<i>3.1 Native interaction of PI4KIII<math>\alpha</math> and CXCR4.....</i>	<i>23</i>
<i>3.1.1 Results. ....</i>	<i>24</i>
<i>3.1.2 Endogenous PI4KIII<math>\alpha</math> interaction with CXCR4 in PC3 cells. ....</i>	<i>26</i>
<i>3.1.3 Results. ....</i>	<i>27</i>
<i>3.1.4 Determine endogenous interaction between CXCR4 and PI4KIII<math>\alpha</math> in other PCa cells. .....</i>	<i>27</i>
<i>3.1.5 Results. ....</i>	<i>28</i>

3.1.6 Discussion.....	29
3.2 Determine co-localization using Proximity Ligation Assay.....	30
3.2.1 Results.....	33
3.2.2 Discussion.....	34
3.3 Determine functional significance of CXCR4 interaction with PI4KIII $\alpha$ using GFP-P4M-SidMx2 biosensor.....	35
3.3.1 Results.....	37
3.3.2 Discussion.....	40
<b>CHAPTER 4- DETERMINE ROLE OF ADAPTOR PROTEIN TTC7B IN CANCER CELL INVASION.....</b>	<b>42</b>
4.0 Introduction.....	42
4.1 Determine the impact of adaptor proteins TTC7B in CXCR4-PI4KIII $\alpha$ interaction.....	42
4.1.1 Results.....	43
4.2 Determine the depletion of TTC7B on CXCL12 induced cell invasion.....	44
4.2.1 Results.....	45
<b>CHAPTER 5- DETERMINE ROLE OF PI4KIII<math>\alpha</math> IN CANCER CELL INVASION AND PROLIFERATION.....</b>	<b>46</b>
5.0 Introduction.....	46
5.1 Impact of PI4KIII $\alpha$ transient knockdown on CXCL12 induced cell invasion.....	47
5.1.1 Results.....	49
5.2 Characterize PI4KIII $\alpha$ stable knockdown cell models.....	50
5.2.1 Results.....	51
5.3 Impact of PI4KIII $\alpha$ stable knockdown on CXCL12 induced cell invasion.....	52

5.3.1 Results. ....	53
5.4 Perform RNA-Sequencing analysis to determine differential gene expressions and pathways contributing to PI4KIII $\alpha$ function in PCa cell. ....	54
5.5.1 Results. ....	56
5.6 Discussion. ....	66
<b>CHAPTER 6- CLINICAL SIGNIFICANCE OF PI4KIII<math>\alpha</math> IN METASTATIC PROSTATE CANCER BIOPSIES</b> .....	<b>68</b>
6.0 Introduction. ....	68
6.1 Determine the clinical significance of PI4KIII $\alpha$ in human prostate cancer metastasis. ....	69
6.1.1 Results. ....	75
6.2 Discussion. ....	97
<b>MATERIALS AND METHODS</b> .....	<b>101</b>
7.1 Cell Culture. ....	101
7.2 Lentiviral generation of stable cell-lines. ....	101
7.3 Western Blot analysis. ....	102
7.4 Immunoprecipitation. ....	102
7.5 PI4KIII $\alpha$ lipid kinase assay. ....	103
7.6 Cell proliferation and invasion assays. ....	103
7.7 Fluorescence microscopy. ....	104
7.8 Proximity Ligation Assay. ....	104
7.9 Gene Expression Omnibus Database. ....	104
7.10 Patient and Clinical data. ....	104

<i>7.11 RNA-sequencing analysis</i> .....	105
<i>7.12 Gene Set Enrichment Analysis</i> .....	105
<i>7.13 Pathway Analysis</i> .....	105
<i>7.14 Statistical Analysis</i> .....	106
<i>7.15 Antibody links</i> .....	106
<b>REFERENCES</b> .....	108
<b>ABSTRACT</b> .....	139
<b>AUTOBIOGRAPHICAL STATEMENT</b> .....	141

## LIST OF TABLES

<b>Table 1. Conditions used with the GFP-P4M-SidMx2 biosensor. ....</b>	<b>36</b>
<b>Table 2. Gene sets enriched in phenotype scrambled compared to PI4KA knockdown cell-lines. ....</b>	<b>57</b>
<b>Table 3. Common Gene sets enriched in phenotype scrambled compared to PI4KA knockdown cell-lines. ....</b>	<b>57</b>
<b>Table 4. Common Gene sets enriched in phenotype PI4KA knockdown compared to scrambled cell-lines. ....</b>	<b>58</b>
<b>Table 5. Common Gene sets enriched between phenotype scrambled and high PI4KIII<math>\alpha</math> expressing TCGA-Firehose Legacy prostate adenocarcinoma cohort (total n=498). ....</b>	<b>59</b>
<b>Table 6. Cox regression analysis of Overall Survival of bone metastasized PCa. ....</b>	<b>80</b>
<b>Table 7. Pearson Correlation between the interacting proteins. ....</b>	<b>82</b>
<b>Table 8. Gene sets enriched in phenotype high-PI4K-Bone (n=13). ....</b>	<b>85</b>
<b>Table 9. Gene sets enriched in phenotype Non-AA-Bone (n=19). ....</b>	<b>91</b>

## LIST OF FIGURES

<b>Figure 1. Schematic progression of Prostate cancer.....</b>	<b>3</b>
<b>Figure 2. Inositol ring anchored to the lipid bilayer on PM. ....</b>	<b>4</b>
<b>Figure 3. Metabolism of the different phosphoinositide species and their subcellular localization. ....</b>	<b>5</b>
<b>Figure 4. Domain structure of PI4KIII<math>\alpha</math>. ....</b>	<b>6</b>
<b>Figure 5. Localization of Phosphatidylinositol 4 kinase III<math>\alpha</math> to the plasma membrane.....</b>	<b>8</b>
<b>Figure 6. Characterization of PC3-CXCR4 and PC3-shCXCR4 cells.....</b>	<b>17</b>
<b>Figure 7. Schematic representation of the SILAC analysis was performed.....</b>	<b>17</b>
<b>Figure 8. Proteins identified as interactors of CXCR4 through SILAC analysis. ....</b>	<b>18</b>
<b>Figure 9. Characterization of protein expression and lipid kinase activity of PC3-CXCR4 and PC3-shCXCR4 cells.....</b>	<b>20</b>
<b>Figure 10. CXCR4 interaction with PI4KIII<math>\alpha</math> leads to cancer cell invasion and metastasis? .....</b>	<b>21</b>
<b>Figure 11. PI4KIII<math>\alpha</math> complex recruitment to the PM.....</b>	<b>23</b>
<b>Figure 12. CXCR4 interacts with adaptor proteins of PI4KIII<math>\alpha</math> in tagged gene transfected immunoprecipitations.....</b>	<b>25</b>
<b>Figure 13. CXCR4 interacts with adaptor protein of PI4KIII<math>\alpha</math> in stable CXCR4 overexpressing PC3 cells - under basal, and increases under ligand conditions. ....</b>	<b>27</b>
<b>Figure 14. CXCR4 interacts with adaptor protein of PI4KIII<math>\alpha</math> in native PCa cells - under basal, and increases under ligand conditions. ....</b>	<b>29</b>
<b>Figure 15. Schematic representation of how the Proximity Ligation Assay (PLA) was performed. (Sigma Duolink DUO92101-1 kit) .....</b>	<b>32</b>

<b>Figure 16. CXCR4 co-localizes with adaptor protein of PI4KIII<math>\alpha</math> in native PCa cell - under basal, and increases under ligand conditions. ....</b>	<b>34</b>
<b>Figure 17. PI4P production is induced under CXCL12 ligand conditions in native PCa cell lines.....</b>	<b>40</b>
<b>Figure 18. TTC7B depletion disrupts the CXCR4-PI4KIII<math>\alpha</math> interaction.....</b>	<b>43</b>
<b>Figure 19. TTC7B regulates invasion in PCa through CXCL12 and other chemokines, under both basal and ligand induced conditions. ....</b>	<b>45</b>
<b>Figure 20. Overall progression of cancer.....</b>	<b>47</b>
<b>Figure 21. PI4KIII<math>\alpha</math> regulates invasion in PCa through CXCL12 and other chemokines, under both ligand induced and basal conditions. ....</b>	<b>50</b>
<b>Figure 22. PI4KIII<math>\alpha</math> knockdown using lentiviral shRNA shows decreased expression and activity.....</b>	<b>51</b>
<b>Figure 23. PI4KIII<math>\alpha</math> regulates invasion in PCa through CXCL12, under basal ligand induced conditions. ....</b>	<b>53</b>
<b>Figure 24. Gene expression validation of RNA-seq analysis of PC3-CXCR4 cell lines.....</b>	<b>60</b>
<b>Figure 25. Pathway analysis of genes differentially expressed in PI4KIII<math>\alpha</math> shRNA vs scrambled C4-2B cell-lines. ....</b>	<b>62</b>
<b>Figure 26. Pathway analysis of genes differentially expressed in PI4KIII<math>\alpha</math> shRNA vs scrambled PC3-CXCR4 cell-lines.....</b>	<b>64</b>
<b>Figure 27. Differentially expressed altered gene and pathway meta-analysis between PI4KIII<math>\alpha</math> shRNA vs scrambled in PC3-CXCR4 and C4-2B cell-lines. ....</b>	<b>66</b>
<b>Figure 28. PI4KIII<math>\alpha</math> expression is higher in metastatic tumors compared to its matched primary tumors. ....</b>	<b>75</b>

<b>Figure 29. PI4KIII<math>\alpha</math> expression profile in .....</b>	<b>77</b>
<b>Figure 30. Better OS and PSA progression is associated with low PI4KIII<math>\alpha</math> and CXCR4 expression in bone biopsies. ....</b>	<b>80</b>
<b>Figure 31. Better OS and PSA progression is associated with low PI4KIII<math>\alpha</math> in bone biopsies with Bicalutamide treatment in addition to ADT. ....</b>	<b>85</b>
<b>Figure 32. GSEA of proliferation-associated gene set in PI4KIII<math>\alpha</math> high and low expressing bone biopsies.....</b>	<b>87</b>
<b>Figure 33. Heatmap representation of individual expression levels of top 50 features for each phenotype in Expression dataset in metastatic bone biopsies of mHSPC patient samples. ....</b>	<b>88</b>
<b>Figure 34. GSEA of Hallmark Androgen Response in AA metastatic biopsies of all tissues. ....</b>	<b>89</b>
<b>Figure 35. GSEA of proliferation-associated gene set in Non-AA bone biopsies.....</b>	<b>90</b>
<b>Figure 36. GSEA using A) Meta-55, B) Balk et al, and C) Chandran et al- Metastasis-Up D) Chandran et al- Metastasis-Down-regulated gene signatures .....</b>	<b>93</b>
<b>Figure 37. GSEA using Kegg pathway database. ....</b>	<b>94</b>
<b>Figure 38. Immune expression profile. ....</b>	<b>97</b>
<b>Figure 39. CXCR4 interacts with PI4KIII<math>\alpha</math> leading to PCa invasion and metastasis.....</b>	<b>100</b>

## CHAPTER 1- INTRODUCTION

**1.1 Prostate Cancer.** Prostate cancer (PCa) is the second most diagnosed cancer, most prevalent among men 65 and older, and of non-Hispanic, African-American and Caucasian descent, with estimated new cases of 268,490 in the United States in 2022. In 2021, PCa was estimated to account for 13.1% of all new cancer cases, and 5.6% of all cancer deaths. Even though the 5-year relative survival rate is ~97.5%, with most cases belonging to the localized stage, it is the second leading cause of cancer death (Surveillance, Epidemiology, and End Results (SEER) 18 registries, National Cancer Institute). This increased survival rate can be contributed to early detection through diligent screenings using prostate specific antigen (PSA) testing and digital rectal exams (DREs); and Active Surveillance for men with low-risk tumors and some intermediate-risk cases.

The morbidity rate from PCa can significantly progress after diagnosis by spreading to lymph nodes, liver, and mainly metastasizing to the bone (65-75%)<sup>8, 9</sup>. They can lie dormant, which is a unique characteristic of PCa, other than estrogen positive breast cancer<sup>10</sup>. With increased improvement in risk stratification of patients, the better treatment of course for metastasized patient seems to be an initial treatment of chemotherapy than just androgen deprivation therapy (ADT) alone<sup>11</sup>. Also, in chemotherapy-naïve and chemotherapy-refractory patients, Abiraterone that targets the de novo steroidogenesis, and anti-androgen Enzalutamide are approved single-agent treatments, and also used together in Combined androgen blockade (CAB) treatments. These drugs improve the survival status of patients but not as curative treatments. The increase in poor outcomes and mortality rate are seen in advanced stages of metastatic castrate resistant PCa (mCRPC), and display sensitivity to ADT and androgen receptor signaling inhibitor (ARSi) only from 24-36 months, and have a median survival of less than 2 years<sup>12</sup>. These are due to the acquired resistance to these modern-day treatments, that are generally categorized as

‘restored AR signaling’, ‘AR bypass signaling’ and ‘complete AR independence’<sup>13, 14</sup>. The first line of treatment for mCRPC is usually docetaxel<sup>15</sup>- a microtubule stabilizer, along with ADT, as most mCRPC’s are still reliant on androgen signaling. Also, ARSi abiraterone and prednisolone is added to the regiment, after multiple trials proving the benefits of addition of these agents at these metastatic stages. Second line of ARSi treatments is the androgen targets such as enzalutamide and apalutamide, providing higher efficacy, especially in non-metastatic CRPC. Cabazitaxel is provided to men resistant to docetaxel in advanced mCRPC as a second-line of treatment<sup>16, 17</sup>.

With inherent or acquired resistance still being a problem, more research into biomarkers, mechanisms of resistance and new-generation AR metabolite inhibitors are being researched<sup>13</sup>; along with alternate treatments that include other hormonal therapies with anti-androgens, radiation therapy using radium-223<sup>18</sup>, immune therapies using Sipuleucel-T and bone-targeting agents<sup>11</sup>- to alleviate secondary complications, such as impaired mobility, fractures and hypercalcemia. With the spread of PCa to distant sites, the 5-year relative survival rate decreases to 30.6% (SEER), making this indolent cancer, still a leading cause of cancer death in men.

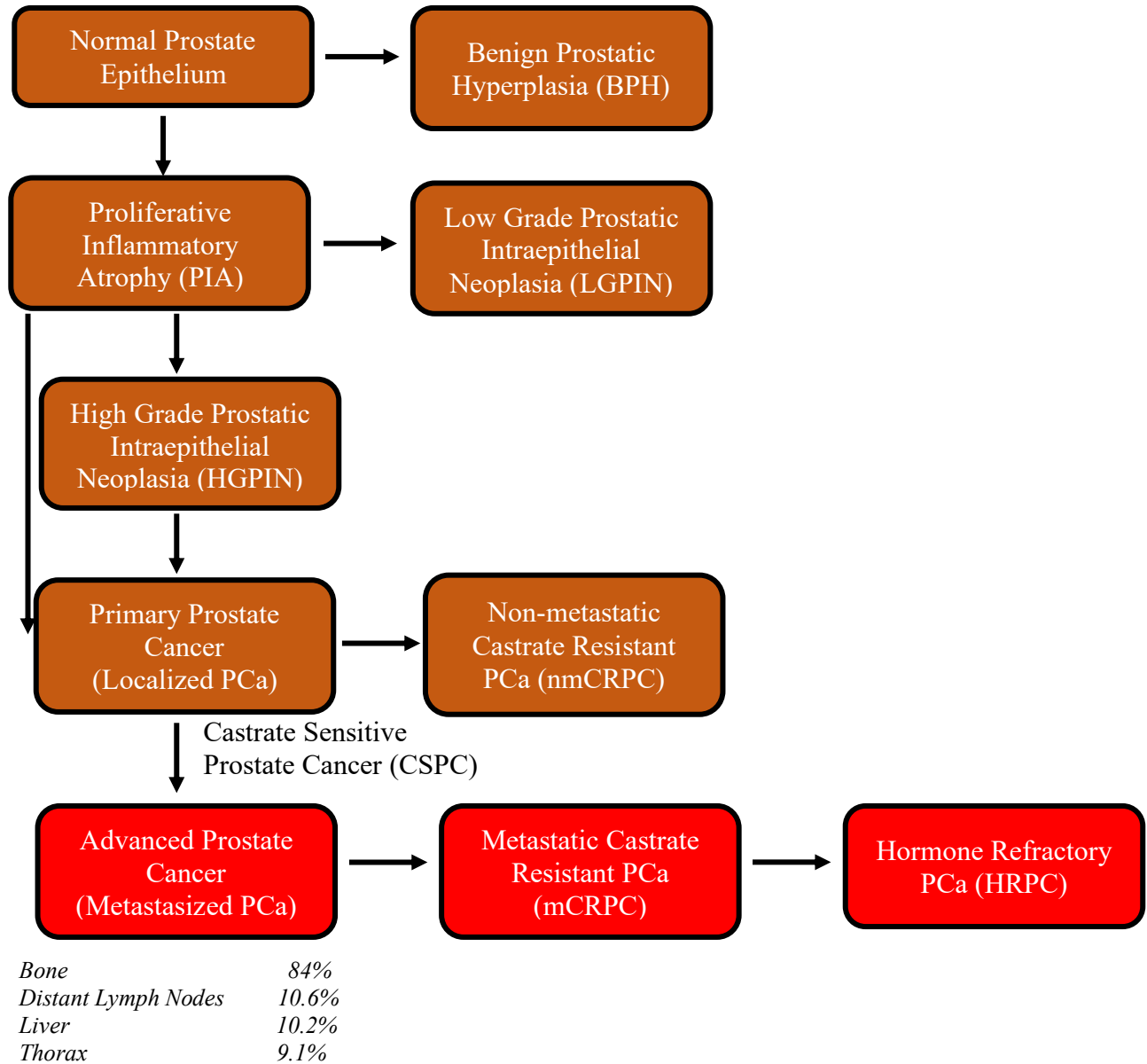


**Figure 1. Schematic progression of Prostate cancer.**

Representation of progression of normal prostate epithelium with PIA and PIN as a precursor of Advanced PCa<sup>7, 8</sup>, as adapted from Abaloff Clinical Oncology 6<sup>th</sup> edition.

**1.2 Phosphatidylinositol metabolism.** Phosphoinositides represent a minor component of the eukaryotic plasma and organelle membranes and are involved in key functions of the cell physiology<sup>19, 20</sup>. They are formed by phosphorylation of the inositol ring at the 3,4,5 position of a phosphatidylinositol (PtdIns) (Fig. 2), resulting in seven phosphoinositide species (Fig. 3).

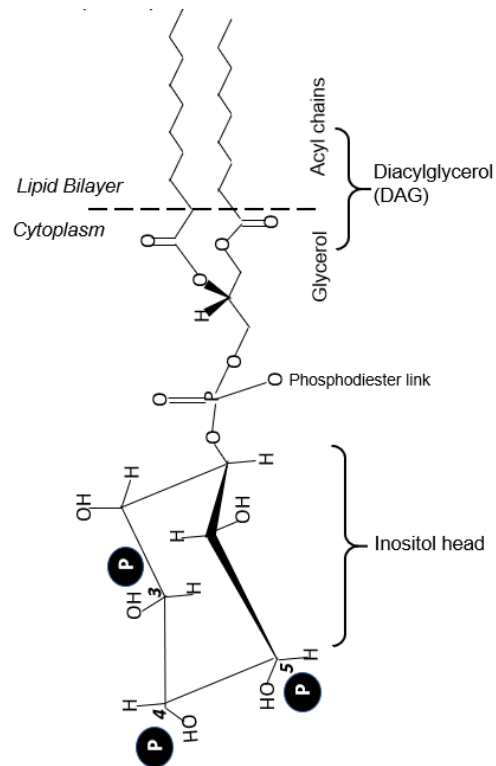


**Figure 2. Inositol ring anchored to the lipid bilayer on PM.**

Phosphorylation of inositol ring at the 3,4,5 position producing phosphatidylinositol.

---

PtdIns(4)P along with PtdIns(4,5)P<sub>2</sub>, PtdIns(3,4,5)P<sub>3</sub> and their downstream metabolites are critical in signal transduction, organelle identity and functions, vesicular trafficking, cell motility, cell proliferation and as a result play important role in cancer and its metastasis<sup>19-24</sup>. The dynamic fluctuations of the membrane phosphoinositide concentrations are critical, as they mediate cellular functions under tight control. They are regulated by their specific kinases, phosphatases and phospholipases and often localized to the subcellular locations where their

substrates are produced (Fig. 3)<sup>19, 25</sup>. This spatiotemporal location of these phosphoinositides are critical and are under tight control, as they provide the organelle identity and synchronized membrane trafficking for the regular functioning of a cell<sup>19</sup>.

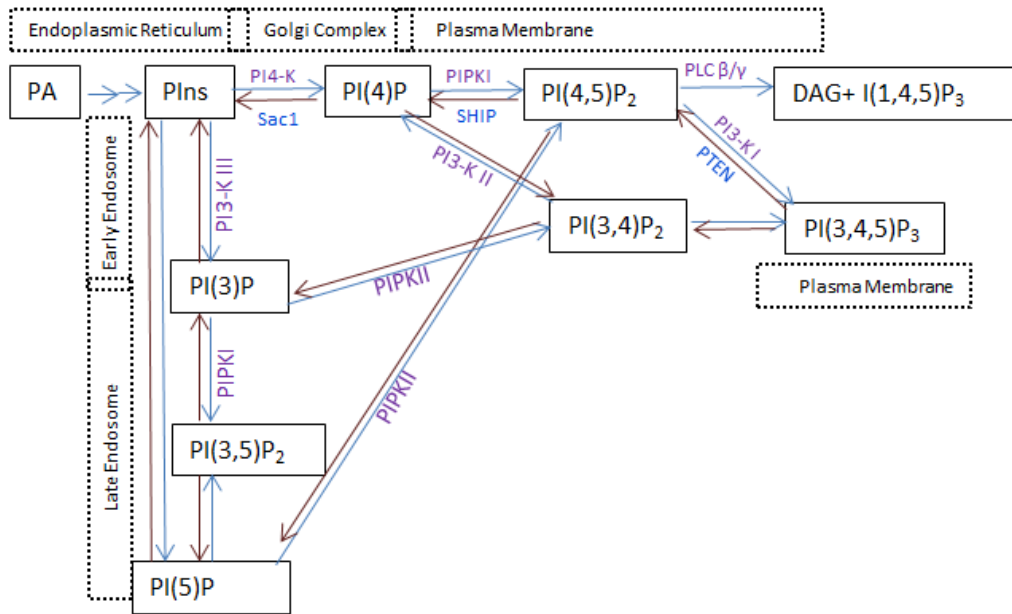


**Figure 3. Metabolism of the different phosphoinositide species and their subcellular localization.**

The seven main phosphoinositide species are PI4P, PI3P, PI5P, PI(4,5)P<sub>2</sub>, PI(3,5)P<sub>2</sub>, PI(3,4)P<sub>2</sub> and PI(3,4,5)P<sub>3</sub>. The kinases and phosphatases that are responsible for their production are shown in purple and blue respectively. The subcellular localization of these species is as listed above.

---

The initial step is catalyzed by phosphatidylinositol 4-kinase (PI4-Kinase) to form PtdIns(4)P, which plays a crucial step in signal transduction as the precursor of PtdIns(4,5)P<sub>2</sub><sup>26</sup>. Hence the PI4-kinase complex has been associated with many cellular functions like maintaining the plasma membrane composition and identity, regulation of coat adaptors for endosomal trafficking, act as regulators of effectors of PI4P proteins such as FAPP2 and OSBP<sup>23, 24, 27-29</sup>. The mammalian genome consists two families of PI4-kinases with four isoforms: Type III

Phosphatidylinositol 4 Kinases- PI4KIII $\alpha$  and PI4KIII $\beta$  (encoded by PI4KA and PI4KB, and homologues of yeast PI4-kinases stt4 and Pik1), that is responsible for PtdIns(4)P generation in the plasma membrane (PM), ER and Golgi complex respectively. Type II Phosphatidylinositol 4 Kinases- PI4KII $\alpha$  and PI4KII $\beta$  (encoded by PI4K2A and PI4K2B, and homologues of yeast PI4-kinase Lsb6), and function mainly in the Golgi complex and endosomal system. Amongst these PI4KIII $\alpha$  is considered to be essential for life<sup>30</sup>, and is implicated as a critical host factor for the hepatitis C virus life cycle<sup>31-33</sup>, other viral<sup>34</sup> and bacterial<sup>35</sup> infections.

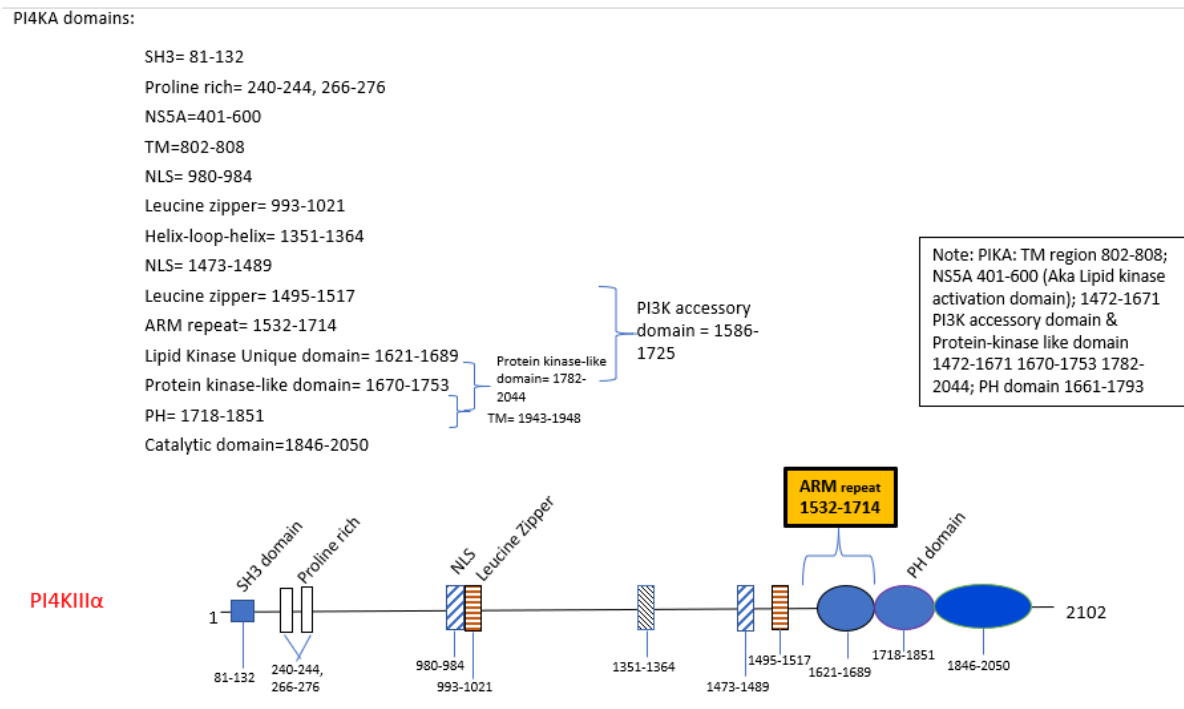


**Figure 4. Domain structure of PI4KIII $\alpha$ .**

Detailed organization of the various domains that comprises PI4KIII $\alpha$ .

---

PI4KIII $\alpha$  is recruited to the PM by a complex super assembly of accessory and regulatory proteins - EFR3 (a palmitoylated scaffold protein), TTC7 and FAM126. Two heterodimeric complexes of PI4KIII $\alpha$ -TTC7-FAM126 dimerizes with each of their C-terminal portions forming a super assembly, with TTC7-FAM126 directly interacting with c-terminus of EFR3 and recruited

to the PM. This lipid kinase complex is conserved from yeast to humans<sup>28, 36-39</sup>. This localization of the PI4KIII $\alpha$  to the PM is extremely crucial for maintaining the PM integrity, identity and its phosphoinositide balance<sup>28</sup>. PI4KIII $\alpha$  has dual functions of regulating PIP binding proteins involved in vesicular trafficking; and generate PtdIns(4,5)P<sub>2</sub> in the PM, by maintaining steady pools of PtdIns(4)P. Also, the structural domain regulates the activity of vesicular trafficking proteins<sup>40</sup>. PtdIns(4)P phosphatase -Sac1, expressed in the ER, along with its corresponding kinase PI4KIII $\alpha$ , is a critical regulator of PtdIns(4)P levels in the PM, Golgi and at the ER. This requires exchange of lipid molecules such as cholesterol through the oxysterol-binding homology (Osh) proteins, which localizes to the PM/ER contact sites, acting as sensors of the PM PI4P levels, which can stimulate SAC1 activity in vitro. This also requires 6 other ER membrane proteins such as VAP, for this exchange and maintenance of cholesterol levels at the PM, by depletion of PI4P at the ER. Thus, the counter-transport of lipids through non-vesicular traffic is driven by the concentration-gradient of PI4P levels at the membrane, maintaining the levels is made possible by SAC-1 phosphatase and Osh protein sensors using the membrane contact sites of PM/ER<sup>41-45</sup>.

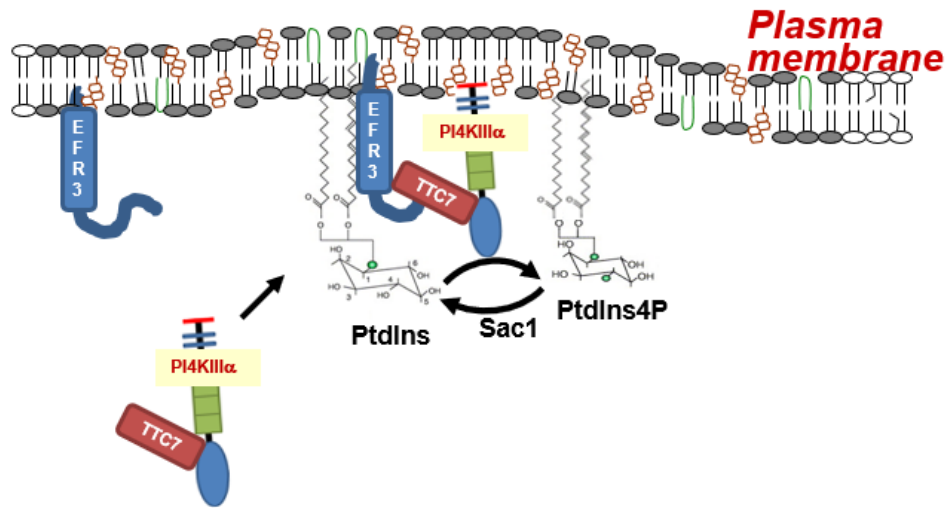


**Figure 5. Localization of Phosphatidylinositol 4 kinase III $\alpha$  to the plasma membrane.**

A complex regulation of accessory proteins mediates PI4KIII $\alpha$  localization to PM, where it participates in generation of PtdIns4P. EFR3B is a GPI anchored plasma membrane protein and TTC7B is cytosolic PI4KIII $\alpha$  adaptor protein. TTC7B and PI4KIII $\alpha$  complexes targeted to plasma membrane through interaction with EFR3B.

---

The PtdIns(4)P generated from PI4-kinases phosphorylation has many other crucial functions other than generating PtdIns(4,5)P<sub>2</sub>. It acts as an effector protein for binding of adaptor and coat complexes (eg: AP-1, GGA proteins, epsinR), as well as lipid-transfer proteins (eg: OSBP, CERT and FAPP proteins), for Golgi-membrane localization, and giving membrane domain identity and organelle specific specialization for that membrane<sup>19, 24</sup>. More specifically the PI4P from PI4KIII $\alpha$ , induces curvature in the plasma membrane playing a role in the biophysical identity of that helps in many of its biochemical characteristics<sup>27</sup>. In addition, PI4P gives an identity to the cytoplasmic side of the plasma membrane as negatively charged along with other negatively charged phosphoinositide species, making it possible to recruit proteins with polybasic lipid binding domains like K-Ras<sup>46, 47</sup>. Thirdly, is to regulate ion channels like transient receptor potential vanilloid 1 (TRPV1) cation channel<sup>46</sup>.

The signal transduction is carried to the downstream effectors from the PM through the help of phosphoinositides and their interacting proteins, along with the dynamic fluctuations of their levels on the PM. The PtdIns(4,5)P<sub>2</sub> produced can be hydrolyzed by phospholipases such as PLC leading to amplification of signals or converted to PtdIns(3,4,5)P<sub>3</sub> that can respond to growth factor stimulation, mediating a wide variety of effects. PtdIns(4,5)P<sub>2</sub> primarily is produced from PtdIns(4)P, as there is very little PtdIns(5)P in cells. It is now known that PI4KIII $\alpha$  is the primary kinase involved in the maintenance of the PtdIns(4)P pool on the PM during PLC signaling after GPCR stimulation, and Ca<sup>2+</sup> signaling<sup>48-50</sup>. Small amounts of this enzyme are sufficient to maintain the house-keeping functions of this kinase and maintain the previously mentioned steady-state membrane phosphoinositide pools<sup>30, 49</sup>, even after receptor stimulation with hormones, for sustained PLC activation and Ca<sup>2+</sup> signaling<sup>48</sup>.

**1.3 Phosphatidylinositol kinases in Cancer.** The deregulation of the normal functions of the PI kinases are found in many cancers leading to tumorigenesis and metastasis in association with phosphoinositides<sup>21, 51, 52</sup>. One of the most frequently mutated PI-kinases is the Class I Phosphoinositide 3-kinases (*generate PIP3 from PIP2*) especially the PIK3CA gene encoding the p110 $\alpha$  catalytic subunit, with mutations that often alter the enzymatic activity and are found in many cancers<sup>53</sup> and other malignancies. The other catalytic subunit p110 $\beta$ , although not commonly mutated promotes tumorigenesis in cancers with PTEN loss<sup>54, 55</sup>. The regulatory subunit of Class I PI3-kinase p85 $\alpha$  is known to have somatic mutations that hinders its ability to inhibit PI3K in endometrial and colon cancers<sup>56, 57</sup>. Currently there are multiple on-going and completed trials of pan, isoform-specific and dual PI3K/mTOR inhibitors that are more target specific and can overcome resistance to therapies. Some of these inhibitors have been tested as single-agents or as

combination therapies, for drug toxicities and other issues associated with PI3K inhibition. These are tested in multiple cancers, and are in various phases of the trials<sup>58</sup>.

So far, no activating/driving mutations or deletions of PI4-kinases in general have been discovered in any cancer. Although irregular vesicular trafficking leading to faulty receptor signaling and misinterpreted organelle identities seemed to play contributing factors, in cancers associated with PI4K expression. Depleting PI4P to limit supply for growth factor signaling and proliferation through AKT signaling proves ineffective, as results show AKT signaling in various cell lines is PI4K-isoform dependent and cell-type dependent<sup>59</sup>.

Increased PI4KII $\alpha$  expression is observed in cancers like breast cancer, thyroid papillary carcinoma, bladder transitional carcinoma et cetera<sup>21</sup>. and is associated with promotion of tumor angiogenesis by altering HER2-PI3K kinases- ERK signaling cascade and increasing production of VEGF and hypoxia-induced factors<sup>60</sup>. It is also shown to be important in the EGFR signaling and subsequent endosomal trafficking of the activated EGFR<sup>61</sup>. This kinase is involved in the Wnt signaling, a crucial signaling pathway in cell-fate determination and thus many malignancies<sup>62, 63</sup>.

Conversely, PI4KII $\beta$ s role in oncogenic signaling has been tied to growth factor signaling<sup>64</sup> with anti-metastatic contribution in hepatocellular carcinoma leading to inhibition of cell migration through actin remodeling<sup>65</sup>.

The other family of PI4-kinases is equally implicated in carcinogenesis. PI4KIII $\beta$  stimulation by eEF1A2, a protein elongation factor, has been associated with development of metastatic breast cancer<sup>66, 67</sup>. Similarly, PI4KIII $\alpha$  gene expression is associated with more invasive and metastatic phenotypes in pancreatic<sup>68</sup> and prostate<sup>1</sup> cancer, as well as chemoresistance<sup>69, 70</sup>. Very recently the EFR3A-PI4KIII $\alpha$  interaction on the PM has been implicated in many KRAS dependent tumors, and treatments with PI4KIII $\alpha$  inhibitors along with KRAS inhibitors, or MAPK

and PI3K inhibitors have proved to improve efficacy<sup>71, 72</sup>. Whereas loss of PI4KIII $\alpha$  expression is linked to developmental abnormalities<sup>73</sup>, neuronal impairments<sup>74</sup> and neurological dysfunctions<sup>75, 76</sup>. Pharmacological blockade or genetic inactivation leads to sudden death in-vivo and embryonic lethality<sup>28, 30</sup>. Majority of these dysregulations are attributed to the MAP kinase signaling cascade.

Of particular interest in our lab, is the function of PI4KIII $\alpha$  in cell signaling, especially in Prostate Cancer (PC).

**1.4 Biological Functions of CXCR4.** CXCR4/Fusin is a seven transmembrane G-protein coupled receptor (GPCR), with an only confirmed chemokine ligand known as CXCL12/SDF. CXCL12 can also bind to another chemokine receptor- type 7 CXCR7. CXCR4 receptor activation is mediated through coupling to an intracellular heterotrimeric G-protein associated inside the PM (inactive state - G $\alpha$ , G $\beta$ , G $\gamma$  bound to GDP (vs) active state upon ligand binding- dissociate into G $\beta\gamma$  dimer and G $\alpha$  bound to GTP). GTP is rapidly hydrolyzed to GDP, after signal transduction, and the heterotrimeric protein reverses back to its inactive state and associates with the receptor. The signaling is further desensitized, by phosphorylation at the serine sites, of the CXCR4 C-terminus by G-protein receptor kinases (GRK), resulting in  $\beta$ -arrestin recruitment and clathrin-mediated endocytosis<sup>77</sup>. The homodimerization and heterodimerization of CXCR4 with other receptors such as CXCR7, CCR7, CCR2 and CCR5- the coordinated binding of ligands, the multiple pathway activation and the mechanism of desensitization is under investigation<sup>77-79</sup>.

This interaction results in downstream signaling involving broad biological processes such as chemotaxis, cell proliferation, migration, differentiation, homing and activation through many divergent pathways. CXCR4 is widely expressed in many cell types; it plays an essential role in embryogenesis during development of heart, brain and vasculature. It is also known for its role in leukocyte chemotaxis and adhesion; along with immune-cell recruitment and retention during

adulthood. Another crucial function is for homing circulating progenitors at sites of tissue injury<sup>80-82</sup> and hematopoietic stem cells into the bone marrow niche, and has to be constitutively active for subsequent retention in the marrow in adulthood<sup>83</sup>. This axis is involved in development of embryonic pluripotent stem-cells and many tissue-committed stem-cells<sup>84</sup>.

**1.5 CXCR4 function in tumor microenvironment and cancer metastasis.** This CXCR4-CXCL12-CXCR7 axis play crucial roles in several types of cancers and can act as an independent predictor of poor survival in patients<sup>85, 86</sup>. Hypermethylation of CXCL12 resulting in downregulation of this ligand, yet over-expressing CXCR4 results in selective metastasis to specific organs with high CXCL12 secretion<sup>87</sup>. This axis is involved in tumor proliferation, angiogenesis, metastasis, cell migration and invasion, survival, maintain cancer stemness with self-renewing capacity<sup>88, 89</sup> and influence the tumor microenvironment by recruiting more immunosuppressive cells<sup>90-100</sup>. This aiding in tumor progression is by direct involvement in the signaling pathways that promote cancer growth and also indirectly by recruiting CXCR4 positive cancer-cells to sites that express CXCL12. Through these multiple roles, it also fosters a chemoresistant phenotype in cancers<sup>101</sup>. Both CXCR4 and CXCL12 are highly expressed in PCa playing the above-mentioned roles in the progression and resistance<sup>97, 102</sup>. In prostate cancer patient tumors, TMPRSS2-ERG fusion gene is frequently expressed due to fusing of androgen responsive TMPRSS2 promoter with ERG transcription factor coding sequence. It has been shown that ERG transcriptionally regulates CXCR4 gene in PCa cells, thus androgens can regulate CXCR4 through TMPRSS2-ERG fusion expressing tumors<sup>103-105</sup>.

The tumor growth and survival have been attributed to the many downstream signaling cascades activated by this axis. The CXCR4-CXCL12 activation of MAPK and phosphorylation of downstream proteins like c-Myc have known to form a positive feedback loop to aid in the

proliferative signaling<sup>106</sup>. Increase in EGF/EGFR signaling proteins<sup>107</sup>, activation of canonical Wnt pathway<sup>108</sup>, increased NF- $\kappa$ B signaling through activation of AKT and ERK<sup>109</sup> are some of the ways leading to increased cell proliferation through this axis. This NF- $\kappa$ B activation, along with MAPK-ERK and PI3K pathways also leads to anti-apoptotic characteristics<sup>110</sup>.

The angiogenic properties of tube formation and migration of vessels require CXCR4-CXCL12 signaling and this is achieved by upregulation through other transcription factors like Foxc<sup>111</sup>, promotion of VEGF, bFGF, COX-2<sup>112, 113</sup> and other angiogenesis-associated genes such as IL-6, SOCS2, cyclooxygenase-2, mainly through PI3K-Akt and NF- $\kappa$ B<sup>114</sup> signaling. There have also been growing evidence of CXCR4-CXCL12 mediating metastasis in many cancers<sup>115, 116</sup>. Prostate cancer is known to predominantly metastasize to the bone, this is established to be mediated by this axis, as PCa cells directly compete with the hematopoietic stem-cell niche and drives them to differentiate<sup>117</sup>, and neutralization of this axis through CXCR4 antibodies reduces the metastatic load<sup>118</sup>. This axis also promotes intraosseous growth after the PCa cells home to the bone through transactivation of HER2<sup>119, 120</sup> and EGFR on lipid-raft membrane mediated by Src and G $\alpha$ <sub>i2</sub> proteins. And blocking this axis impedes the initial tumor establishment in bone without an effect on established tumors suggesting CXCL12/CXCR4 axis contributes to the initial establishment in bone microenvironment<sup>121</sup>.

CXCL12/CXCR4 axis has shown to be a significant contributor to changes in tumor microenvironment leading to metastasis. This axis has been shown to be activate signaling pathways such as SHH<sup>122</sup>; MEK/ERK, PI3K/AKT, Wnt/B-catenin<sup>123</sup>; upregulation of survivin<sup>93</sup>; production of MMP-9<sup>119</sup>, MMP-13 expression<sup>124</sup>; attracting CXCR4-positive cancer stem cells to areas of hypoxia through HIF-1 production resulting in CXCL12 upregulation<sup>84</sup>; promote expression of  $\alpha$ 5 and  $\beta$ 3 integrins on tumor cells to enhance adhesion of tumor cells to the ECM<sup>125</sup>.

all to facilitate the invasion through the process of the Epithelial-to-mesenchymal transition (EMT)<sup>126</sup>. NF- $\kappa$ B activation through MEK/ERK signaling is also seen to play a role in preferential adhesion and transendothelial migration (TEM) of PC3 cells to the marrow stroma by overexpressing CXCR4<sup>127</sup>.

<sup>128</sup>The influence on this axis on the tumor and its microenvironment is evident as CXCL12 secreted by carcinoma associated fibroblasts (CAFs) can aid tumor growth in cancer cells that express high CXCR4 on the cell-surface promoting invasiveness, and also attract endothelial progenitor cells promoting angiogenesis<sup>129</sup>. Specifically, in PCa the CAF cells can secrete transforming growth factor- $\beta$  (TGF- $\beta$ ) resulting in CXCR4 stimulation propagating AKT signaling in prostate epithelium indicative of the tumor stromal cooperation in carcinogenesis<sup>130</sup>.

This axis can also act as a chemoattractant and aid in metastasis by attracting CXCR4 expressing cancer cells to sites of high CXCL12 expression like liver, lungs and bone marrow<sup>131</sup>. As mentioned this is especially true in PCa, as this cancer majorly metastasizes to the bone in advanced PCa. Also, this characteristic aids in tumor development by attracting other CXCR4 expressing inflammatory, vascular, immune and stromal cells that can provide a tumor nourishing and immunosuppressive environment<sup>128</sup>. CXCL12 secreted by CAFs and M2 macrophages induces myeloid derived suppressor cells (MDSCs)<sup>132</sup> and attracted regulatory T (Tregs)<sup>133</sup> cells, weakening an anti-tumor response.

The chemoresistance of many cancers is shown to develop upregulation of CXCR4 and CXCL12 after chemotherapy<sup>134, 135</sup>. This phenomenon can also be seen in patient that develop distant recurrence<sup>136</sup>, and in some cancers with the maintenance of cancer progenitor cells in treatment-resistant cancers<sup>137</sup>. This chemoresistance is abled by activation of downstream PI3K/AKT pathway and NF- $\kappa$ B and thus downregulating apoptotic proteins<sup>138</sup>.

There are targeted therapies in trials aimed towards this axis in preclinical and clinical cancer treatments. Some of the pre-clinical studies for this axis include. CTCE-9908- a peptide CXCL12 analog<sup>139-141</sup>, Olaptosed-pegol- a CXCL12 PEGylated mirror-image<sup>142</sup>, AMD3465- small-molecule CXCR4 antagonist<sup>143</sup>, BKT140- new-generation peptide CXCR4 inhibitor<sup>144</sup>, and POL5551- a CXCR4 antagonist<sup>145</sup>. The only FDA approved CXCR4 antagonist thus far is plerixafor (AMD3100), to be used for autologous stem-cell transplantation in patients with Non-Hodgkin's lymphoma or multiple myeloma. It is used in combination with granulocyte-colony stimulating factor (G-CSF) to replenish hematopoiesis after chemotherapy<sup>146</sup>. The clinical trials involving plerixafor currently involve using this drug as a combination with chemotherapy in AML and multiple myeloma<sup>147, 148</sup>, radiochemotherapy in cervical cancer (RTCT)<sup>149</sup>, immunotherapies in many cancer models<sup>150</sup> including ovarian cancer<sup>151</sup>, mesothelioma, and breast cancer<sup>152, 153</sup>.

## CHAPTER 2- HYPOTHESIS & RATIONALE

CXCR4 activation contributes to multiple signaling pathway activation leading to tumor promoting activities culminating in metastasis, we focus our efforts on the immediate molecular-downstream interactors which may involve in CXCR4 mediated tumor metastasis. Towards this end, SILAC (Stable Isotope Labeling by Amino Acids in Cell Culture) a proteomic analysis was performed on prostate cancer cells. This method elucidates the relative proteomic change using the combination of metabolic incorporation of modified stable isotopic nuclei and mass spectrometry.

Our lab identified PI4KIII $\alpha$  as a novel lipid-raft-associated regulator of CXCR4 mediating invasion and metastasis in PC cells<sup>1</sup>.

For the SILAC we first characterized the cells that will be used in this analysis- PC3 cells overexpressing (CXCR4) and underexpressing CXCR4 (shCXCR4) using stable lentiviral transductions. The mRNA level of the CXCR4 in these cell-lines were verified using qPCR, and the cell-surface expression was characterized using FACS analysis. The FACS indicated large CXCR4 overexpression in PC3-CXCR4 cells from the positive shifts in the median fluorescence intensity (MFI), while PC3-shCXCR4 showed a negative shift (Fig 6).

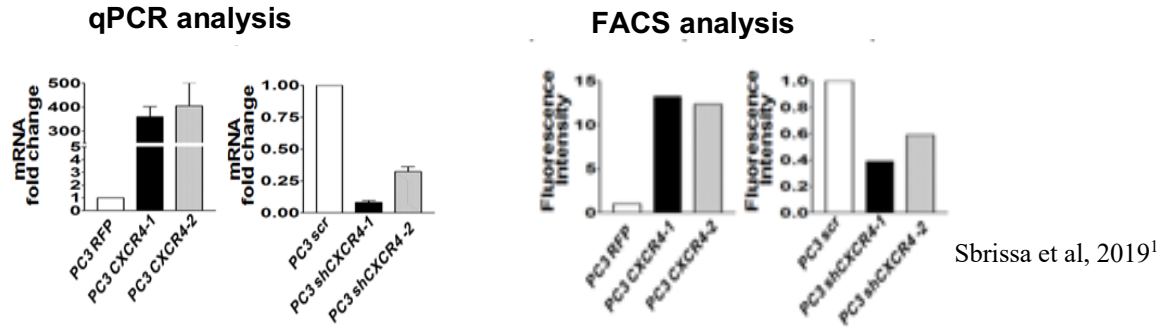
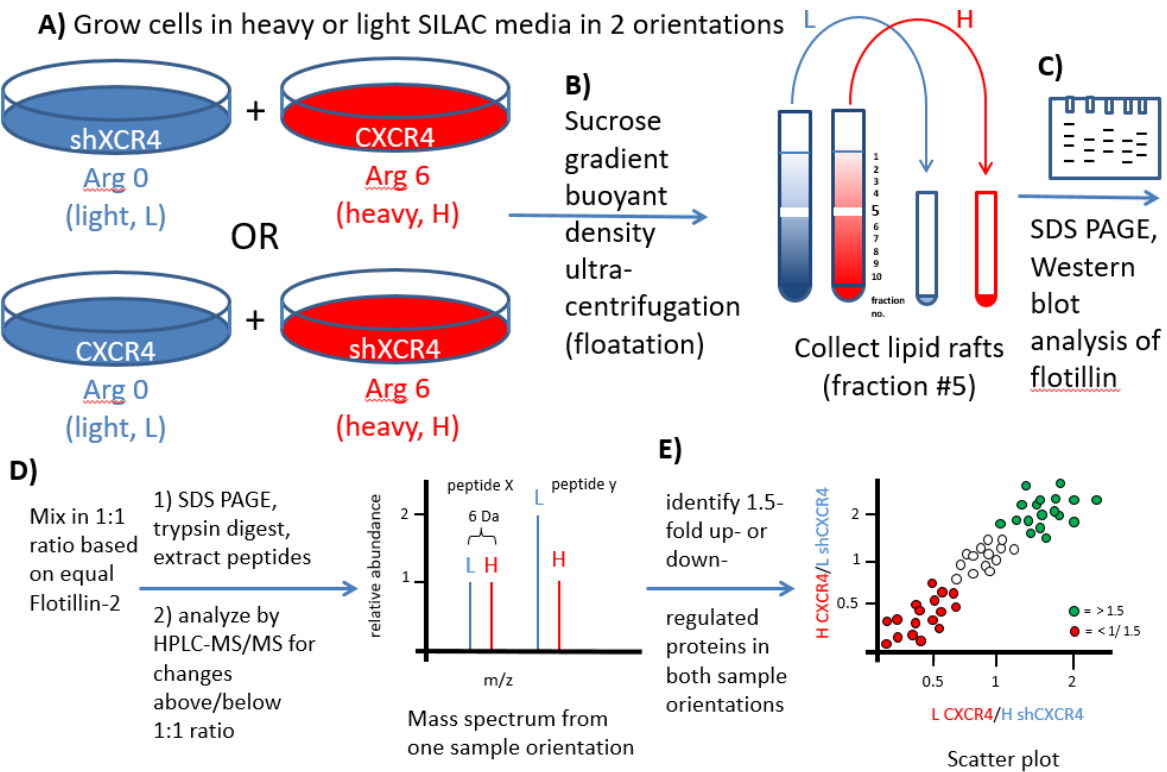


**Figure 6. Characterization of PC3-CXCR4 and PC3-shCXCR4 cells.**

The quantitation of the mRNA levels of CXCR4 after lentiviral transductions were verified using qPCR and the cell-surface expression of CXCR4 was characterized using FACS analysis.



Diego

**Figure 7. Schematic representation of the SILAC analysis was performed.**

SILAC proteomics of lipid-raft microdomains purified by sucrose-gradient buoyant-density ultracentrifugation from PC3-CXCR4 and PC3-shCXCR4 cells were collected and mixed on a 1:1

ratio of H CXCR4:L shCXCR4 or L CXCR4:shCXCR4 based on flotillin levels. The samples were analyzed using HPLC tandem mass-spectrometry.

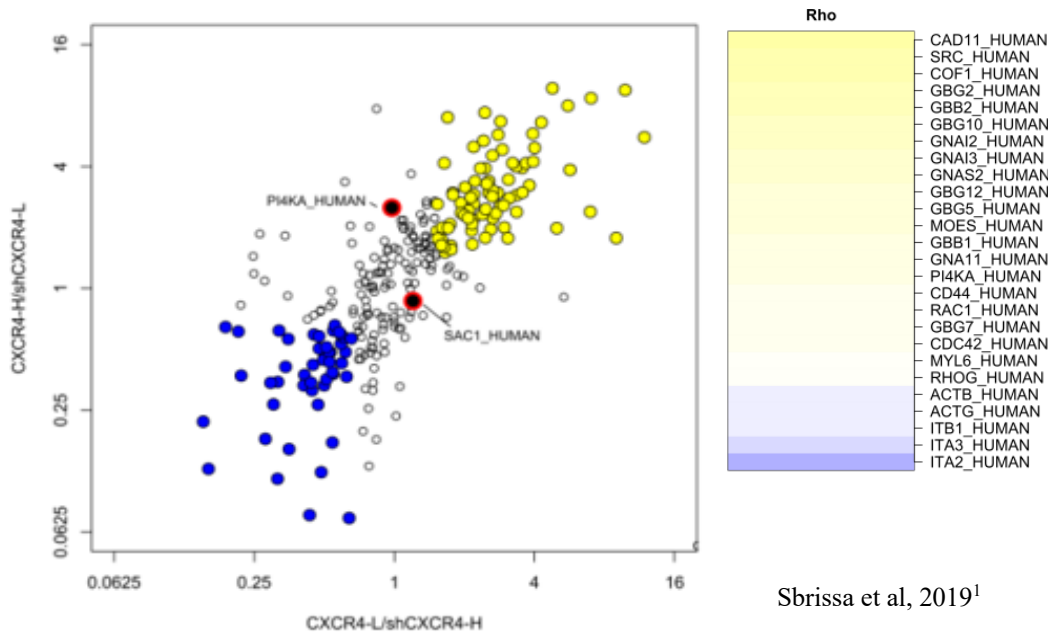


### Figure 8. Proteins identified as interactors of CXCR4 through SILAC analysis.

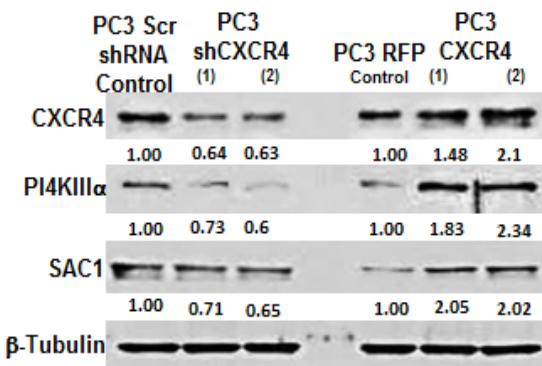
Integration of the two independent flip experiments of H CXCR4:L shCXCR4 and L CXCR4:shCXCR4 lipid raft protein ratios. Overexpressed proteins are shown in yellow and underexpressed proteins are shown in blue. Here you see the presence of PI4KA\_HUMAN expressed in lipid-rafts along with CXCR4.

Here 277 proteins identified from this analysis, were represented as a scatter plot on the basis of, if they were 1.5-fold up (79 proteins) or down (47 proteins) regulated on both the orientations of the sample pools. The proteomics analyzed 2 independent experiments resulting in the scatterplot profile of the same pattern, with proteins of overexpression in yellow and downregulated in blue. The ingenuity pathway database, identified pathways of the proteins overexpressed, as showing enrichment of several pathways that would be associated with CXCR4, like the GPCR interacting proteins, caveolar mediated endocytic pathway and viral entry endocytic

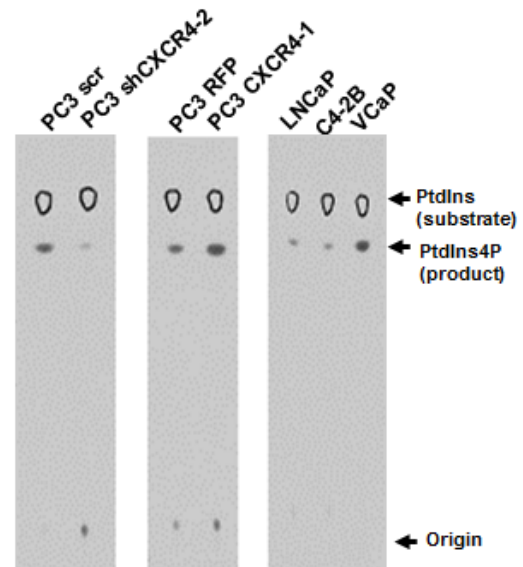
pathway. Interestingly it also showed presence of PI4KIII $\alpha$  and a PI4kinase A-phosphatase- Sac1, as being overexpressed in the lipid rafts with CXCR4 overexpressing cells.

With our SILAC showing enrichment of PI4KIII $\alpha$  with CXCR4 in the lipid rafts. Next, we characterized the interaction between CXCR4 and PI4KIII $\alpha$  using - PC3-CXCR4 and PC3-shCXCR4 cell model system.

### A WB analysis



### B Lipid kinase activity assay



Sbrissa et al, 2019<sup>1</sup>

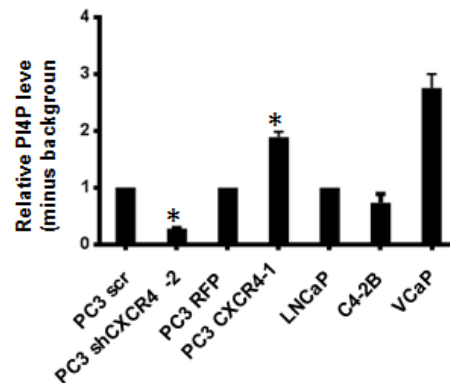


**Figure 9. Characterization of protein expression and lipid kinase activity of PC3-CXCR4 and PC3-shCXCR4 cells.**

A)WB analysis of total cellular proteins isolate from PC3-CXCR4 and PC3-shCXCR4 cells. These are representative data from 3 different experiments, showing down regulation of CXCR4, PI4KIII $\alpha$  and Sac1 in shCXCR4 cell lines and an increase in CXCR4 overexpressing cell lines.

B)Lipid Kinase activity. Representative autoradiograms from TLC analysis of PI4KIII $\alpha$  lipid kinase activity, in CXCR4 overexpressing and downregulated cell lysates vs their parental controls, and in other PCa cell lines, from 3 independent experiments.

---

The characterization of the expression and kinase activity, show that PI4KIII $\alpha$  and SAC1 expression correlates with CXCR4 expression as can be seen in CXCR4 knock-down and overexpressing PC3 cell lines. PC3-CXCR4 cell line shows a 2-fold increase in PI4KIII $\alpha$  levels compared to the parental PC3 cell line (Fig 9A). Interestingly there is no change in gene expression levels of PI4KIII $\alpha$  and Sac1 between the parental and overexpressing cell line, indicating a post-transcriptional modification to alter PI4KIII $\alpha$  protein expression in CXCR4 overexpressing cells<sup>1</sup>. Similarly, to check the activity of this increased PI4KIII $\alpha$  levels, an in-vitro lipid kinase assay was performed from the immunoprecipitated PI4KIII $\alpha$  from these lysates. The kinase activity also correlated with the expression of PI4KIII $\alpha$ , with almost 2-fold increase in CXCR4 overexpressing cells, indicative of the PI4P product formed. Also, amongst the various PCa cell-lines tested VCaP has the highest kinase activity<sup>1</sup>. The high expression and kinase activity in VCaP as seen in Sbrissa et al, could potentially be contributed to the high CXCR4 expression through the increased ERG transcription, as VCaP cells are TMPRSS2-ERG fusion positive, thus providing another evidence of CXCR4 regulating PI4KIII $\alpha$ .

We also see from the preliminary data presented here and the literature of these respective proteins, we hypothesize that CXCR4 interacts with PI4KIII $\alpha$  using its adaptor proteins leading to cellular invasion.

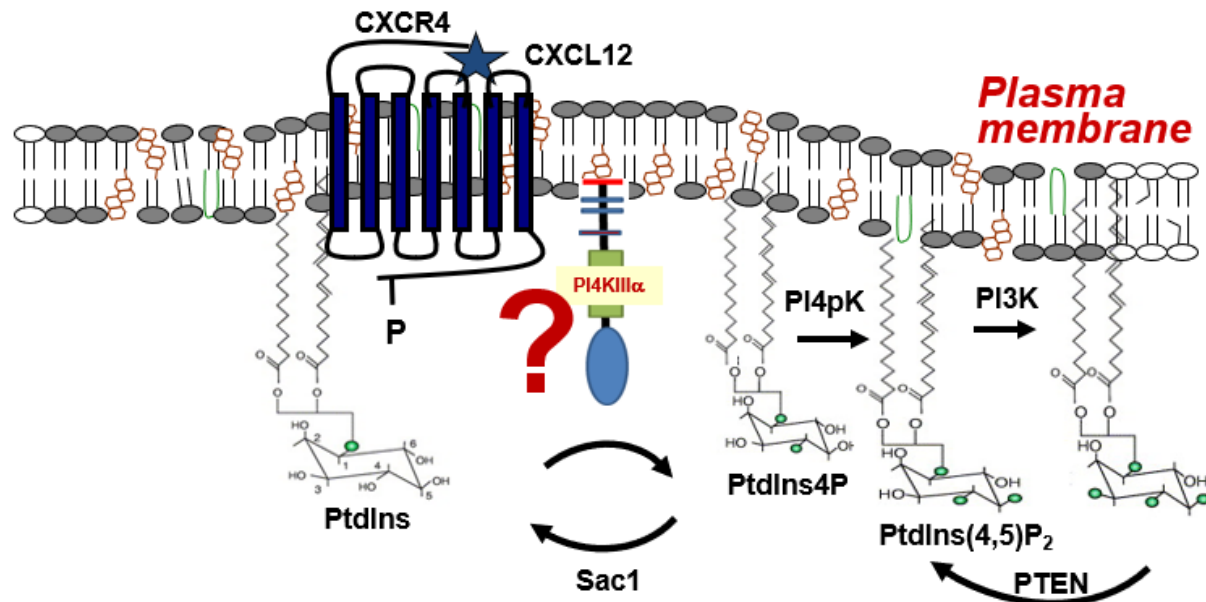


**Figure 10. CXCR4 interaction with PI4KIII $\alpha$  leads to cancer cell invasion and metastasis?**

In this study we investigate further the association of PI4KIII $\alpha$  and CXCR4 in Prostate cancer cells, along with stable overexpression of CXCR4 and knockdown of PI4KIII $\alpha$ . This will be achieved by functionally characterizing the interaction between PI4KIII $\alpha$ , its adaptor proteins in relation to CXCR4, and also determining their roles in CXCR4 induced invasion.

This relationship will be additionally studied in patient metastatic biopsies with mHSPC for their clinical relevance. The differentially expressed genes and the predominant signaling pathways between these conditions and their relation to cancer cell invasion and proliferation will be explored.

## CHAPTER 3- DETERMINE THE MECHANISMS OF PI4KIII $\alpha$ INTERACTION WITH CXCR4 IN PROSTATE CANCER

**3.0 Introduction.** CXCR4 has many interactor proteins either through direct or indirect interactions. signaling involves activation of multiple downstream pathways leading to cellular homing to their respective target sites.<sup>154</sup> Here as established from the preliminary studies, we identified lipid kinase PI4KIII $\alpha$  as a novel interacting partner of CXCR4 and may play an important role in the cellular and biological functions of CXCR4.

PI4KIII $\alpha$  (Stt4p in yeast) has few critical adaptor proteins as mentioned that are required for its recruitment to the PM. The accessory and regulatory proteins, super-complex consist of EFR3, TTC7 (Ypp1p in yeast) and FAM126 (this subunit not present in yeast). The PI4KIII $\alpha$ -TTC7-FAM126 heterotrimers form homodimers with each of their C-terminal portions, forming a ~700-kDa assembly<sup>38</sup>. TTC7 is initially required for the stability of this complex in-vivo, and the TTC7-FAM126 interacts with the c-terminus of EFR3, and phosphorylation of this terminus hinders PI4KIII $\alpha$  recruitment<sup>37, 38</sup>.

Here we elucidate this interaction between CXCR4 and PI4KIII $\alpha$  along with the adaptor proteins EFR3B and TTC7B.

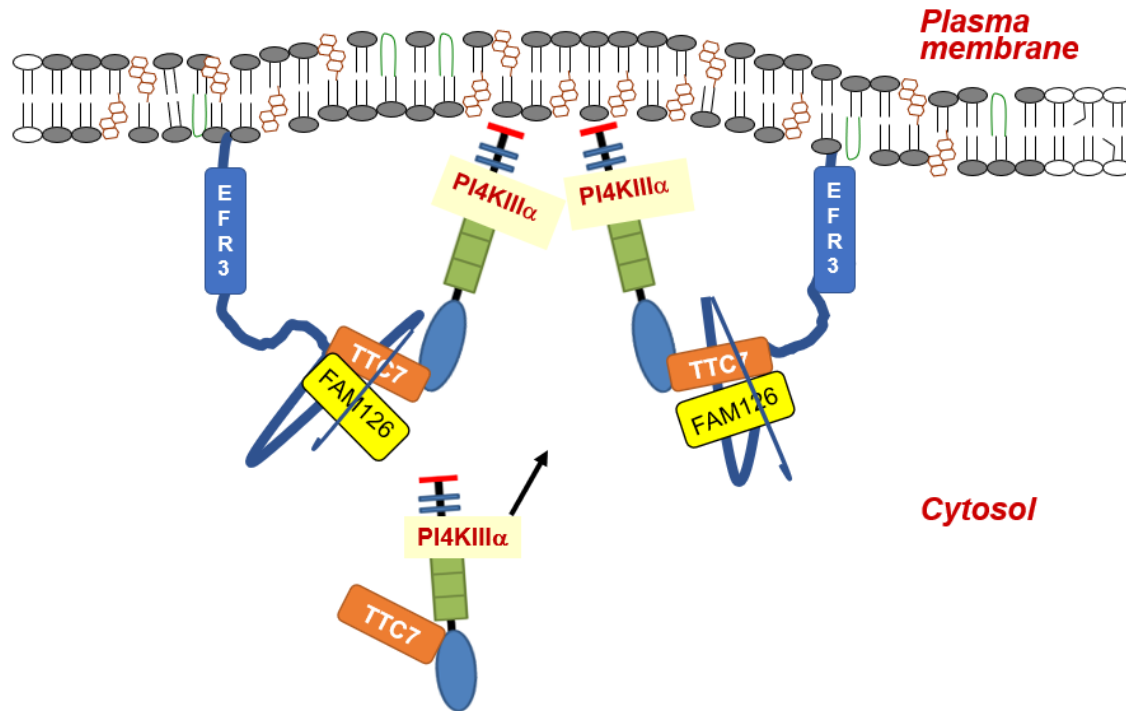


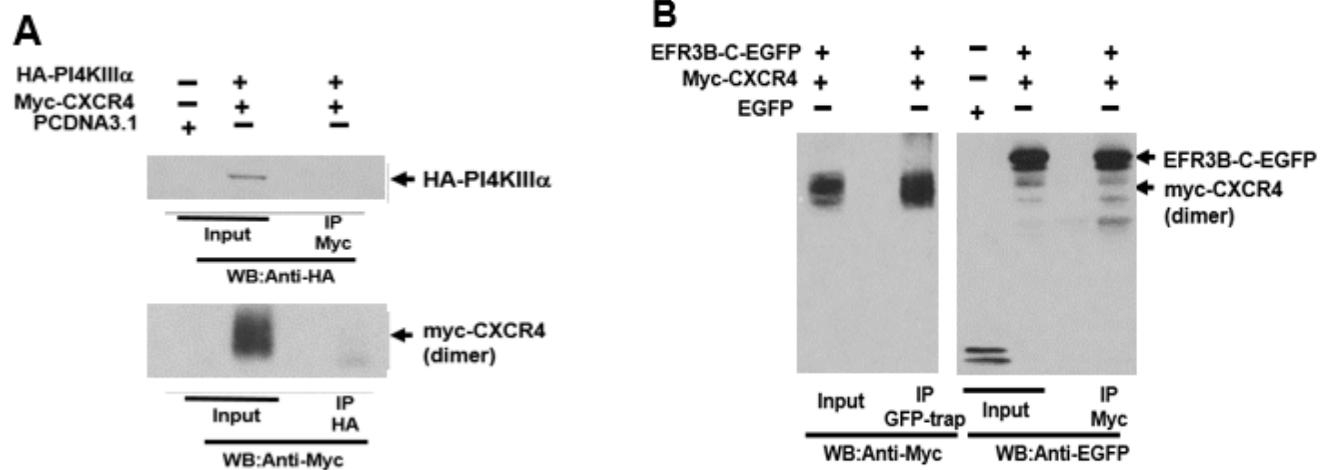
**Figure 11. PI4KIII $\alpha$  complex recruitment to the PM.**

EFR3 localizes to the PM at its N terminus, along with the N-terminal palmitoylation. PI4KIII $\alpha$  is recruited by an interaction with TTC7-FAM126 and the C-terminus of EFR3.

**3.1 Native interaction of PI4KIII $\alpha$  and CXCR4.** To characterize the interaction that we observed in the SILAC enrichment, we performed interaction studies by pulling down for CXCR4 using immunoprecipitation (IP) assays. Initially we tested our IP system in Cos-7 cells, after transfecting with tagged-proteins of interest (Fig 12). We conclude from this study that the CXCR4 and PI4KIII $\alpha$  interaction is not direct, as we do not see the presence of PI4KIII $\alpha$  in the pull-downs of CXCR4 lysates (Fig 12A). So, we tested if CXCR4 binds to any of the adaptor and regulatory proteins mentioned above. We see that CXCR4 binds to both EFR3B and TTC7B. More specifically EFR3B binds to CXCR4 dimers whereas TTC7B binds to CXCR4 monomers (Fig 12B and 12C). The other chemokine receptors such as CXCR7 and CXCR1 also have this interaction profile of binding to EFR3B and TTC7B, but this is not the case for all GPCRs, such

as Gprc6a or ADR2B1. This data suggest that chemokine receptor family members interact with PI4KIII $\alpha$  through the adaptor proteins. Now we wanted to test for the presence of PI4KIII $\alpha$ , when we pull-down CXCR4 after performing a triple transfection with the HA-PI4KIII $\alpha$ , Myc-CXCR4 and EFR3B-C-EGFP plasmids. As demonstrated here, when we transfect CXCR4 and PI4KIII $\alpha$ , with an adaptor protein, we found PI4KIII $\alpha$  in a complex with CXCR4 (Fig 12D), indicating that the interaction between them is facilitated by the adaptor protein EFR3B. As seen in the SILAC studies, this data supports that chemokine receptors could regulate PI4KIII $\alpha$  through its adaptor proteins, and in this way recruit PI4KIII $\alpha$  to the PM for further downstream signaling.

### 3.1.1 Results.



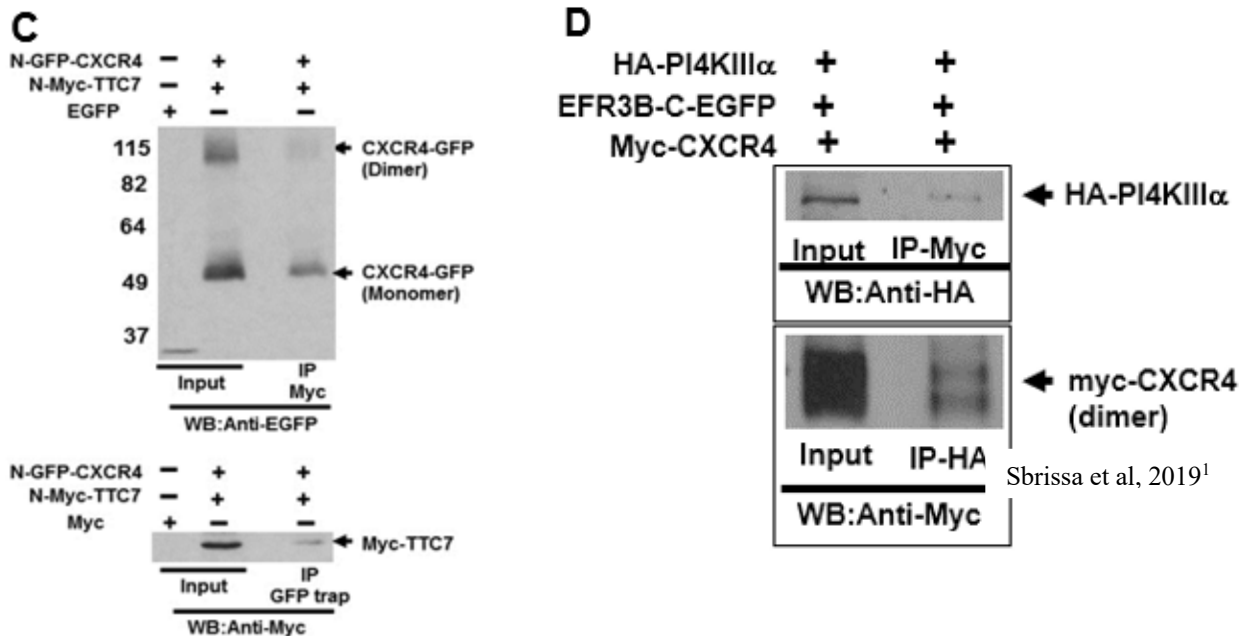


**Figure 12. CXCR4 interacts with adaptor proteins of PI4KIII $\alpha$  in tagged gene transfected immunoprecipitations.**

Cos-7 cells transfected with plasmid expressing fusion genes as mentioned, were co-immunoprecipitated followed by western blot analysis. A) CXCR4 pull-down was performed using Myc antibody and immunoblotted for HA to see the presence of PI4KIII $\alpha$ ; and reciprocal PI4KIII $\alpha$  pull-down was performed using HA antibody. B) CXCR4 pull-down was performed using Myc antibody and immunoblotted for GFP to see the presence of EFR3B; and reciprocal EFR3B pull-down was performed using GFP antibody. C) CXCR4 pull-down was performed using GFP antibody and immunoblotted for Myc to see the presence of TTC7B; and reciprocal TTC7B pull-down was performed using Myc antibody. D) Triple transfection of CXCR4, EFR3B, and PI4KIII $\alpha$  in Cos-7 cells was followed by CXCR4 pull-down with Myc antibody and immunoblotted for HA to see the presence of PI4KIII $\alpha$ ; and reciprocal PI4KIII $\alpha$  pull-down was performed using HA antibody.

**3.1.2 Endogenous PI4KIII $\alpha$  interaction with CXCR4 in PC3 cells.** We tested endogenous interaction between CXCR4 and PI4KIII $\alpha$  in CXCR4 overexpressing and knockdown PC3 cells. We observe that there is a basal level of interaction between the adaptor protein -TTC7B, PI4KIII $\alpha$  and CXCR4, , in PC3-CXCR4 overexpressing cell-line (Fig 13A). Whereas this interaction is enhanced almost 2 and 3.5 folds of TTC7B and PI4KIII $\alpha$  respectively, under CXCL12 treatment.(Fig 13A). In CXCR4 knock-down cell-line of PC3-shCXCR4, we see no observable interaction between TTC7B, PI4KIII $\alpha$  and CXCR4, in the presence or absence of CXCL12 (Fig 13B). These data suggest that in CXCR4 expressing PC3 cells a complex is formed between CXCR4, PI4KIII $\alpha$  and TTC7B and this complex formation further enhanced in the presence of CXCR4 ligand CXCL12.

### 3.1.3 Results.

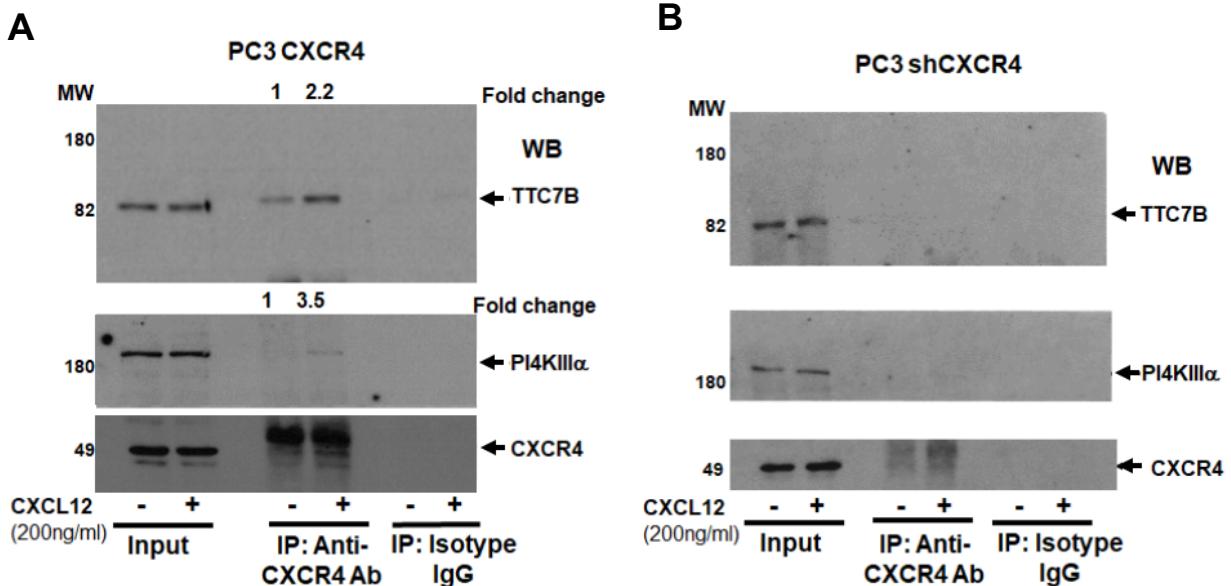


**Figure 13. CXCR4 interacts with adaptor protein of PI4KIII $\alpha$  in stable CXCR4 overexpressing PC3 cells - under basal, and increases under ligand conditions.**

PC3 cells stably transfected with CXCR4 were serum starved and induced with either no ligand or with CXCL12 (200ng/ml). The lysates were immunoprecipitated with CXCR4 antibody and observed for the presence of TTC7B and PI4KIII $\alpha$  in A) in CXCR4 overexpressing cells - PC3-CXCR4 and B) in CXCR4 downregulated cells – PC3 shCXCR4.

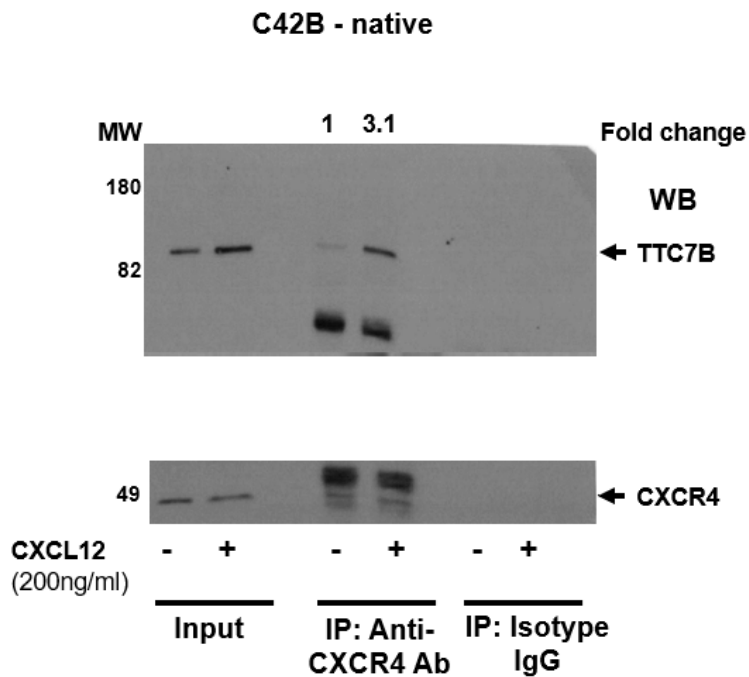
### 3.1.4 Determine endogenous interaction between CXCR4 and PI4KIII $\alpha$ in other PCa cells.

We tested endogenous interaction between CXCR4 and PI4KIII $\alpha$  in C4-2B and VCaP cells. - we observe the mechanism of the CXCR4 regulation of PI4KIII $\alpha$  in native PCa cell-lines. These endogenous native interactions were observed in C4-2B and VCaP cell lines. These interactions were tested after induction under, with or without ligand CXCL12 conditions. Similar conditions as above of serum starvation and concentration of ligand for induction were followed for the immunoprecipitation assays.

We observe that there is a basal level of interaction with the adaptor protein in both C4-2B and VCaP in the absence of ligand (Fig 14A,14B). And as seen in CXCR4 overexpressing cells (Fig 13), this interaction is enhanced almost 3 folds in C4-2B and 8 folds in VCaP, under CXCL12 treatment. Of all the prostate cell-lines, it would be interesting to recall we observed that VCaP has the highest kinase activity and PI4P levels (Fig 9B). From these immunoprecipitation studies, we demonstrate that there is a basal level of interaction between CXCR4, TTC7B and PI4KIII $\alpha$ , and with CXCL12 treatment, this interaction is enhanced in PCa cells.

### 3.1.5 Results.

**A**



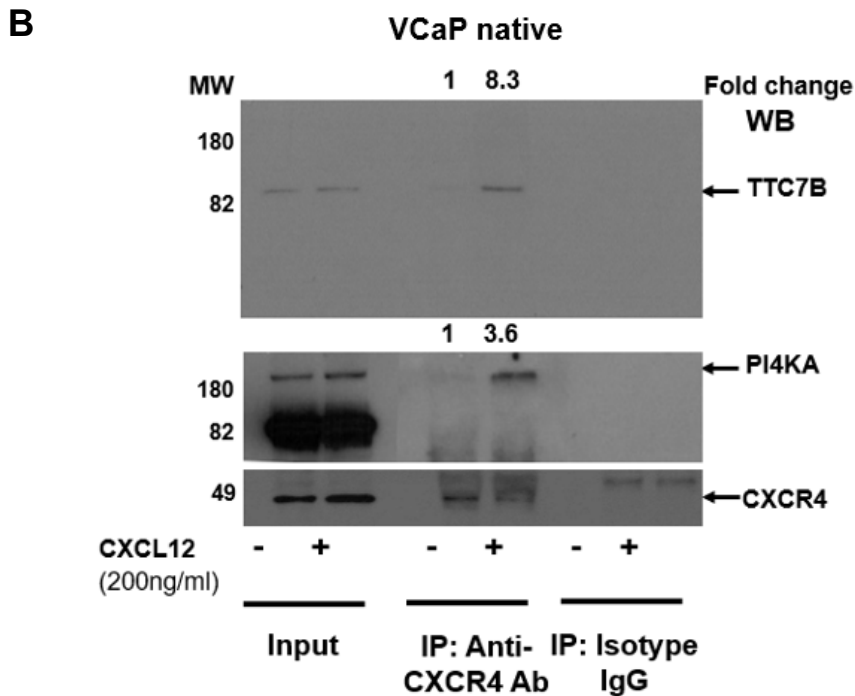


**Figure 14. CXCR4 interacts with adaptor protein of PI4KIII $\alpha$  in native PCa cells - under basal, and increases under ligand conditions.**

C4-2B and VCaP cells were serum starved and induced with either no ligand or with CXCL12. The lysates were immunoprecipitated with CXCR4 antibody and observed for the presence of TTC7B interactions. A) in C4-2B cell line, TTC7B interacts with CXCR4 under basal conditions. Under CXCL12 induction the interaction increases ~3 fold with TTC7B. B) in VCaP cell line, TTC7B and PI4KIII $\alpha$  interacts with CXCR4 under basal conditions. Under CXCL12 induction the interaction increases ~8 fold with TTC7B and ~4 fold with PI4KIII $\alpha$  respectively.

**3.1.6 Discussion.** These data support the initial observations in the SILAC studies, that chemokine receptor CXCR4 interacts with PI4KIII $\alpha$  kinase as seen with the enrichments in the lipid rafts. These immunoprecipitation studies show that these are facilitated through its adaptor proteins, and thus recruited to the PM. These interactions are also shown to be common to some chemokine

receptors such as CXCR7 and CXCR1 but not with other G-protein coupled receptors such as Gprc6a and human  $\alpha 2b$  adrenergic receptors (ADR2B)<sup>1</sup>.

From current studies we can conclude that CXCR4 does not directly bind to PI4KIII $\alpha$ , but through the adaptor proteins EFR3B and TTC7B in Cos-7 and PCa cell lines (Fig 12-14). These adaptor proteins and their interaction with PI4KIII $\alpha$  are well established and evolutionarily conserved, with EFR3 a membrane targeted protein through its palmitoylation, interacts with cytosolic TTC7 bound to PI4KIII $\alpha$ , acting as a docking site on the membrane<sup>28, 36-39</sup>. These specific interactions are seen in relation with CXCR4 with EFR3B binding to CXCR4 dimers and TTC7B binding to CXCR4 monomer, and whether these interactions are affected by a characteristic of CXCR4 receptors to homodimerize or heterodimerize with other GPCRs including chemokine receptors are yet to be elucidated.

**3.2 Determine co-localization using Proximity Ligation Assay.** Immunoprecipitation involve lysing cells with detergents and this process may aid artificial interaction of proteins, to overcome this issue proximity ligation assay was performed to determine the CXCR4 interaction with adaptor protein TTC7 in prostate cancer cells. Target specific antibodies from different host species (TTC7B-rabbit and CXCR4-mouse) are used and colocalization assay performed as specified in the Sigma Duolink DUO92101-1 kit. This is an assay performed with intact cells that detects proximity, through hybridization of connector oligos, which yields rolling circle amplification products, if the two proteins of interest are within 40nm of distance, proving co-localization.

This assay validates the co-localization of CXCR4 with the adaptor protein TTC7B, observed as red punctates from oligo probes attached to red fluorophores (Fig 16B). As determined from the immunoprecipitation studies, there is a basal level of red punctate formation with no

ligand induction, indicative of basal level of co-localization. When induced with CXCL12 the number of red punctates increase as confirmed with quantitation, indicating increase in co-localization, thus increased interaction of CXCR4 and TTC7B complex formation in cells.

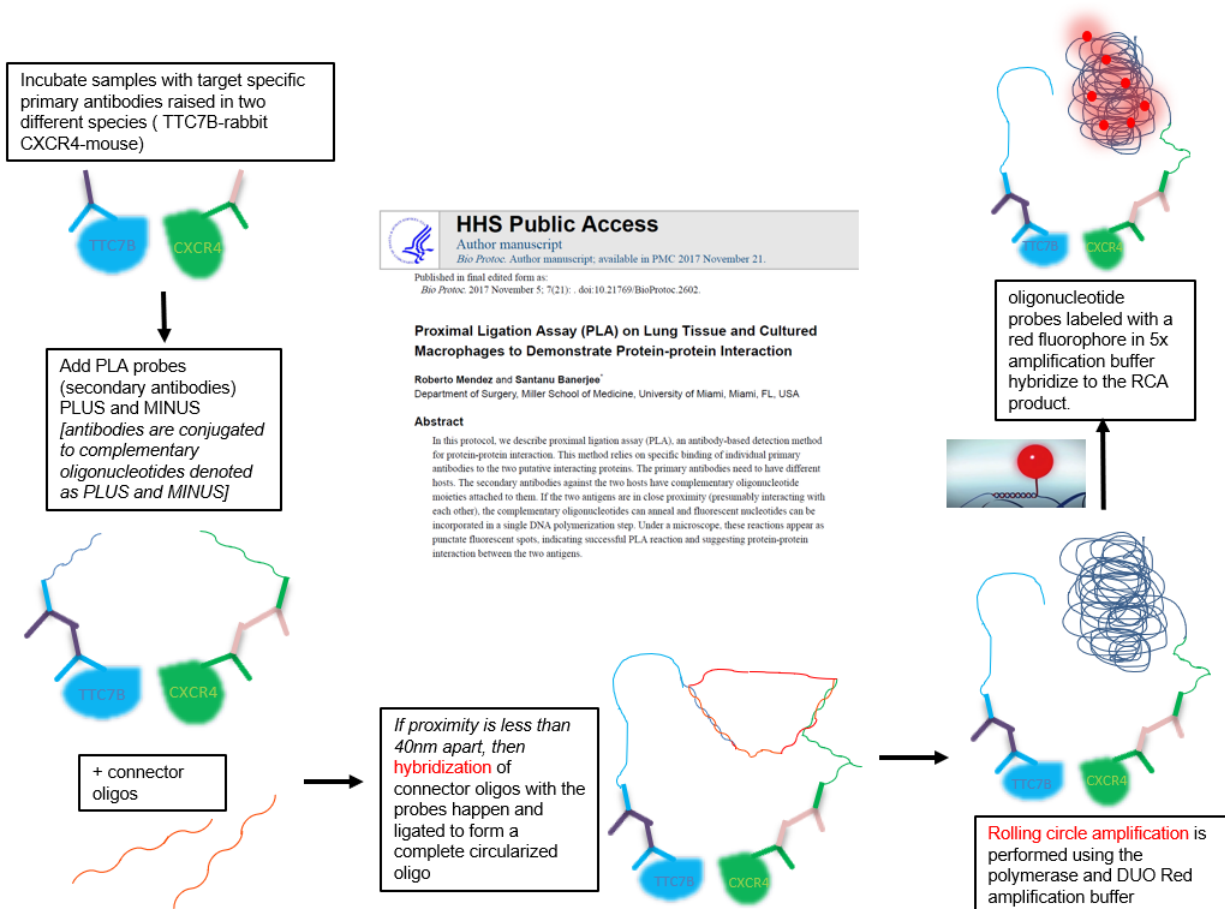


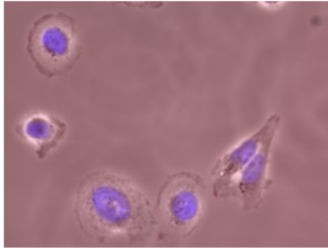
**Figure 15. Schematic representation of how the Proximity Ligation Assay (PLA) was performed. (Sigma Duolink DUO92101-1 kit)**

The samples are initially incubated with target specific antibodies and further incubated with the PLA probes that are conjugated to secondary antibodies, provided as part of the kit. The connector oligos hybridize if the two proteins of interest, are less than 40nm apart, and form a circularized oligo. This is further amplified into rolling circle amplification products through the DUO polymerase and amplification buffer. The resulting products hybridize to red fluorophores, by incubating with oligonucleotide probes attached to red fluorophore. The assay can be imaged using fluorescence microscopy and quantitated.

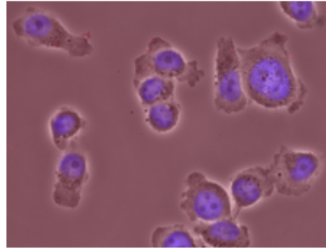
### 3.2.1 Results.

**A**

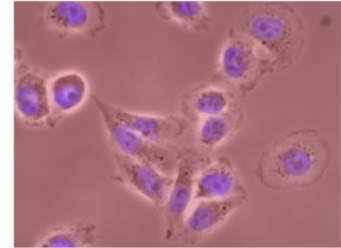
No Primary Antibody



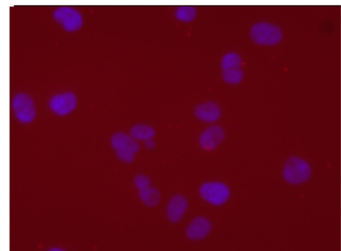
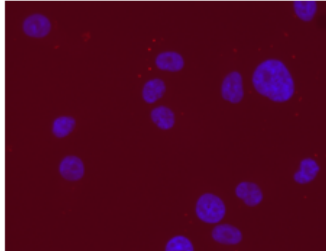
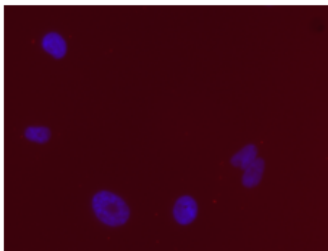
Only  $\alpha$ -CXCR4 Antibody



Only  $\alpha$ -TTC7B antibody



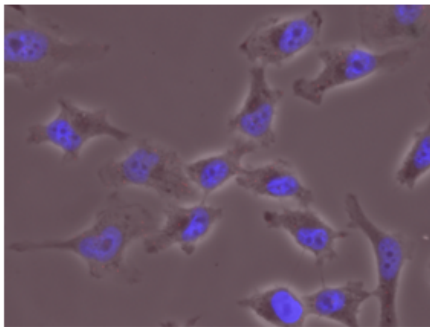
Merged image of phase contrast, DAPI and Red fluorescence



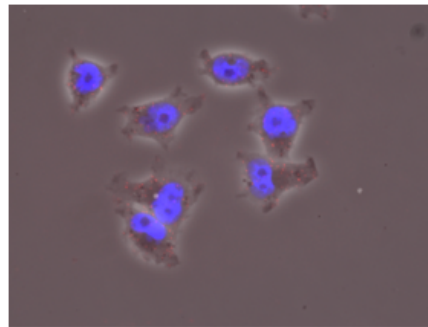
Merged image of DAPI and Red fluorescence

**B**

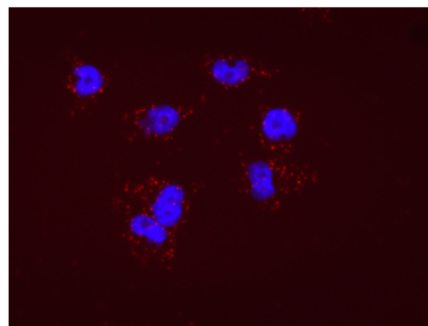
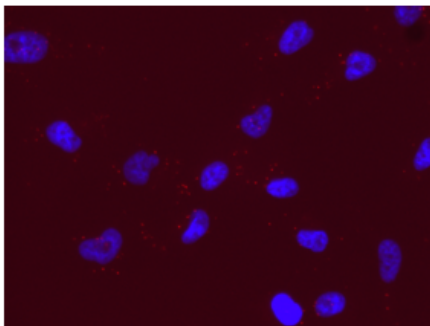
Control



CXCL12



Merged image of phase contrast, DAPI and Red fluorescence



Merged image of DAPI and Red fluorescence

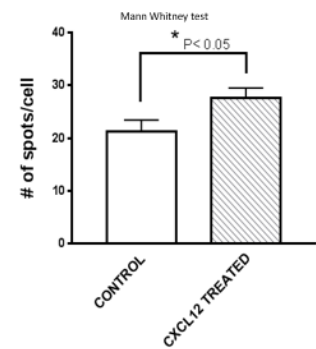


**Figure 16. CXCR4 co-localizes with adaptor protein of PI4KIII $\alpha$  in native PCa cell - under basal, and increases under ligand conditions.**

C4-2B were serum starved and induced with either no ligand or with CXCL12. The cells were fixed with 4%PFA and permeabilized with mild buffer 0.01% tween-20 in PBS. The cells were further treated as per the Sigma Duolink DUO92101-1 kit. CXCR4-mouse and TTC7B-rabbit antibodies were used for primary incubation and observed for the presence of co-localization of CXCR4 and TTC7B. A) in C4-2B cell line, the fluorescence images show very minimal presence of red fluorophores in the control conditions of no primary antibody, only CXCR4, or only TTC7B antibody. B) here we see TTC7B co-localizes with CXCR4 under basal conditions. Under CXCL12 induction the co-localization increases ( $P < 0.05$ ) between CXCR4 and TTC7B.

---

**3.2.2 Discussion.** The proximity assay further confirms the interaction studies of CXCR4 interacting with the PI4KIII $\alpha$  adaptor protein TTC7B. The co-localizations show that the PI4KIII $\alpha$  interactions are indeed facilitated through these adaptor proteins and thus recruited to the PM. These endogenous interactions initially confirmed from cell lysates in native PCa cell lines, are also proved in intact cell lines with this PLA assay.

As with fluorescence interaction techniques there are always limitations to these assays. PLA has non-linear effects, as it is shown to have saturation effects at higher expression levels, so can be considered semi-quantitative when tested for some conditions. So, this might be a factor to consider, and another alternate fluorescence technique would be the fluorescence resonance energy transfer (FRET), as it is shown to have linear effects with protein expression levels. The limitation of FRET is that, it can detect co-localization of 10nm or less only, whereas PLA also detects co-localization more than 10nm and less than 40nm, as in the case with complex assemblies, that may

not necessarily be within 10nm. So, in this study with the super-complex formation of PI4KIII $\alpha$ -TTC7B-EFR3B and their interaction with CXCR4, PLA might after all be a more dependable technique, if we do not simply just rely on quantitation alone.

These results so far suggest that there is a basal constitutive level of interaction of PI4KIII $\alpha$  kinase with the CXCR4 on the membrane, and induction with CXCL12 enhances the interaction, potentially suggesting this interaction is both constitutive and ligand induced.

### **3.3 Determine functional significance of CXCR4 interaction with PI4KIII $\alpha$ using GFP-P4M-**

**SidMx2 biosensor.** To determine the functional significance of the CXCR4- PI4KIII $\alpha$  interaction we used biosensors to detect PI4P production on plasma membranes, which is an indicative of PI4KIII $\alpha$  function. The GFP-P4M-SidMx2 (Addgene #51472) biosensor<sup>155</sup> has been characterized and well established for visualization in membrane studies<sup>46, 155, 156</sup>. PC3, C4-2B and VCaP cells were transfected with this biosensor and the functionality under different conditions were observed in fixed cells and quantitated. The peak max obtained from ImageJ was used, and the areas quantitated are shown within the inset (Fig 17). The quantitation method was adopted from the seminal papers that were used in the characterization of this biosensor, further validating the CXCR4- PI4KIII $\alpha$  crosstalk. Here we observed basal level of PI4P production on the PM of the PCa cells. Upon induction with CXCL12, we observe enhanced GFP localizing to the membrane, indicating increased PI4P production on PM. To determine this PI4P production is specific to PI4KIII $\alpha$  we treat the cells with GSK-F1 which is a PI4KIII $\alpha$  inhibitor. PI4KIII $\alpha$  inhibition in cells leads to decreased GFP-P4M-SidMx2 biosensor accumulation on PM as detected by fluorescence signal originating from GFP suggesting that CXCL12 induced PI4P production is mediated through PI4KIII $\alpha$  in PM. Similarly, we determined CXCL12 induced PI4P is mediated through CXCR4 using small molecule CXCR4 inhibitor, AMD-3100. In the presence of AMD3100 the

PI4P production on PM also reverted back to baseline suggesting CXCL12 induced PI4P production is mediated through CXCR4 on PM. These data demonstrate that the PI4P production is dependent on the induction of the CXCR4- PI4KIII $\alpha$  crosstalk (Fig 17A 17B 17C).

	<u>Cells</u>	<u>Treatment</u>	<u>Expected PI4P levels</u>
1	PC3, C42B, VCaP	Regular media	Baseline
2	PC3, C42B, VCaP	+CXCL12 (200ng/ml)	Increase
3	PC3, C42B, VCaP	+GSK-F1 (2uM) +CXCL12 (200ng/ml)	Decrease
4	PC3, C42B, VCaP	+ AMD3100 (4ug/ml) +CXCL12 (200ng/ml)	Decrease

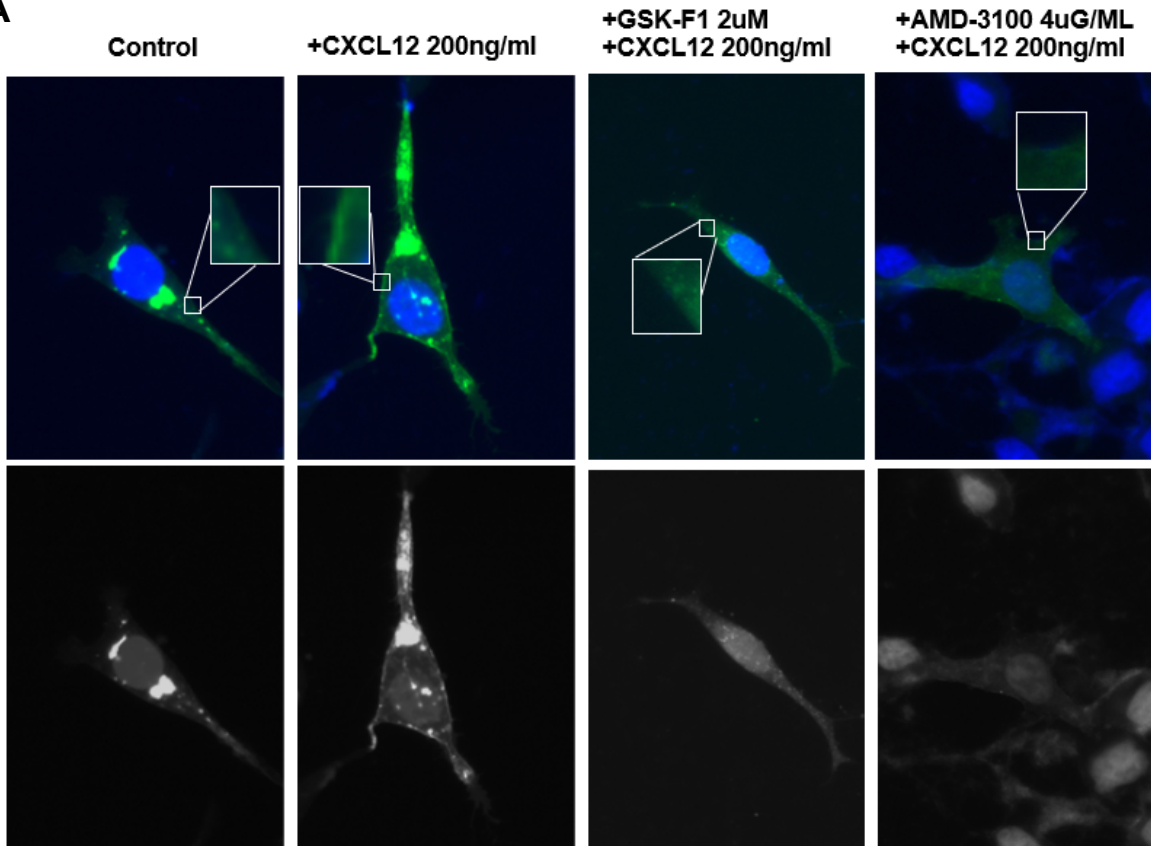
**Table 1. Conditions used with the GFP-P4M-SidMx2 biosensor.**

The table shows the various conditions used for the fluorescence imaging of the PC3 and C4-2B cell lines transfected with the GFP-P4M-SidMx2 biosensor.

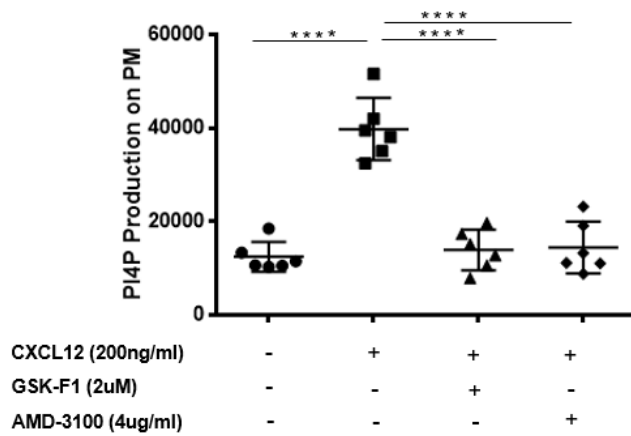
---

## 3.3.1 Results.

A

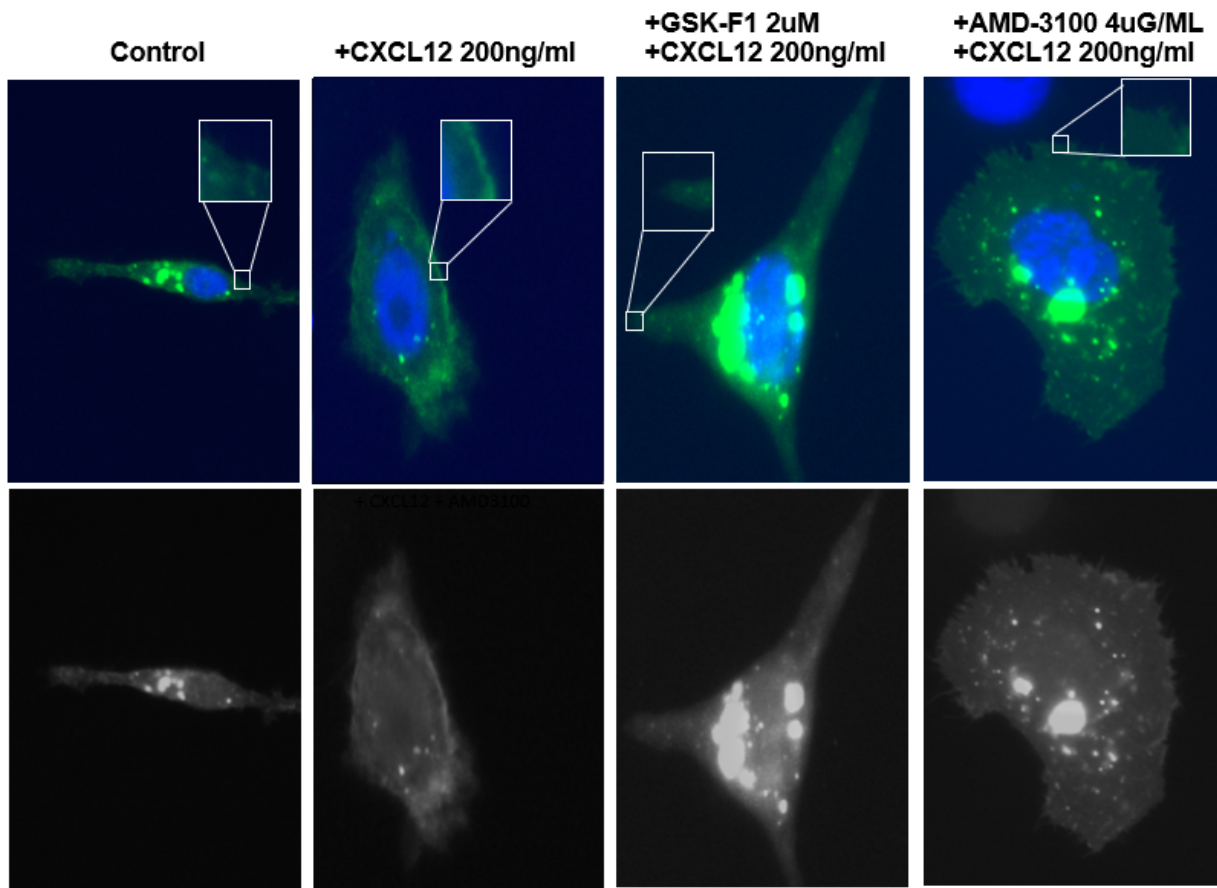


GFP-P4M-SidMX2 transfected C42B

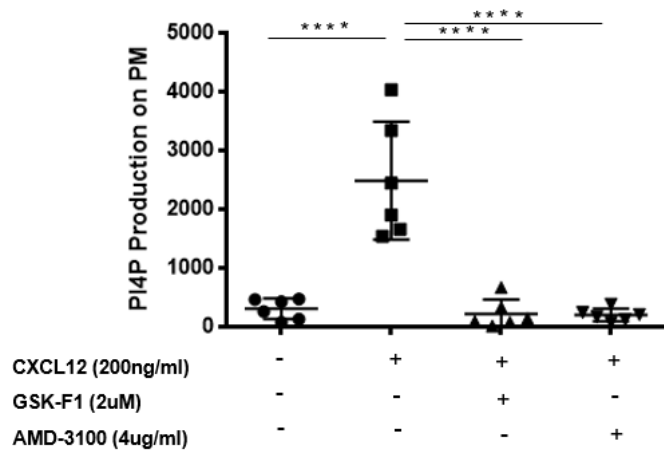


Anova  
followed  
by Tukey  
post-test

B

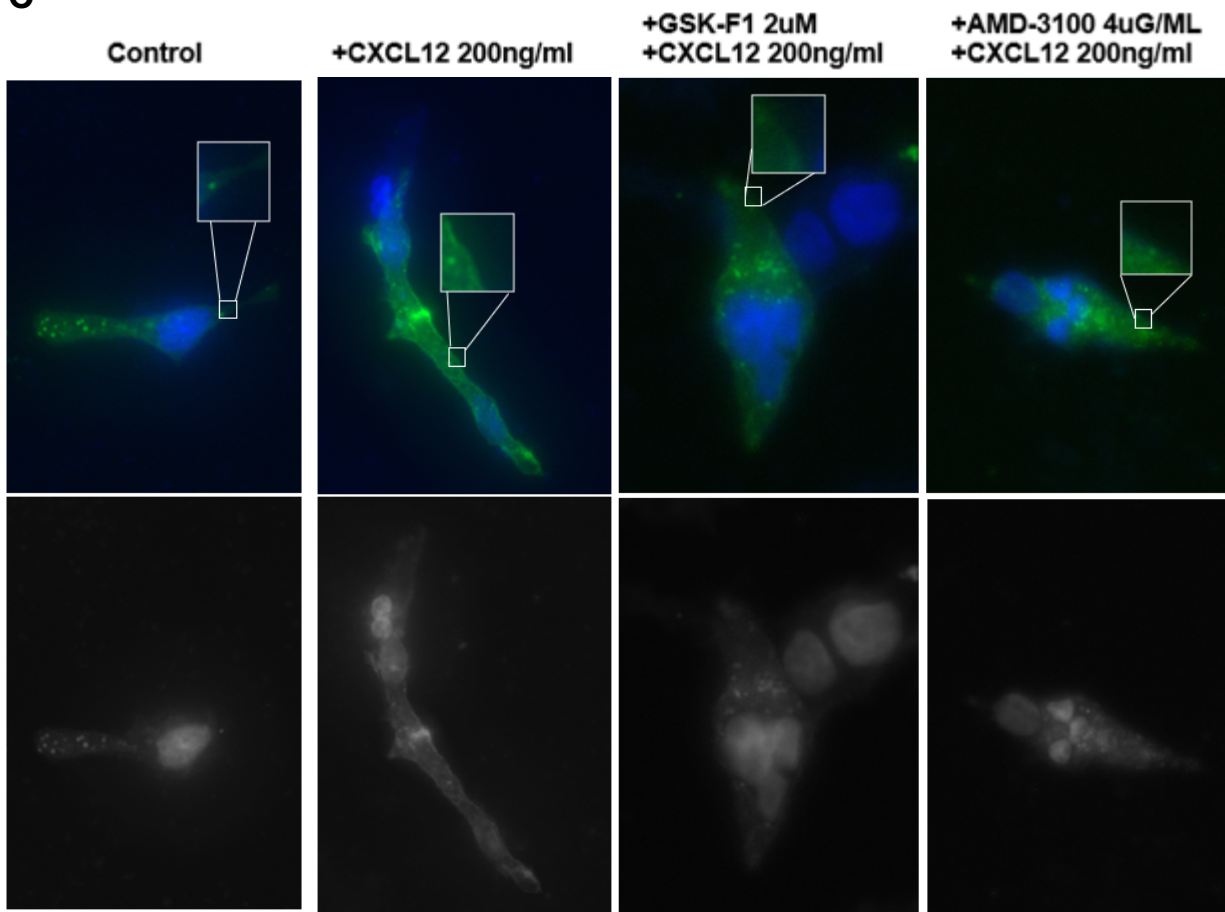


GFP-P4M-SidMX2 transfected PC3

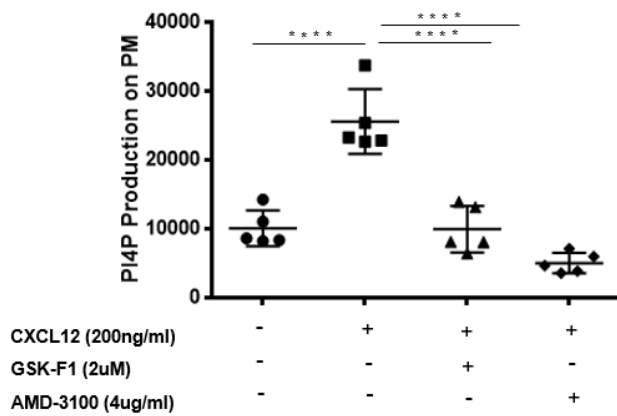


Anova  
followed  
by Tukey  
post-test

C



GFP-P4M-SidMX2 transfected VCaP



Anova  
followed  
by Tukey  
post-test

**Figure 17. PI4P production is induced under CXCL12 ligand conditions in native PCa cell lines.**

A) C4-2B B) PC3 C) VCaP cells were grown on cover-slips and transfected with 2.5ug of GFP-P4M-SidMx2. They were serum starved and treated with the following conditions as seen in Table 1. The cells were fixed with 4%PFA and 0.2% glutaraldehyde and washed with 50mM NH<sub>4</sub>Cl in PBS. Condition 1) there is a basal level of fluorescence as seen in the insets with no ligand induction. 2) there is an increase in fluorescence with CXCL12 induction 3) decrease in fluorescence after treatment with GSK-F1. 4) decrease in fluorescence after treatment with AMD-3100.

---

**3.3.2 Discussion.** We utilized a novel PI4P probe designed by Balla and Hammond<sup>155</sup> that exploits the P4M domain binding capacity to the PI4P lipids, isolated from *L.pneumophila* SidM. This probe is shown to be highly specific and efficient in localizing to PI4P in live cells, compared to previous probes, and is shown to detect in localization in organelles such as PM, Golgi and late endosomes. Especially another advantage of using this probe in our study is that, the probes ability to detect the fluctuating PI4P abundance on the PM has already been validated in this paper, owing its ability to have just the appropriate amount of affinity to PI4P, as opposed to the very high affinity of P4M when intact with SidM in vitro, eliminating background or false positive fluorescence. Nonetheless, this biosensor in conjunction with a PI4P binding protein, may not be able to distinguish different organelles, as it is shown to localize in the three different organelles, unless used with another organelle-specific targeting molecules or proteins. In our case the CXCL12 induction of CXCR4 is widely researched and strictly studied to be on the PM, so we focus on the fluorescence fluctuations on the PM when studying this CXCR4-PI4KIII $\alpha$  crosstalk.

As seen from the immunoprecipitation studies and proximity assays, this fluorescence imaging further validates that, there is a basal constitutive level of interaction of PI4KIII $\alpha$  kinase with the CXCR4 on the membrane. And induction with CXCL12 enhances the interaction, potentially suggesting this interaction is both constitutive and ligand induced., as indicated through PI4P production, sensed using GFP-P4M-SidMx2.

## CHAPTER 4- DETERMINE ROLE OF ADAPTOR PROTEIN TTC7B IN CANCER CELL INVASION

**4.0 Introduction.** As we see the wide implications of CXCR4 and PI4KIII $\alpha$  in various cancers from our background information, here we determined the influence of the adaptor proteins of PI4KIII $\alpha$  in PCa. Briefly, PI4KIII $\alpha$  is recruited to the PM by these evolutionarily conserved adaptor proteins forming a stable complex, which includes EFR3, TTC7 and FAM126. EFR3A has been implicated in KRAS-dependent pancreatic cancer, that shows TCGA datasets with a positive correlation between KRAS and EFR3A mRNA expressions<sup>72</sup>. Also, EFR3A alterations is associated with reduced survival, and increased expression is observed in tumor samples of various pancreatic cancer datasets. This study also demonstrated that EFR3A binds to KRAS through immunoprecipitation and size-exclusion chromatography assays<sup>71</sup>. Here we examine the functional attributes of the adaptor protein TTC7B in invasion using PCa cells.

### **4.1 Determine the impact of adaptor proteins TTC7B in CXCR4-PI4KIII $\alpha$ interaction.**

PI4KIII $\alpha$  regulates chemokine mediated invasion in PCa cells, as studied through native interactions in PC3-RFP parental cell line, along with PC3-CXCR4 and other PCa cells, under different chemokine ligand conditions (Fig 21). We characterize the effect of TTC7B knockdown on invasion using siRNA, and also determine the impact of these knockdowns directly on the interaction of CXCR4 and PI4KIII $\alpha$ . Briefly, from Fig 18, we have established that CXCR4 interacts with PI4KIII $\alpha$  through its adaptor proteins – cytosolic TTC7B. This interaction is enhanced with CXCL12 from its basal level, and is tested in various PCa cell lines, including PC3-CXCR4. Now using the same PC3-CXCR4 cell line, we learn from CXCR4 antibody pull-down assays that siRNA knockdown of TTC7B, almost completely disrupts PI4KIII $\alpha$  interaction with CXCR4 (Fig 18B), while no change in CXCR4 (Fig 18C) is observed. This further validates the

knockdown efficiency of this TTC7B siRNA for use in our invasion assays (Fig 18A). From these data we can confirm that endogenous expressions of TTC7B are required for the CXCR4- PI4KIII $\alpha$  crosstalk.

#### 4.1.1 Results.

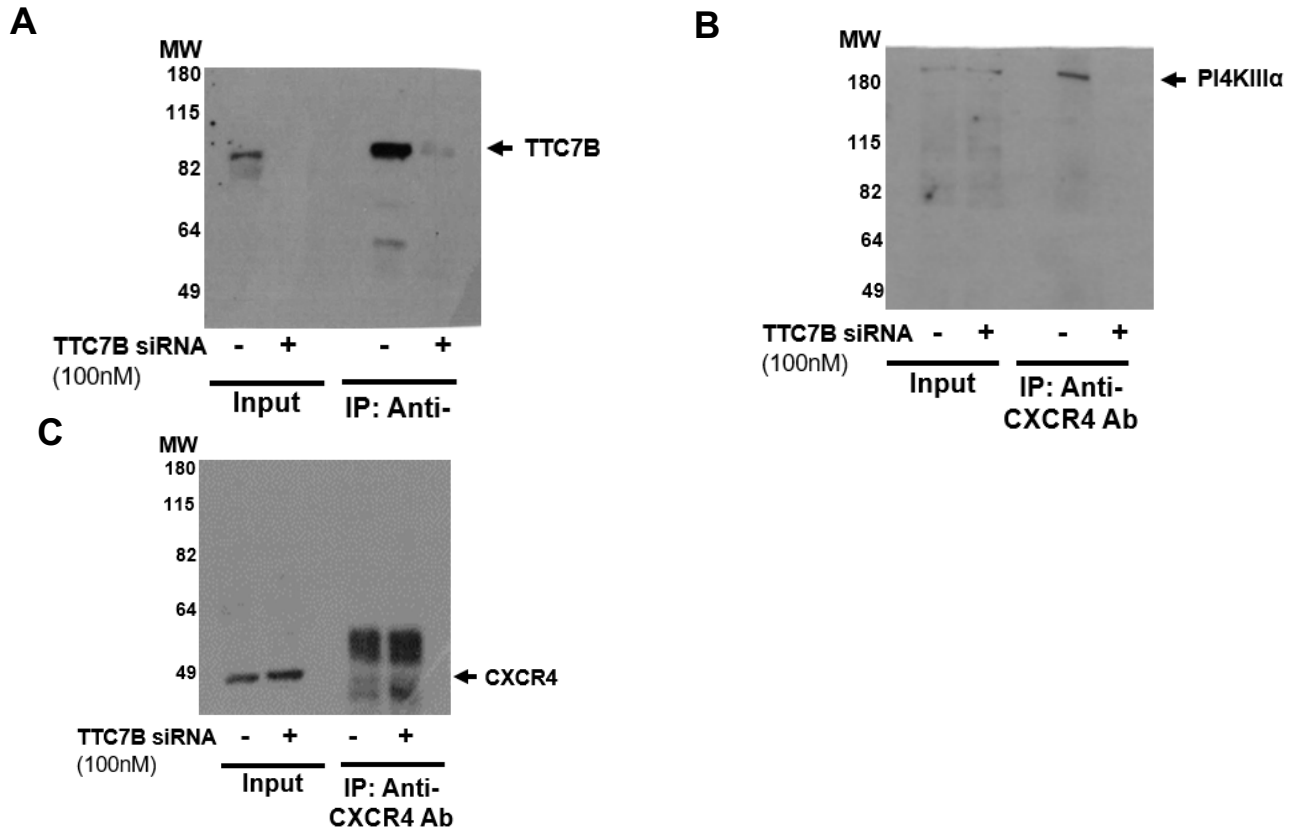


**Figure 18. TTC7B depletion disrupts the CXCR4-PI4KIII $\alpha$  interaction.**

PC3-CXCR4 were transfected with TTC7B siRNA (100nM final) and lysates were immunoprecipitated with 4 $\mu$ g CXCR4 antibody and observed for the presence of A) TTC7B B) PI4KIII $\alpha$ . C) and CXCR4.

**4.2 Determine the depletion of TTC7B on CXCL12 induced cell invasion.** Now that the TTC7B siRNA was validated for efficient knockdown, we used them to observe the effect of their depletion in CXCL12 induced invasion, and determine if their effects closely correlate with that of PI4KIII $\alpha$  knockdown. These chemokine invasion studies were performed with PC3-CXCR4 cell line in Matrigel coated inserts as before and stained with crystal violet. There is an increase in cell invasion in ligand induced conditions of CXCL12 compared to untreated levels in both scrambled (Scr) siRNA and TTC7B siRNA conditions. But within these conditions between Scr and TTC7B siRNA, the knockdown cells have decrease in invasion almost 2-fold in both the basal and ligand conditions, to their respective Scr siRNA levels (Fig 20A-B). This suggests that this adaptor protein TTC7B has important roles in both basal and ligand induced invasion.

Furthermore, we tested if this effect of TTC7B on invasion is restricted to CXCR4-CXCL12 axis or any other chemokine mediated cell invasions as well. So, we also tested another chemoattractant CXCL8, which is known to mediate invasion in PCa. In Scr siRNA between the untreated and CXCL8 conditions, there is an almost 1.5-fold increase in invasion upon ligand stimulation. And when treated with the adaptor protein siRNAs of TTC7B, there is a 3-fold and 2-fold decrease in invasion respectively compared to Scr siRNA, under induced ligand conditions. Between the untreated samples of Scr siRNA and the adaptor protein knockdown, there was not much significant difference (Fig 20A-B).

This data suggests that the adaptor protein of PI4KIII $\alpha$ - TTC7B might be common to other chemokine induced invasions other than CXCL12. TTC7B plays a role in invasion under both basal and ligand induced conditions with stimulants such as CXCL12 and CXCL8, as tested here.

## 4.2.1 Results

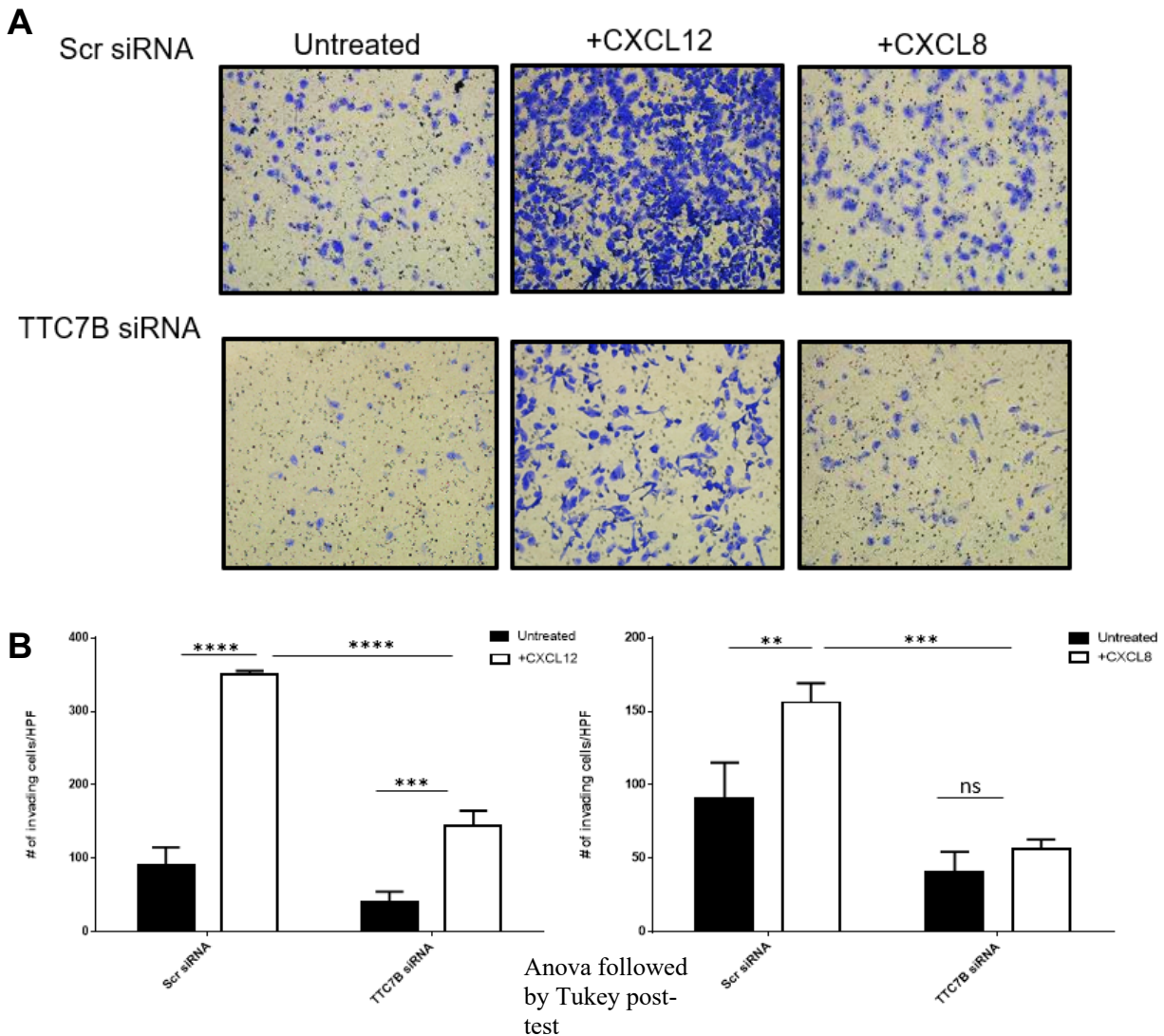


**Figure 19. TTC7B regulates invasion in PCa through CXCL12 and other chemokines, under both basal and ligand induced conditions.**

A) PC3-CXCR4 were transfected with TTC7B siRNA (100nM final) and were serum starved. PC3-CXCR4-TTC7B siRNA cells were plated on Matrigel coated 8uM insert transwells, bottom wells were supplemented with media and appropriate ligand conditions (CXCL12 200ng/ml, CXCL8 50ng/ul). Next day inserts were stained with crystal violet, imaged and quantified. B) Quantitation of the same is shown, with an Anova followed by Tukey post-test ( $P < 0.0001$ ).

## CHAPTER 5- DETERMINE ROLE OF PI4KIII $\alpha$ IN CANCER CELL INVASION AND PROLIFERATION

**5.0 Introduction.** Here we study the influence of this CXCR4-PI4KIII $\alpha$  crosstalk in PCa. Briefly CXCR4-CXCL12 is involved in many facets of cancer progression from proliferation to the various stages of metastasis including invasion, angiogenesis and survival. PCa has a high expression of CXCR4 and CXCL12 contributing to the progression and chemoresistance<sup>88, 97, 102, 115, 116</sup>. CXCR4 expression is also transcriptionally regulated in TMPRSS2-ERG fusion positive PCa, increasing CXCR4 expression and tumorigenicity of these cancers. This axis aids in the PCa metastasizing to the bone, as high CXCR4 expression on the cell surface aids directly to compete for the hematopoietic stem-cell niche in the bone marrow, and in further colonization through intraosseous growth after homing<sup>117, 119, 120</sup>. Also, the CAF cells associated with PCa can secrete CXCL12 and TGF- $\beta$  resulting in tumor growth promoting invasiveness and tumor growth<sup>129, 130</sup>. Likewise, PI4KIII $\alpha$  gene expression is shown to be associated with more invasive and metastatic phenotypes in prostate cancer<sup>1</sup>, as well as chemoresistance<sup>69, 70</sup>.

So, we observe the role of CXCR4-PI4KIII $\alpha$  crosstalk in cancer progression, specifically how it impacts the proliferation and invasion of these PCa cells. For these we perform cell-based assays and hope to elucidate how these proteins play a role in these steps. In this study we further analyze the differential gene expressions and pathways that are involved in control and low expressing PI4KIII $\alpha$  cell-lines that were stably knockdown of PI4KIII $\alpha$ . These were examined and studied through RNA-sequencing analyses and provided further insight into the processes that promote these characteristics of invasion and proliferation.

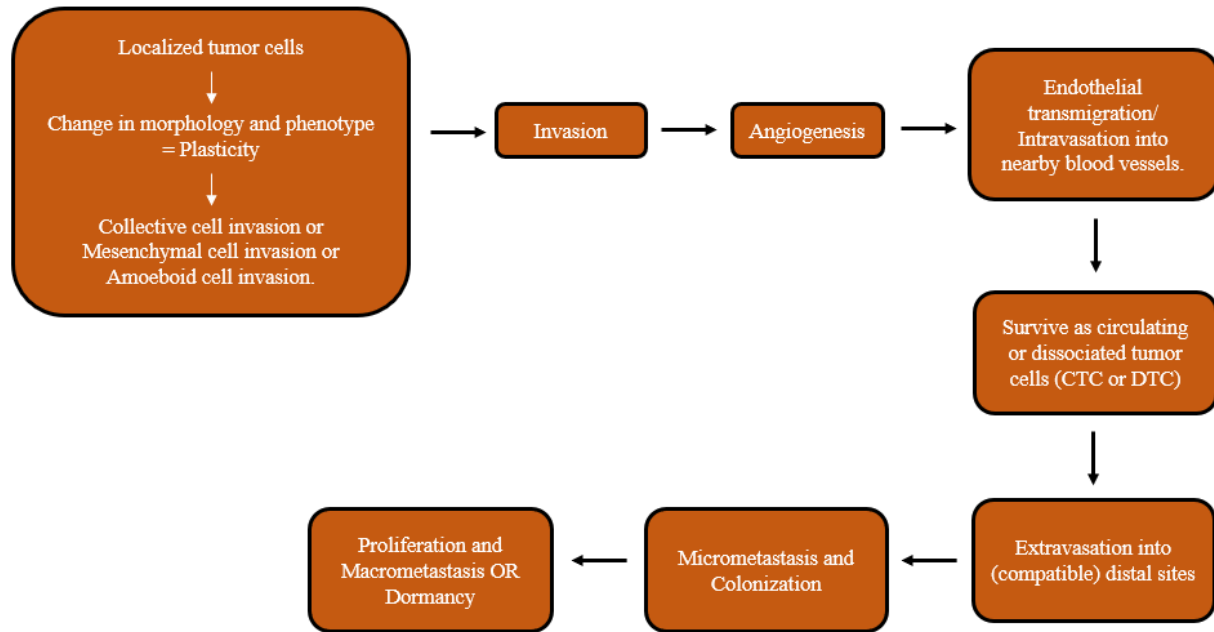


**Figure 20. Overall progression of cancer.**

Representation of progression of a localized tumor into an advanced staged metastasis or into dormancy<sup>2-6</sup>.

**5.1 Impact of PI4KIII $\alpha$  transient knockdown on CXCL12 induced cell invasion.** As observed in (Fig 17), higher PI4P production is seen on the PM with CXCL12 induction. CXCR4-CXCL12 axis plays a role in cancer progression, so the role of PI4KIII $\alpha$  in cellular invasion was studied, as PI4KIII $\alpha$  is shown to interact with CXCR4, and this was performed in prostate cancer cells overexpressing CXCR4. The PI4KIII $\alpha$  effects were studied in PC3-CXCR4 cells by transient knockdown studies using siRNA. Between parental cell line PC3 and CXCR4 overexpressing PC3; the cell invasion was enhanced under both basal and CXCL12 stimulation in PC3-CXCR4 cells. Under basal conditions, PCR-CXCR4 had 3-fold more invasion than PC3-RFP, and with CXCL12 stimulated induction there were 6-fold more invasion (Fig 21A). When PI4KIII $\alpha$  is knockdown, this severely hinders the invasion capacity (Fig 21B), even when CXCR4 is overexpressed. Under

basal conditions, PC3-CXCR4 PI4KIII $\alpha$  siRNA had 3-fold decrease in invasion than PCR-CXCR4 Scr siRNA, and with CXCL12 stimulated induction there were 6-fold less invasion.

Furthermore, we wanted to test if this effect of PI4KIII $\alpha$  on invasion is restricted to CXCR4-CXCL12 axis or many other chemokine mediated cell invasions as well. Other chemoattractants tested were CXCL11, CXCL8 and CCL21, which are known to play some function in mediating invasion in PCa. PI4KIII $\alpha$  knockdown showed a decrease in invasion in both basal and other chemokines induced cell invasion (Fig 21C). This suggests PI4KIII $\alpha$  is common to many chemokines induced invasions under basal and ligand induced conditions. Within the parameters of our cellular invasion protocol, PI4KIII $\alpha$  knockdown, showed no significant effect on cell proliferation.

## 5.1.1 Results.

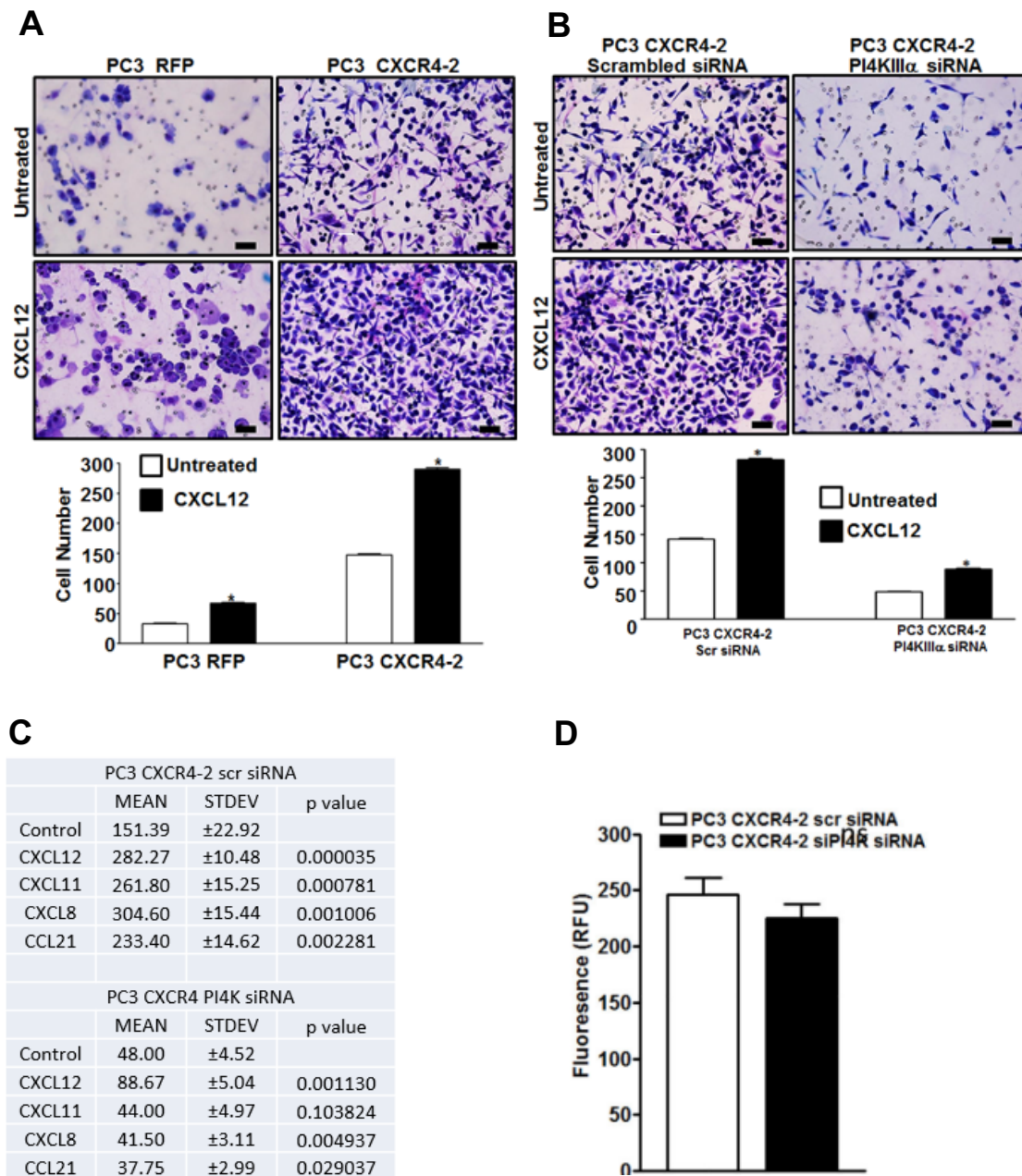


**Figure 21. PI4KIII $\alpha$  regulates invasion in PCa through CXCL12 and other chemokines, under both basal and ligand induced conditions.**

A) PC3-RFP, PC3-CXCR4 were plated on Matrigel coated 8uM insert transwells, bottom wells were supplemented with media and stimulated with CXCL12 for 10 minutes. Next day inserts were stained with crystal violet, imaged and quantified. B) PC3-CXCR4 were transfected with PI4KIII $\alpha$  siRNA (100nM final) and were serum starved. PC3-CXCR4- PI4KIII $\alpha$  siRNA cells were plated on Matrigel coated 8uM insert transwells, bottom wells were supplemented with media and stimulated with CXCL12 for 10 minutes. Next day inserts were stained with crystal violet, imaged and quantified. C) Cell invasion studied under the presence of CXCL12, CXCL11, CXCL8 and CCL21 with Scr and PI4KIII $\alpha$  siRNA cell lines. D) Cell proliferation assay of PC3-CXCR4 cells between Scr and PI4KIII $\alpha$  siRNA transfected cells.

---

**5.2 Characterize PI4KIII $\alpha$  stable knockdown cell models.** To understand the effects of stable knockdown of PI4KIII $\alpha$  on invasion and use them for RNA-seq to identify differential gene expressions (DEG) in cells, C4-2B and PC3-CXCR4 were stably knockdown using lentiviral transduction of PI4KIII $\alpha$  using the following sequences:

A) 27 PI4KIII $\alpha$  shRNA sequence = V2LHS\_170027

Mature antisense: TAGATCTCCAGTTGGCCAC (NM\_058004 : 4660-4678)

B) 30 PI4KIII $\alpha$  shRNA sequence = V3LHS\_352630

Mature antisense: TCACTAACTCCACATCGCT (NM\_058004 : 5516-5534)

(Source: Biobanking and Correlative Sciences Core- Karmanos Cancer Institute)

Both the PI4KA shRNA #27 and #30 show decrease in protein expression compared to Scr. The kinase activity also is highly reduced in the #27 shRNA, showing lesser PI4P production,

using PI4KIII $\alpha$  specific antibody pull-down and analysis by TLC (Fig 22A,B). These characterizations validate the knockdown efficiency of the shRNA used, and hence we used #27 shRNA cells along with Scr for the subsequent experiments.

### 5.2.1 Results.

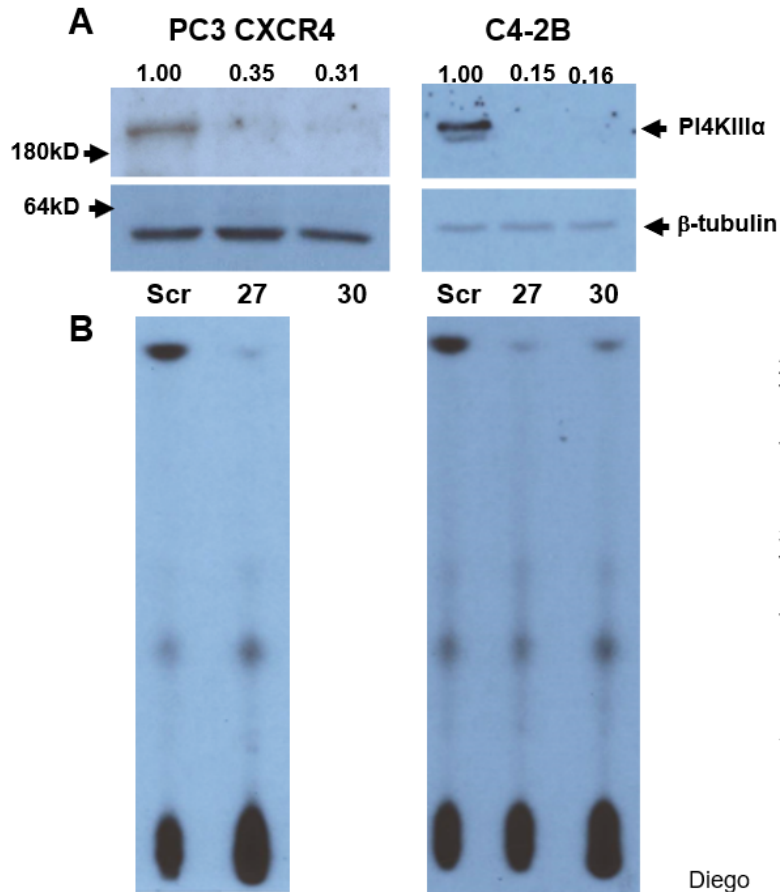


**Figure 22. PI4KIII $\alpha$  knockdown using lentiviral shRNA shows decreased expression and activity.**

Stably knocked down PI4KIII $\alpha$  using the shRNA sequences mentioned characterized in C4-2B and PC3-CXCR4 cells using A) protein expression from Western blots. B) kinase activity through lipid kinase assay.

**5.3 Impact of PI4KIII $\alpha$  stable knockdown on CXCL12 induced cell invasion.** The stable shRNA knockdowns were used to study the effect of PI4KIII $\alpha$  depletion in CXCL12 induced invasion studies. These chemokine invasion studies were performed with PC3-CXCR4 cell line in Matrigel coated inserts as before and stained with crystal violet. There is an increase in cell invasion in CXCL12 induced conditions compared to untreated levels in Scr and PI4KIII $\alpha$  27, 30 shRNA conditions. There is almost a 1.3-2-fold decrease in invasion in PI4KIII $\alpha$  knockdown cells in both the basal and CXCL12 induced conditions (Fig 23). These effects are more in #30 PI4KIII $\alpha$  shRNA and suggests that PI4KIII $\alpha$  has an important role in both basal and ligand induced invasions. We already established through PI4KIII $\alpha$  siRNA studies that PI4KIII $\alpha$  is common to many chemokines induced invasion under both basal and ligand induced conditions (Fig 21). These provide evidence that PI4KIII $\alpha$  is an essential mediator of cell invasion along with its adaptor protein TTC7B (Fig 19).

### 5.3.1 Results.

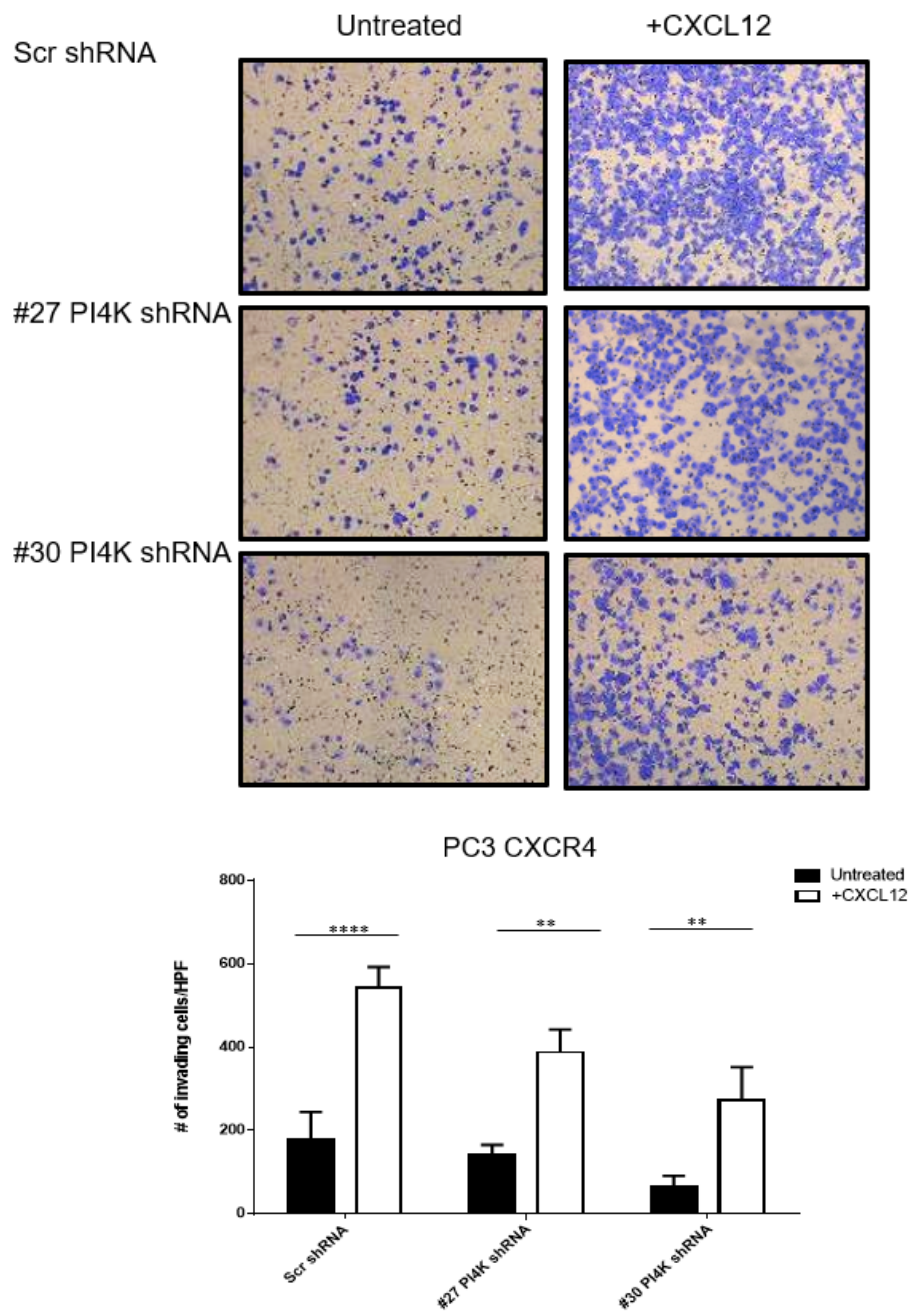


**Figure 23. PI4KIII $\alpha$  regulates invasion in PCa through CXCL12, under basal ligand induced conditions.**

A) Stable knockdown of PI4KIII $\alpha$  in PC3-CXCR4 were serum starved and were plated on Matrigel coated 8uM insert transwells, bottom wells were supplemented with media and appropriate ligand

conditions (CXCL12 200ng/ml). Next day inserts were stained with crystal violet, imaged and quantified. B) Quantitation of the same is shown, with an Anova followed by Tukey post-test ( $P < 0.05$ ).

---

**5.4 Perform RNA-Sequencing analysis to determine differential gene expressions and pathways contributing to PI4KIII $\alpha$  function in PCa cell.** The cell-lines used for the following analysis were again C4-2B (androgen insensitive, androgen receptor positive, high tumorigenicity, osteoblastic, LnCaP derived), and PC3-CXCR4 (Parental PC3: androgen insensitive, androgen receptor negative, high tumorigenicity, osteolytic), with Scr and stable PI4KIII $\alpha$  knockdown #27 shRNA lines. The DEG were analyzed using both Advaita's iPathway guide and the Gene Set Enrichment Analysis (GSEA) software using the Molecular Signatures Database (MSigDB).

When we knockdown PI4KIII $\alpha$  and TTC7B we see a decrease in invasion (Fig 19, 21B, 23). Here we used #27 PI4KA stable knockdown cells and analyzed pathways involved in this invasive phenotype using the GSEA software. This showed reciprocal enrichment of many pathways involved in cell-proliferation such as E2F targets, P53 pathways, PI3K-AKT-MTOR signaling, Il6-JAK-STAT3 and MTORC1 signaling between the C4-2B and PC3-CXCR4 cell-lines in the Scr compared to PI4KIII $\alpha$  knockdown cell-lines (Table 2). Interestingly C4-2B cell-lines being androgen receptor positive, and androgen-insensitive, showed significant upregulation and reciprocal enrichment of androgen response ( $p=0$ , NES=-2.18) signaling in the Scr compared to PI4KIII $\alpha$  knockdown cell-lines. Among the leading-edge pathway analysis enriched between PI4KIII $\alpha$  knockdown cell-lines vs Scr, the top-most significant hallmark pathways are as seen in the reciprocal enrichment plots, i.e. enriched in Scr and as highlighted in yellow in the gene set table (Table 2) (FDR  $q\text{-val} < 0.05$  and  $P < 0.05$ ). We also validated our RNA-seq reads through qPCR

for genes that were expressed as the top 50 genes for each phenotype on the heatmap in PC3-CXCR4 cell-line (Fig 27) (Fig 28).

To study the overlap between pathways of the cells used for our RNA-seq and publicly available data set, we performed a GSEA analysis. For this we utilized the TCGA Firehose legacy database with n=498 for prostate adenocarcinoma, and categorized the dataset into high PI4KIII $\alpha$  expressing and low PI4KIII $\alpha$  expressing cohort to represent the PI4KIII $\alpha$  knockdown cell-line. (Table 5) We found some overlap of pathways enriched between the Scr of both C4-2B and PC3-CXCR4, along with the high PI4KIII $\alpha$  expressing cohort, and this includes E2F targets, G2M checkpoints, mitotic spindle and protein secretion.

We also performed an ingenuity pathway analysis using Advaita Bioinformatics software to validate our analysis of different expressed genes and pathways. (Fig 29) (Fig 30) Comparison between PI4KIII $\alpha$  shRNA and Scr in C4-2B and PC3-CXCR4 show 562 and 222 genes significantly differentially expressed with a log fold change of 0.6 and above and corrected P value of  $\leq 0.05$ . Both the cell-lines show the KEGG pathway map of “neuroactive ligand-receptor interaction” as the most significantly impacted pathway in the PI4KIII $\alpha$  shRNA cell-lines. The gene ontology also lists processes and functions that were significantly impacted in these knockdown cell-lines (Fig 29 iii iv) and v)), (Fig 30 iii iv) and v)). A meta-analysis between these cell-lines also revealed several altered pathways and functions that were mutually altered between these cell-lines. Interestingly many of these biological processes such as ‘cell-surface receptor signaling pathway’, ‘regulation of locomotion’, ‘regulation of cell migration’ and ‘cell population proliferation’; as well as molecular functions such as ‘cytokine activity’ and ‘G protein-coupled receptor binding’ (highlighted in yellow) (Fig 31) all show significantly altered between PI4KIII $\alpha$

shRNA and Scr cell-lines, suggesting that PI4KIII $\alpha$  activation in cancer cells contributes to above described biological processes and molecular functions.

### 5.5.1 Results.

**A**

	GS follow link to MSigDB	GS DETAILS	SIZE	ES	NES	NOM p-val	FDR q-val	FWER p-val	RANK AT MAX	LEADING EDGE
1	<a href="#">HALLMARK_MYC_TARGETS_V1</a>	<a href="#">Details ...</a>	200	-0.64	-2.80	0.000	0.000	0.000	8450	tags=91%, list=32%, signal=132%
2	<a href="#">HALLMARK_E2F_TARGETS</a>	<a href="#">Details ...</a>	200	-0.59	-2.63	0.000	0.000	0.000	8330	tags=81%, list=32%, signal=118%
3	<a href="#">HALLMARK_G2M_CHECKPOINT</a>	<a href="#">Details ...</a>	200	-0.56	-2.44	0.000	0.000	0.000	9163	tags=79%, list=35%, signal=120%
4	<a href="#">HALLMARK_OXIDATIVE_PHOSPHORYLATION</a>	<a href="#">Details ...</a>	200	-0.55	-2.43	0.000	0.000	0.000	8223	tags=71%, list=31%, signal=103%
5	<a href="#">HALLMARK_MYC_TARGETS_V2</a>	<a href="#">Details ...</a>	58	-0.67	-2.42	0.000	0.000	0.000	6137	tags=83%, list=23%, signal=108%
6	<a href="#">HALLMARK_UNFOLDED_PROTEIN_RESPONSE</a>	<a href="#">Details ...</a>	113	-0.57	-2.37	0.000	0.000	0.000	10298	tags=87%, list=39%, signal=142%
7	<a href="#">HALLMARK_MTORC1_SIGNALING</a>	<a href="#">Details ...</a>	200	-0.50	-2.19	0.000	0.000	0.000	7980	tags=66%, list=30%, signal=93%
8	<a href="#">HALLMARK_ANDROGEN_RESPONSE</a>	<a href="#">Details ...</a>	100	-0.55	-2.18	0.000	0.000	0.000	7320	tags=65%, list=28%, signal=90%
9	<a href="#">HALLMARK_PROTEIN_SECRETION</a>	<a href="#">Details ...</a>	96	-0.53	-2.10	0.000	0.000	0.000	10275	tags=79%, list=39%, signal=129%
10	<a href="#">HALLMARK_UV_RESPONSE_UP</a>	<a href="#">Details ...</a>	158	-0.48	-2.05	0.000	0.000	0.000	7632	tags=60%, list=29%, signal=84%
11	<a href="#">HALLMARK_MITOTIC_SPINDLE</a>	<a href="#">Details ...</a>	198	-0.47	-2.05	0.000	0.000	0.000	11263	tags=80%, list=43%, signal=139%
12	<a href="#">HALLMARK_TNFA_SIGNALING_VIA_NFKB</a>	<a href="#">Details ...</a>	200	-0.44	-1.95	0.000	0.000	0.000	6663	tags=47%, list=25%, signal=62%
13	<a href="#">HALLMARK_DNA_REPAIR</a>	<a href="#">Details ...</a>	150	-0.46	-1.94	0.000	0.000	0.000	11558	tags=80%, list=44%, signal=142%
14	<a href="#">HALLMARK_P53_PATHWAY</a>	<a href="#">Details ...</a>	200	-0.43	-1.93	0.000	0.000	0.000	9832	tags=60%, list=37%, signal=94%
15	<a href="#">HALLMARK_REACTIVE_OXYGEN_SPECIES_PATHWAY</a>	<a href="#">Details ...</a>	49	-0.53	-1.88	0.000	0.000	0.001	8293	tags=73%, list=32%, signal=107%
16	<a href="#">HALLMARK_ADIPOGENESIS</a>	<a href="#">Details ...</a>	199	-0.42	-1.86	0.000	0.000	0.002	7425	tags=51%, list=28%, signal=71%
17	<a href="#">HALLMARK_IL6_JAK_STAT3_SIGNALING</a>	<a href="#">Details ...</a>	87	-0.47	-1.80	0.000	0.000	0.006	7034	tags=43%, list=27%, signal=58%
18	<a href="#">HALLMARK_CHOLESTEROL_HOMEOSTASIS</a>	<a href="#">Details ...</a>	74	-0.48	-1.80	0.000	0.000	0.006	8037	tags=58%, list=31%, signal=83%
19	<a href="#">HALLMARK_PI3K_AKT_MTOR_SIGNALING</a>	<a href="#">Details ...</a>	105	-0.45	-1.79	0.000	0.000	0.007	7222	tags=60%, list=27%, signal=82%
20	<a href="#">HALLMARK_APOPTOSIS</a>	<a href="#">Details ...</a>	161	-0.40	-1.70	0.000	0.002	0.029	8083	tags=53%, list=31%, signal=77%
21	<a href="#">HALLMARK_ESTROGEN_RESPONSE_EARLY</a>	<a href="#">Details ...</a>	200	-0.38	-1.70	0.000	0.002	0.029	6810	tags=46%, list=26%, signal=61%

**B**

	GS follow link to MSigDB	GS DETAILS	SIZE	ES	NES	NOM p-val	FDR q-val	FWER p-val	RANK AT MAX	LEADING EDGE
1	<a href="#">HALLMARK_OXIDATIVE_PHOSPHORYLATION</a>	<a href="#">Details ...</a>	200	-0.54	-2.08	0.000	0.000	0.000	10382	tags=81%, list=39%, signal=132%
2	<a href="#">HALLMARK_G2M_CHECKPOINT</a>	<a href="#">Details ...</a>	200	-0.48	-1.91	0.000	0.000	0.000	7841	tags=49%, list=30%, signal=69%
3	<a href="#">HALLMARK_MYC_TARGETS_V1</a>	<a href="#">Details ...</a>	200	-0.48	-1.87	0.000	0.000	0.001	12687	tags=86%, list=48%, signal=164%
4	<a href="#">HALLMARK_E2F_TARGETS</a>	<a href="#">Details ...</a>	200	-0.47	-1.85	0.000	0.001	0.002	7943	tags=49%, list=30%, signal=69%
5	<a href="#">HALLMARK_DNA_REPAIR</a>	<a href="#">Details ...</a>	150	-0.48	-1.82	0.000	0.000	0.002	11999	tags=77%, list=46%, signal=141%
6	<a href="#">HALLMARK_MITOTIC_SPINDLE</a>	<a href="#">Details ...</a>	198	-0.45	-1.76	0.000	0.001	0.005	11906	tags=73%, list=45%, signal=133%
7	<a href="#">HALLMARK_ADIPOGENESIS</a>	<a href="#">Details ...</a>	199	-0.44	-1.72	0.000	0.002	0.011	9780	tags=62%, list=37%, signal=98%
8	<a href="#">HALLMARK_FATTY_ACID_METABOLISM</a>	<a href="#">Details ...</a>	158	-0.41	-1.56	0.000	0.015	0.096	10983	tags=67%, list=42%, signal=115%
9	<a href="#">HALLMARK_PROTEIN_SECRETION</a>	<a href="#">Details ...</a>	96	-0.43	-1.55	0.007	0.016	0.118	10153	tags=65%, list=39%, signal=105%
10	<a href="#">HALLMARK_P53_PATHWAY</a>	<a href="#">Details ...</a>	200	-0.38	-1.50	0.007	0.025	0.200	8279	tags=51%, list=31%, signal=73%
11	<a href="#">HALLMARK_CHOLESTEROL_HOMEOSTASIS</a>	<a href="#">Details ...</a>	74	-0.42	-1.41	0.027	0.058	0.425	8159	tags=49%, list=31%, signal=70%
12	<a href="#">HALLMARK_ALLOGRAFT_REJECTION</a>	<a href="#">Details ...</a>	200	-0.35	-1.39	0.011	0.068	0.527	5688	tags=34%, list=22%, signal=43%
13	<a href="#">HALLMARK_ESTROGEN_RESPONSE_LATE</a>	<a href="#">Details ...</a>	200	-0.35	-1.39	0.017	0.064	0.532	7999	tags=44%, list=30%, signal=62%
14	<a href="#">HALLMARK_BILE_ACID_METABOLISM</a>	<a href="#">Details ...</a>	112	-0.35	-1.30	0.056	0.150	0.853	8795	tags=49%, list=33%, signal=73%
15	<a href="#">HALLMARK_UNFOLDED_PROTEIN_RESPONSE</a>	<a href="#">Details ...</a>	113	-0.36	-1.29	0.074	0.154	0.885	11858	tags=57%, list=45%, signal=103%
16	<a href="#">HALLMARK_MTORC1_SIGNALING</a>	<a href="#">Details ...</a>	200	-0.32	-1.28	0.041	0.155	0.902	11296	tags=61%, list=43%, signal=106%
17	<a href="#">HALLMARK_SPERMATOGENESIS</a>	<a href="#">Details ...</a>	135	-0.34	-1.28	0.053	0.150	0.910	6787	tags=40%, list=26%, signal=54%
18	<a href="#">HALLMARK_APOPTOSIS</a>	<a href="#">Details ...</a>	161	-0.34	-1.28	0.052	0.143	0.911	9326	tags=56%, list=35%, signal=86%
19	<a href="#">HALLMARK_REACTIVE_OXYGEN_SPECIES_PATHWAY</a>	<a href="#">Details ...</a>	49	-0.40	-1.26	0.123	0.162	0.949	8530	tags=53%, list=32%, signal=78%
20	<a href="#">HALLMARK_HEME_METABOLISM</a>	<a href="#">Details ...</a>	198	-0.32	-1.25	0.050	0.160	0.958	9574	tags=51%, list=36%, signal=79%
21	<a href="#">HALLMARK_PEROXISOME</a>	<a href="#">Details ...</a>	104	-0.35	-1.23	0.108	0.183	0.976	9795	tags=54%, list=37%, signal=85%

**Table 2. Gene sets enriched in phenotype scrambled compared to PI4KA knockdown cell-lines.**

In A) C4-2B B) PC3-CXCR4. Gene sets reciprocally enriched in these endogenous levels of PI4KIII $\alpha$  expressing cell-lines when compared to PI4KIII $\alpha$  knockdown show enrichment in pathways involved in cell-proliferation ((FDR q-val < 0.05 and P<0.05).

H: hallmark gene sets (GSEA- Molecular signatures database)	C42B Scr shRNA			PC3 CXCR4-OX Scr shRNA		
	NES	NOM p-val	FDR q-val	NES	NOM p-val	FDR q-val
Myc-Targets V1	-2.80	0.000	0.000	-1.87	0.000	0.000
E2F Targets	-2.63	0.000	0.000	-1.85	0.000	0.000
G2M Checkpoints	-2.44	0.000	0.000	-1.91	0.000	0.000
Oxidative Phosphorylation	-2.43	0.000	0.000	-2.08	0.000	0.000
Unfolded Protein Response	-2.31	0.000	0.000	-1.29	0.074	0.154
MTROC1 Signaling	-2.19	0.000	0.000	-1.28	0.041	0.155
Androgen Response	-2.18	0.000	0.000	-1.08	0.306	0.458
Mitotic Spindle	-2.05	0.000	0.000	-1.76	0.000	0.001
DNA Repair	-1.94	0.000	0.000	-1.82	0.000	0.000
P53 Pathway	-1.93	0.000	0.000	-1.50	0.007	0.025
Reactive Oxygen Species Pathway	-1.88	0.000	0.000	-1.26	0.123	0.102
Adipogenesis	-1.86	0.000	0.000	-1.72	0.002	0.000
Cholesterol Homeostasis	-1.80	0.000	0.000	-1.41	0.027	0.058
Apoptosis	-1.70	0.000	0.000	-1.28	0.052	0.143

**Table 3. Common Gene sets enriched in phenotype scrambled compared to PI4KA knockdown cell-lines.**

Gene sets reciprocally enriched in these endogenous levels of PI4KIII $\alpha$  expressing cell-lines when compared to PI4KIII $\alpha$  knockdown ((FDR q-val < 0.05 and P<0.05 is considered significant), as analyzed by the Hallmark Gene set collection of MSigDB.

H: hallmark gene sets (GSEA- Molecular signatures database)	C42B PI4K shRNA			PC3 CXCR4-OX PI4K shRNA		
	NES	NOM p-val	FDR q-val	NES	NOM p-val	FDR q-val
HALLMARK_ANGIOGENESIS	1.26	0.152	0.136	1.83	0.003	0.003
HALLMARK_COAGULATION				1.42	0.010	0.094
HALLMARK_KRAS_SIGNALING_DN	1.46	0.004	0.048	1.41	0.000	0.066
HALLMARK_EPITHELIAL_MESENCHYMAL_TRANSITION				1.24	0.058	0.221
HALLMARK_COMPLEMENT				1.18	0.076	0.287
HALLMARK_MYOGENESIS				0.92	0.744	1.000
HALLMARK_HYPOXIA				0.92	0.730	1.000
HALLMARK_TNFA_SIGNALING_VIA_NFKB				0.90	0.858	1.000
HALLMARK_WNT_BETA_CATENIN_SIGNALING				0.86	0.719	1.000
HALLMARK_APICAL_JUNCTION				0.81	0.970	1.000
HALLMARK_UV_RESPONSE_DN				0.75	0.990	0.965
HALLMARK_PANCREAS_BETA_CELLS	1.56	0.030	0.041			
HALLMARK_NOTCH_SIGNALING	0.97	0.498	0.638			
HALLMARK_SPERMATOGENESIS	0.80	0.921	0.907			
HALLMARK_IL6_JAK_STAT3_SIGNALING						

 = Molecular signatures of significance in each PI4K KD cell lines.

**Table 4. Common Gene sets enriched in phenotype PI4KA knockdown compared to scrambled cell-lines.**

Gene sets enriched in these PI4KIII $\alpha$  knockdown when compared to endogenous levels of PI4KIII $\alpha$  expressing cell-lines ((FDR q-val < 0.05 and P<0.05 is considered significant), as analyzed by the Hallmark Gene set collection of MSigDB.

---

H: hallmark gene sets (GSEA- Molecular signatures database)	C42B Scr shRNA			TCGA Firehose PI4KA high cohort		
	NES	NOM p-val	FDR q-val	NES	NOM p-val	FDR q-val
E2F targets	-2.63	0.000	0.000	0.96	0.606	0.773
Mitotic Spindle	-2.05	0.000	0.000	2.35	0.000	0.000
Protein Secretion	-2.10	0.000	0.000	2.08	0.000	0.000
G2M checkpoint	-2.44	0.000	0.000	1.67	0.000	0.002
Androgen Response	-2.18	0.000	0.000	1.90	0.000	0.000
PI3K-AKT-MTOR signaling	-1.79	0.000	0.000	0.94	0.598	0.717

H: hallmark gene sets (GSEA- Molecular signatures database)	PC3-CXCR4 Scr shRNA			TCGA Firehose PI4KA high cohort		
	NES	NOM p-val	FDR q-val	NES	NOM p-val	FDR q-val
Mitotic Spindle	-1.76	0.000	0.001	2.35	0.000	0.000
Protein Secretion	-1.55	0.007	0.016	2.08	0.000	0.000
G2M checkpoint	-1.91	0.000	0.000	1.67	0.000	0.002
E2F targets	-1.85	0.000	0.001	0.96	0.606	0.773

**Table 5. Common Gene sets enriched between phenotype scrambled and high PI4KIII $\alpha$  expressing TCGA-Firehose Legacy prostate adenocarcinoma cohort (total n=498).**

(FDR q-val < 0.05 and P<0.05 is considered significant), as analyzed by the Hallmark Gene set collection of MSigDB.

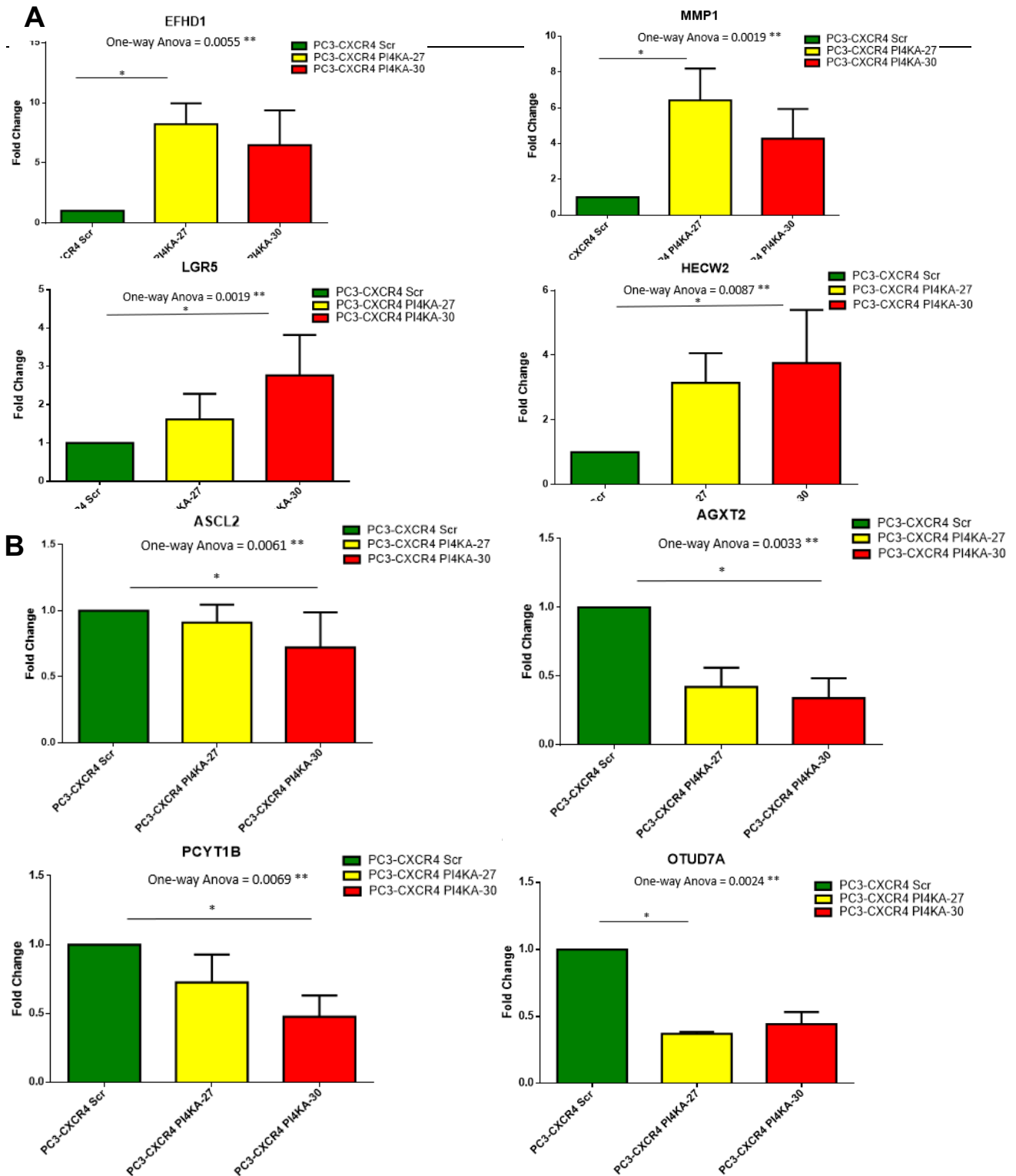
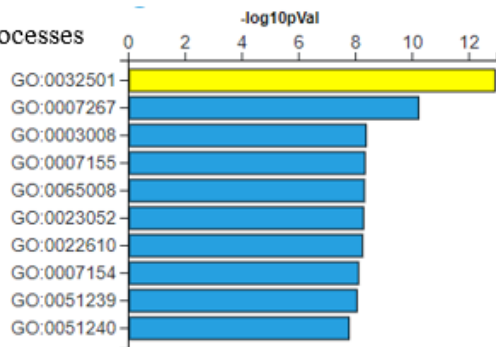


**Figure 24. Gene expression validation of RNA-seq analysis of PC3-CXCR4 cell lines.**

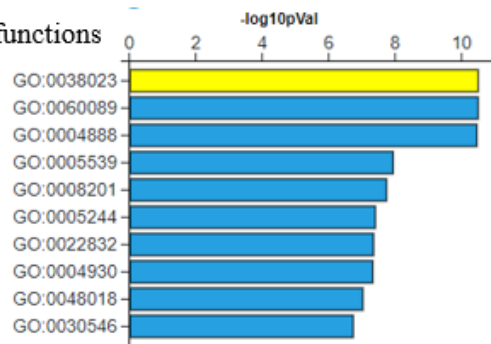
A) Genes that are expressed high in PI4K knockdown cell-lines. B) Genes that are expressed low in in PI4K knockdown cell-lines.

## Biological processes



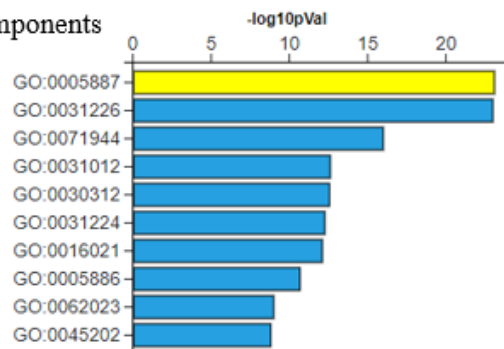
(c) Advaita Corporation 2022

## v) Molecular functions



(c) Advaita Corporation 2022

## w) Cellular components



(c) Advaita Corporation 2022

Name	# genes (DE/ALL)	p-value
multicellular organismal process	227 / 4808	1.300e-13
cell-cell signaling	76 / 1090	6.400e-11
system process	75 / 1173	4.500e-9
cell adhesion	66 / 975	4.900e-9
regulation of biological quality	137 / 2713	5.200e-9
signaling	188 / 4128	5.600e-9
biological adhesion	66 / 980	6.000e-9
cell communication	189 / 4176	8.300e-9
regulation of multicellular organismal process	101 / 1812	9.500e-9
positive regulation of multicellular organismal process	64 / 963	1.800e-8

Name	# genes (DE/ALL)	p-value
signaling receptor activity	54 / 627	3.300e-11
molecular transducer activity	54 / 627	3.300e-11
transmembrane signaling receptor activity	46 / 482	3.600e-11
glycosaminoglycan binding	20 / 135	1.200e-8
heparin binding	17 / 100	1.900e-8
voltage-gated ion channel activity	18 / 118	4.100e-8
voltage-gated channel activity	18 / 119	4.700e-8
G-protein-coupled receptor activity	23 / 190	4.900e-8
receptor ligand activity	22 / 182	9.800e-8
signaling receptor activator activity	22 / 189	1.900e-7

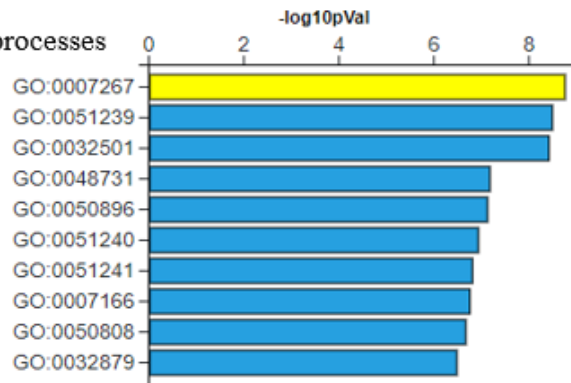
Name	# genes (DE/ALL)	p-value
integral component of plasma membrane	94 / 920	8.800e-24
intrinsic component of plasma membrane	97 / 976	1.100e-23
cell periphery	201 / 3678	1.100e-16
extracellular matrix	41 / 333	2.700e-13
external encapsulating structure	41 / 334	3.000e-13
intrinsic component of membrane	175 / 3280	6.000e-13
integral component of membrane	171 / 3189	8.800e-13
plasma membrane	174 / 3387	2.500e-11
collagen-containing extracellular matrix	30 / 252	1.100e-9
synapse	69 / 988	1.700e-9

**Figure 25. Pathway analysis of genes differentially expressed in PI4KIII $\alpha$  shRNA vs scrambled C4-2B cell-lines.**

i) Analysis of DEG show GO biological processes significantly impacted in the PI4KIII $\alpha$  shRNA C4-2B cell-line, with “cell-cell signaling” significantly impacted ii) Analysis of DEG show GO molecular functions significantly impacted in the PI4KIII $\alpha$  shRNA C4-2B cell-line, with “signaling receptor activity” significantly impacted iii) Analysis of DEG show GO cellular components significantly impacted in the PI4KIII $\alpha$  shRNA C4-2B cell-line, with “integral component of plasma membrane” significantly impacted. All processes and functions of interest to us is highlighted in yellow.

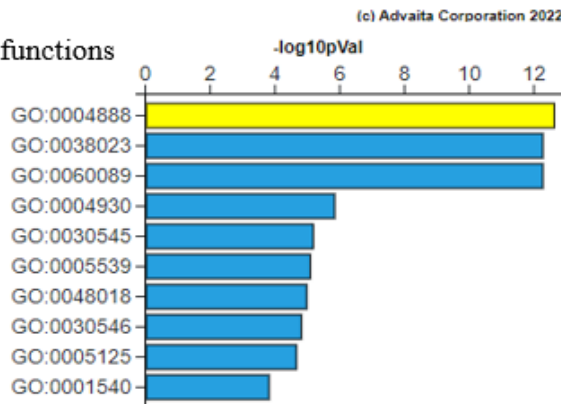
---

## Biological processes



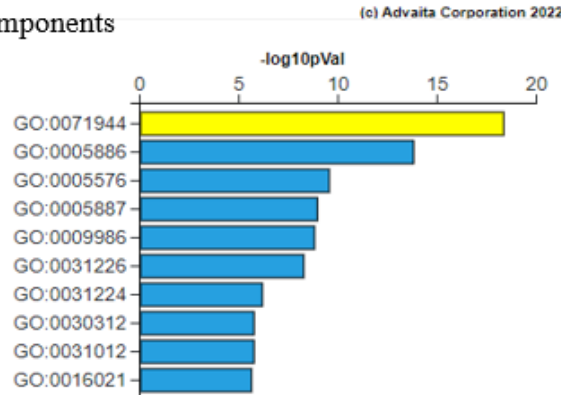
Name	# genes (DE/ALL)	p-value
cell-cell signaling	42 / 984	1.800e-9
regulation of multicellular organismal process	57 / 1649	3.300e-9
multicellular organismal process	108 / 4372	3.900e-9
system development	83 / 3128	6.800e-8
response to stimulus	120 / 5337	7.700e-8
positive regulation of multicellular organismal process	36 / 888	1.200e-7
negative regulation of multicellular organismal process	29 / 625	1.600e-7
cell surface receptor signaling pathway	54 / 1700	1.800e-7
synapse organization	19 / 296	2.200e-7
regulation of localization	56 / 1829	3.400e-7

## Molecular functions



Name	# genes (DE/ALL)	p-value
transmembrane signaling receptor activity	30 / 402	2.500e-13
signaling receptor activity	34 / 536	5.600e-13
molecular transducer activity	34 / 536	5.600e-13
G-protein-coupled receptor activity	12 / 143	1.500e-6
signaling receptor regulator activity	13 / 194	6.900e-6
glycosaminoglycan binding	10 / 115	8.500e-6
receptor ligand activity	12 / 173	1.100e-5
signaling receptor activator activity	12 / 179	1.600e-5
cytokine activity	8 / 79	2.300e-5
amyloid-beta binding	6 / 55	1.600e-4

## Cellular components



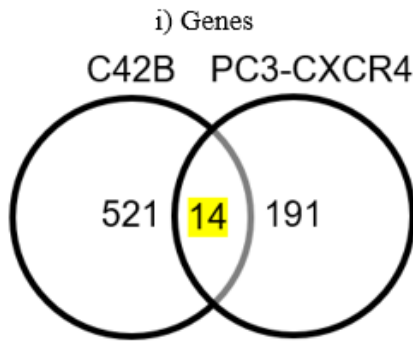
Name	# genes (DE/ALL)	p-value
cell periphery	108 / 3226	4.900e-19
plasma membrane	95 / 2982	1.700e-14
extracellular region	74 / 2371	3.000e-10
integral component of plasma membrane	36 / 752	1.200e-9
cell surface	26 / 419	1.700e-9
intrinsic component of plasma membrane	36 / 797	5.800e-9
intrinsic component of membrane	75 / 2879	7.200e-7
external encapsulating structure	17 / 281	1.900e-6
extracellular matrix	17 / 281	1.900e-6
integral component of membrane	72 / 2804	2.500e-6

(c) Advaita Corporation 2022

**Figure 26. Pathway analysis of genes differentially expressed in PI4KIII $\alpha$  shRNA vs scrambled PC3-CXCR4 cell-lines.**

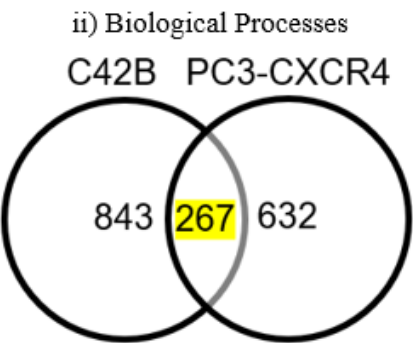
i) Analysis of DEG show GO biological processes significantly impacted in the PI4KIII $\alpha$  shRNA PC3-CXCR4 cell-line, with “cell-cell signaling” significantly impacted ii) Analysis of DEG show GO molecular functions significantly impacted in the PI4KIII $\alpha$  shRNA PC3-CXCR4 cell-line, with “transmembrane signaling receptor activity” significantly impacted iii) Analysis of DEG show GO cellular components significantly impacted in the PI4KIII $\alpha$  shRNA PC3-CXCR4 cell-line, with “cell periphery” significantly impacted. All processes and functions of interest to us is highlighted in yellow.

---



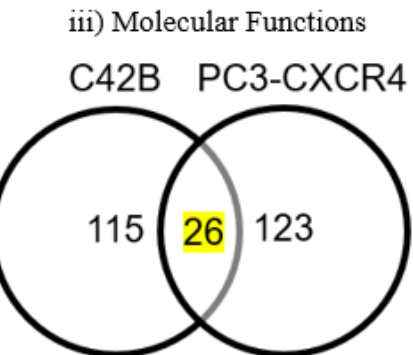
**Genes altered in C42B, PC3-CXCR4 cells**

	P-value PC3-CXCR4	P-value C42B
LONRF2	2.210e-5	9.180e-5
ERBB4	2.678e-5	0.049
SLC8A2	8.818e-5	0.002
DCLK1	1.320e-4	0.003
CD33	4.594e-4	0.002
GRM4	5.312e-4	2.934e-4
ANK2	6.631e-4	0.010
FAM198B	0.002	1.000e-6
INA	0.002	0.011
L1CAM	0.002	0.009
TLR2	0.003	0.048
RDH10-AS1	0.004	0.007
LOC646214	0.017	1.000e-6



**Biological processes altered in C42B, PC3-CXCR4 cells**

	P-value PC3-CXCR4	P-value C42B		P-value PC3-CXCR4	P-value C42B
negative regulation of multicellular organismal process	1.600e-7	6.800e-4	regulation of biological quality	1.500e-5	5.200e-9
cell surface receptor signaling pathway	1.800e-7	4.100e-6	regulation of membrane potential	0.002	4.500e-8
synapse organization	2.200e-7	1.600e-4	positive regulation of ERK1 and ERK2 cascade	0.023	7.700e-8
regulation of locomotion	6.000e-7	7.000e-5	regulation of anatomical structure morphogenesis	1.700e-5	1.600e-7
regulation of cell migration	1.300e-6	9.500e-5	MAPK cascade	0.006	2.200e-7
regulation of cellular component movement	1.500e-6	2.200e-5	cell fate commitment	0.002	3.800e-7
regulation of response to stimulus	2.200e-6	6.100e-4	positive regulation of developmental process	1.600e-4	4.700e-7
regulation of cell motility	3.200e-6	1.400e-4	regulation of MAPK cascade	0.001	5.900e-7
regulation of signaling	8.700e-6	1.100e-4	positive regulation of cell differentiation	0.007	9.500e-7
positive regulation	1.300e-5	0.019			



**Molecular Functions altered in C42B, PC3-CXCR4 cells**

	P-value PC3-CXCR4	P-value C42B		P-value PC3-CXCR4	P-value C42B
cytokine activity	2.300e-5	8.800e-5	adenylate cyclase inhibiting G protein-coupled glutamate receptor activity	0.015	0.014
calcium ion binding	2.100e-4	0.019	triacyl lipopeptide binding	0.015	0.032
G protein-coupled amine receptor activity	5.000e-4	0.014	G protein-coupled glutamate receptor activity	0.015	0.014
molecular function regulator	0.001	2.700e-4	serine-type endopeptidase inhibitor activity	0.016	4.900e-4
heparin binding	0.002	1.900e-8	G protein-coupled receptor binding	0.018	0.029
sulfur compound binding	0.003	2.000e-5			
cyclic nucleotide binding	0.004	0.045			
frizzled binding	0.004	0.001			
GABA receptor activity	0.004	0.039			
growth factor activity	0.006	0.007			
hormone activity	0.007	0.010			
BMP receptor binding	0.008	0.026			
neurotransmitter receptor activity	0.008	0.004			
3',5'-cyclic-AMP phosphodiesterase activity	0.009	0.047			

**Figure 27. Differentially expressed altered gene and pathway meta-analysis between PI4KIII $\alpha$  shRNA vs scrambled in PC3-CXCR4 and C4-2B cell-lines.**

i) shows 14 genes mutually altered in PI4KIII $\alpha$  shRNA cell-lines. (with 521 genes exclusively altered in C4-2B and 191 genes exclusively altered in PC3-CXCR4.). ii) shows 267 biological processes mutually altered in PI4KIII $\alpha$  shRNA cell-lines. (with 843 genes exclusively altered in C4-2B and 632 genes exclusively altered in PC3-CXCR4.). Some of the biological processes of interest have been listed and highlighted in yellow. iii) shows 26 molecular functions mutually altered in PI4KIII $\alpha$  shRNA cell-lines. (with 115 genes exclusively altered in C4-2B and 123 genes exclusively altered in PC3-CXCR4.). Some of the molecular functions of interest have been listed and highlighted in yellow.

---

**5.6 Discussion.** From these above data we can conclude that PI4KIII $\alpha$  contributes to the invasion in PCa cell lines. The localization to the PM in response to ligand induction as seen in Fig 17, further attributes to the role PI4KIII $\alpha$  activity contributing to the PI4P production to the invasive projection in cancer cells from our previously published data<sup>1</sup>, leading to invasion. We see that PI4KIII $\alpha$  knockdown leads to decreased invasion, and this is case when the adaptor protein TTC7B is transiently knocked down as well. These proteins also have a role in other chemokine mediated invasions and might be crucial players in the invasive characteristics of cancer progression. The CXCR4-CXCL12 axis has already been well studied for its role in aiding circulating tumor cells home into the bone marrow, and supporting colonization in the hematopoietic niche.

To study the effect of PI4KIII $\alpha$  knockdown, stable cell-lines were created and characterized for utilization in the functional and DEG studies. These stable knockdown cells showed similar results for invasion compared to the transient knockdowns. The role of adaptor

proteins in contributing to the proliferative nature of PCa cells, remain to be elucidated. PI4KIII $\alpha$ 's key role may be to influence in this homing by contributing towards the attachment, invasion and proliferation at the osteoblastic sites. Additionally, we further evaluated the differential expression with differences in pathways enriched between the control and PI4KIII $\alpha$  knockdown cell-lines. Consistent to our functional characterization, we find many pathways enriched attributing to cell proliferation and invasion in Scr compared to PI4KIII $\alpha$  knockdown cell-lines (Table 2) (Table 3), like the MTROC1 signaling and mitotic spindle. Even the androgen response is significantly enriched compared to PI4KIII $\alpha$  deficient cell-lines in C4-2B, and not so significant levels in PC3-CXCR4 cell-lines as expected as PC3 is androgen receptor negative. Interestingly as we saw in the literature EFR3 and PI4KIII $\alpha$  is crucial for KRAS signaling in cancer<sup>71, 72</sup>. So, when we knockdown PI4KIII $\alpha$ , genes downregulated in KRAS signaling (KRAS\_SIGNALING\_DN) is enriched in this population in both C4-2B and PC3-CXCR4 (Table 4). Furthermore, the enrichment of cell proliferative pathways such as E2F targets and protein secretion in cell-lines is validated using the publicly available TCGA Firehose expressing high PI4KIII $\alpha$  for prostate adenocarcinoma. These gene and pathway alterations are also further validated by similar biological processes and molecular functions impacted by PI4KIII $\alpha$  knockdown using Advaita ingenuity pathway analysis. These include processes such as proliferation, locomotion, response to stimulus and GPCR binding.

Overall these studies are some of the initial efforts in uncovering the novel roles of PI4KIII $\alpha$  and its adaptor protein TTC7B. The study of the interaction by which these proteins mechanistically contribute, through chemokine receptors especially the CXCR4-CXCL12 axis is also quite interesting and sheds light on the various routes by which PI4KIII $\alpha$  transduces its downstream signaling.

## CHAPTER 6- CLINICAL SIGNIFICANCE OF PI4KIII $\alpha$ IN METASTATIC PROSTATE CANCER BIOPSIES

**6.0 Introduction.** In our previous data, we observed the expression changes in primary vs metastatic tumors through IHC staining of matched pairs of PCa tumor biopsies. This showed higher level of PI4KIII $\alpha$  expression in metastatic sample compared to their matched primary tumors (Fig 28). These were some of the early evidences of PI4KIII $\alpha$  expression and its implication in prostate cancer. This trend of PI4KIII $\alpha$  expression levels in metastatic samples were also corroborated with other publicly available datasets showing similar pattern of higher PI4KIII $\alpha$  expression in metastatic samples. The studies we show here are from A) GDS3289: 101 cell populations were isolated using laser-capture microdissection and profiled prostate cancer progression from benign epithelium to metastatic disease<sup>157</sup>. B) Beltran et al: histologically characterized 114 castrate- resistant tumors from 81 patients as prostate adenocarcinoma (CRPC- adeno, n=51) and neuroendocrine prostate-cancer (CRPC-NE, n=30), analyzed these biopsies over different time points from same patients to perform genome-wide DNA methylation analysis<sup>158</sup>. And C) GSE6919: 152 human samples that includes prostate cancer tissues, prostate tissue adjacent to tumor, and metastatic prostate cancer tissues were analyzed for gene expression using various Affymetrix chip sets. These studies support the increased PI4KIII $\alpha$  expression pattern in increasing progression of PCa from benign to metastatic phenotype (Fig 29). Interestingly the corresponding phosphatase SACM1L to the PI4KIII $\alpha$  showed a reciprocal pattern of decrease in GDS3289 (Fig 29A). The adaptor protein EFR3B also showed a similar increase as PI4KIII $\alpha$  expression in Beltran et al, in the castrate resistant neuroendocrine phenotype, a marker for drug resistance and an aggressive variant (Fig 29B).

In pancreatic ductal carcinoma this gene has been associated with invasion and metastasis in differential gene expression analysis<sup>68</sup>. It is known to be involved in chemoresistance to cisplatin in medulloblastoma<sup>69</sup> and gemcitabine resistance in pancreatic cancer<sup>70</sup> from a panel of kinase siRNAs. One of the recent implications of PI4KIII $\alpha$  along with its adaptor protein EFR3A, in association to a commonly mutated gene KRAS in pancreatic cancers<sup>71, 72</sup>, provides yet another evidence of PI4KIII $\alpha$  and its emerging role in commonly mutated cancers.

The stable knockdown of PI4KIII $\alpha$  in PCa cells leads to alterations in pathways and processes responsible for regulation of cell motility, locomotion, proliferation and G-protein coupled receptor binding. Now we analyze the alterations in pathways and functions on the basis of PI4KIII $\alpha$  expression in metastatic biopsies of metastatic hormone sensitive prostate cancer patients (mHSPC). This is in efforts to provide further insight into the processes that promote these characteristics of invasion in samples of high PI4KIII $\alpha$  expression. Here in clinical samples, there is a trend of high tumor cell proliferation, poor overall survival and PSA progression in patients in high PI4KIII $\alpha$  levels in the bone.

### **6.1 Determine the clinical significance of PI4KIII $\alpha$ in human prostate cancer metastasis.**

RNA-seq analysis was performed on biopsies from metastatic hormone sensitive PCa (mHSPC) patients. 50 total metastatic biopsies were used for RNA sequencing from bone (n=32) and soft-tissues (n=18) including liver and lymph-nodes. These biopsies were also used in clinical trial NCT02058706, with total n=71 metastatic biopsies, testing the efficacy of enzalutamide vs bicalutamide, with enzalutamide showing improved outcomes in terms of time to PSA progression, response (7 month and 12 month) and overall survival (OS); with black patients showing even better outcomes to PSA response with enzalutamide<sup>159</sup>. Our RNA-seq analysis was further stratified based on the origin of biopsies and low or high PI4KIII $\alpha$  expression. Kaplan-Meier plots

demonstrated that bone metastasis biopsies have poor OS and PSA progression in cohorts with high PI4KIII $\alpha$  and CXCR4 expression, and there was no significance in these outcomes in correlation to these expression levels in soft-tissue biopsies (Fig 30). It is interesting to note that PCa metastasizes mostly to the bone and this poor outcome trend is also solely noticeable only in bone biopsies and not in soft-tissues. A detailed COX regression analysis implicated the known genes involved in PI4P production (Fig 17). These include two isoforms of PI4K (PI4KA and PI4K2B), all the adaptor proteins involved in the recruitment of PI4KA to the PM, and CXCR4. The increased expressions of the proteins were significant in the poor OS of bone metastasis in PCa (Table 6). Furthermore, the Pearson correlation showed associations of these interacting proteins based on the origin of biopsy, and in particular EFR3B proved to be of significant correlation with PI4KA and TTC7B in bone and not soft-tissue (Table 7). The correlation assessed between PI4KA and CXCR4, and PI4KA and TTC7B showed positive correlation in metastatic tumor biopsies from both bone and soft-tissue.

We further analyzed the efficacies of enzalutamide and bicalutamide post-treatment on the overall patient outcome based on the origin of biopsies, in respect to low vs high PI4KIII $\alpha$  expression levels. (Enzalutamide- Bone n=18, Bicalutamide- Bone n=14, Enzalutamide- Soft-tissue n=8, Bicalutamide- Soft-tissue n=10). We observe that there is poor OS and PSA progression associated with bone biopsies of high PI4KIII $\alpha$  expression levels that received treatment with bicalutamide in combination with ADT and not enzalutamide (Fig 31A) (Fig 31C). We must note that there might be better outcomes associated to PI4KIII $\alpha$  expression levels with the improved next-generation androgen-blockade molecules such as enzalutamide, if the OS and PSA progression were collected and followed-up for longer periods post-treatment. This could be due to the development of drug-resistance to androgen-blockade therapies. Also, we see no

significant overall outcomes to either bicalutamide or enzalutamide in soft-tissue biopsies (Fig 31B) (Fig 31D).

With bone metastatic biopsies showing better outcomes in low PI4KIII $\alpha$  expression level cohorts and interesting outcomes post-treatment with bicalutamide, we additionally analyze the gene sets and pathways differentially expressed between the low and the high PI4KIII $\alpha$  expression levels. The GSEA analysis showed enrichment of gene-sets involved in cell proliferation such as E2F targets, P53 pathways, PI3K-AKT-MTOR signaling, and WNT-Beta-Catenin signaling in high PI4KIII $\alpha$  expressing bone biopsies (Fig 32). These are the pathways implicated in cell proliferation, and that are activated through the CXCR4-CXCL12 axis as we mentioned previously. Among the leading-edge pathway analysis enriched between high PI4KIII $\alpha$  vs low PI4KIII $\alpha$  bone biopsy cohort, the top-most significant hallmark pathways are as seen in the enrichment plots and as highlighted in yellow in the gene set table (Table 8) (FDR q-val < 0.05 and P<0.05).

Additionally, we explored these differential gene expressions based on race, categorizing samples as of African-American (AA) origin or Non-AA, and further categorizing them based on origin of biopsy as well. Overall AA population showed enrichment of Hallmark Androgen Response pathways cumulatively with both bone and soft-tissue biopsies combined (Fig 34). This might explain why AA patients respond well to the next-generation androgen blockade treatments using enzalutamide on the basis of rate and duration of PSA response<sup>159</sup>.

Interestingly, when bone biopsies were analyzed to show molecular signatures in AA bone samples, the result showed reciprocal enrichment, that is enrichment of similar pathways we mentioned for cell proliferation (Fig 35) in Non-AA bone samples, such as E2F targets, KRAS

signaling, PI3K-AKT-MTOR signaling, and IL6-JAK-STAT3 signaling in high PI4KIII $\alpha$  expressing bone biopsies.

This proliferative nature of non-AA bone biopsy samples was also validated using other metastatic signatures, other than the Hallmark GSEA signatures, and re-analyzed with GSEA. The external metastatic signatures utilized for our study were from GSEA and other published sources, and they are as follows: a) meta-55, which is a distinct molecular profile that has a unique MYC/RAS co-activation signature highly associated with PCa metastasis<sup>160</sup> b) the gene signature procured from Balk et al, that listed genes associated with aggressive phenotype and identified genes that mediate androgen metabolism in androgen-independent metastatic tumors.<sup>161</sup> and C) Chandran et al, differential gene expression analysis that show a unique pattern of 415 genes upregulated (Chandran-Metastasis-UP) and 364 genes downregulated (Chandran-Metastasis-DOWN) at least 2 fold in their metastatic samples, and this included pathways related to androgen ablation and other metastasis associated genes. These multiple cross-validations showed similar patterns of non-AA bone biopsies being reciprocally enriched compared to the AA. That is there is an enrichment of these metastasis associated genes including proliferation and invasion in non-AA bone samples compared to AA. And as expected Chandran-Metastasis-DOWN gene signature that includes genes that are down-regulated in overall metastasis levels enriched in AA bone, in comparison to non-AA bone (Fig 36).

As a validation and an overlap of the observations thus far from our cellular functional assays and our biopsies samples, we can confidently state that knockdown of PI4KIII $\alpha$  leads to decrease in cellular invasion and proliferation, and Non-AA bone biopsies show enrichment of cell proliferation pathways. This is further confirmed with the enrichments of phosphatidylinositol signal system (hsa 04070) and the PI3K-AKT signaling pathway (hsa 04151) from the KEGG

pathway database in the Non-AA bone biopsies (Fig 37), indirectly correlating to the increased expression of PI4KIII $\alpha$ , as it is a crucial kinase involved in both the signaling system.

We also analyzed the immune landscape using differential gene expression analysis between the two different origin of biopsies (Bone and Soft-tissue) and within the low and high PI4KIII $\alpha$  expressing metastatic bone biopsies. PCa is known to have a very immunosuppressive environment from the various regulatory immune cell profiles such as T-regulatory cells<sup>162, 163</sup>, tumor associated macrophages (TAMS)<sup>164-166</sup>, and myeloid-derived suppressor cells (MDSCs)<sup>167</sup>. The tumor microenvironment is also bathed with the cytokine fluids and proteins from the surrounding tumor stromal cells and fibroblasts, that act as immunosuppressants such as TGF- $\beta$ , adenosine from prostatic acid phosphatase, PD-L1, VEGF, prostaglandin E2 and IL-6,8,10. With clinical trials in PCa targeting each of the individual mechanisms, optimal clinical efficacy is yet to be achieved. Patient classification based on genomic profiling, if they have more susceptible genes that are part of an immunosuppressive signature, along with use of combination therapies and combined immunotherapeutic targets, might be a way to address the many mechanisms of drug and other immunotherapy resistances in PCa<sup>168</sup>. To gather the immune profile between our biopsy samples and within our metastatic bone biopsies, the CIBERSORTX tool was utilized to understand the differential gene expression using the LM22 signature, that is inbuilt within the platform.

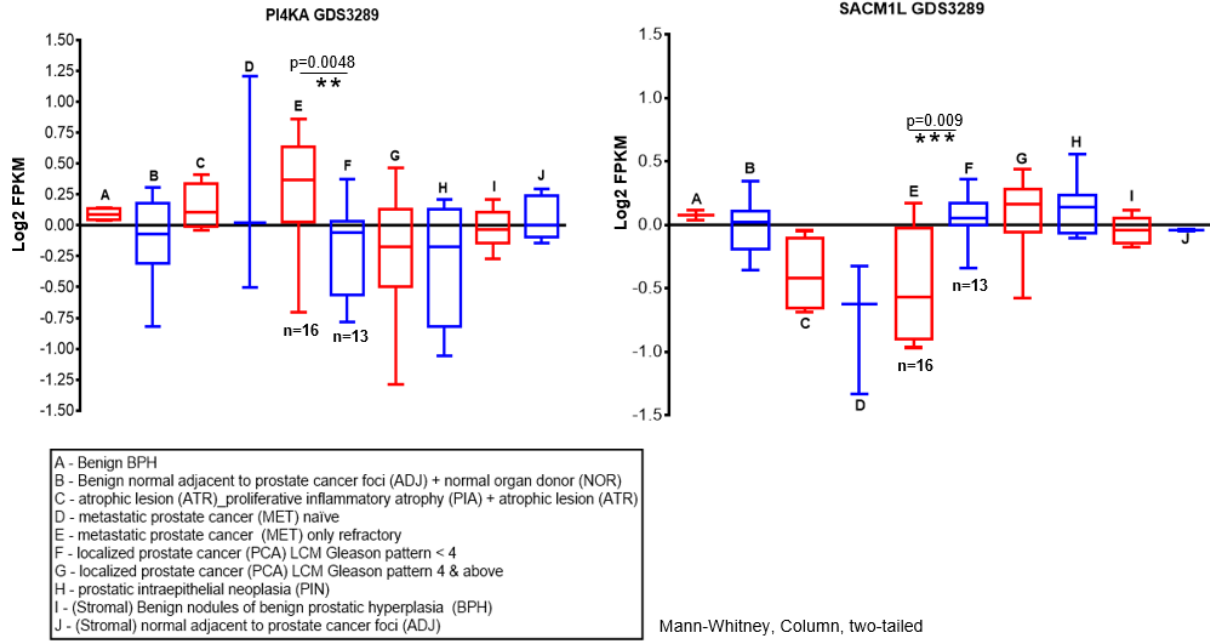
Our analysis showed that metastatic bone biopsies showed a more immunosuppressive phenotype with the macrophage profile, with a higher presence of resting macrophages (M0) and immunosuppressive macrophages (M2), while soft-tissues showed a more immune-active phenotype with an increased presence of immune-active macrophages (M1). Naive T-cells CD4 were shown to be of higher expression in their unprimed state in high PI4KIII $\alpha$  expressing bone

biopsies, along with T-cells gamma delta (Fig 38A). The latter cell type gamma-delta is known to have both pro-tumor and anti-tumor effects depending on the subset of gamma-delta<sup>169</sup>, but this CIBERSORTX platform does not allow us to differentiate between the subsets. This was an interesting trend to see between the biopsies, with bone showing a higher presence of naïve and immunosuppressive cells, considering that the majority of the PCa cells metastasizes to the bone.

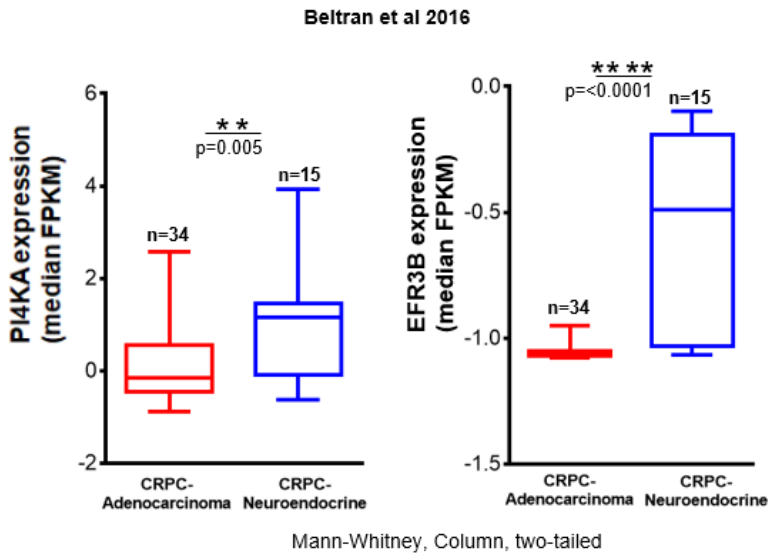
Within the low and high PI4KIII $\alpha$  expressing metastatic bone biopsies, high PI4KIII $\alpha$  expressing bone biopsies showed a more immunosuppressive phenotype, with increased expression of M0 and M2 macrophages. Although the expression of M1 immune-active macrophages were similar between low and high PI4KIII $\alpha$  biopsies, the presence of M0 and M2 makes the environment more irresponsive to any anti-tumor immune activity. Interestingly other immune cells of significance in the profiling such as mast cells, natural killer cells (NK) and T-cells CD4 memory cells were of higher expression in their resting state in high PI4KIII $\alpha$  expressing biopsies, whereas they were of higher expression in their active state in low PI4KIII $\alpha$  expressing bone biopsies (Fig 38B). Other immunosuppressive cells like t-regulatory cells showed no change between soft-tissue vs bone or low vs high PI4KIII $\alpha$  bone metastatic biopsies.



**A**



**B**



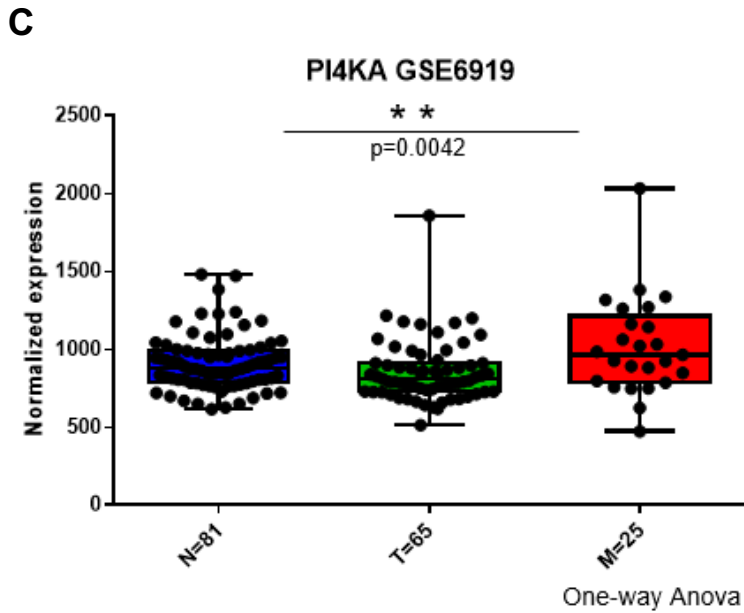
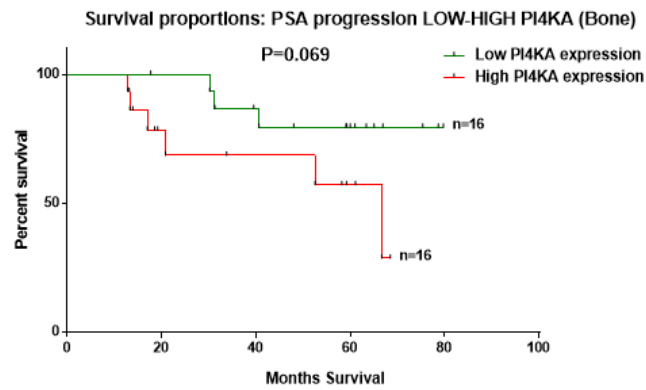
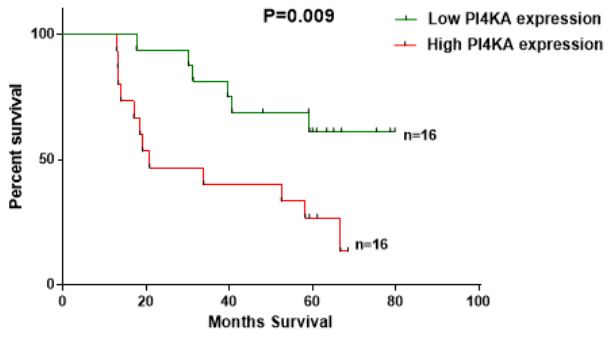


**Figure 29. PI4KIII $\alpha$  expression profile in**

A) GDS3289: show high PI4KIII $\alpha$  expression, between population E to F, E= metastatic prostate cancer, only refractory, F= Localized prostate cancer, gleason pattern <4. SACML1 expression, which is the corresponding phosphatase between the progression of E to F. B) Beltran et al: show high PI4KIII $\alpha$  and EFR3B expression in castrate resistant neuroendocrine population compared to adenocarcinoma. C) GSE6919: PI4KIII $\alpha$  expression from N=normal to T= localized prostate tumor to M= metastatic tumor population.

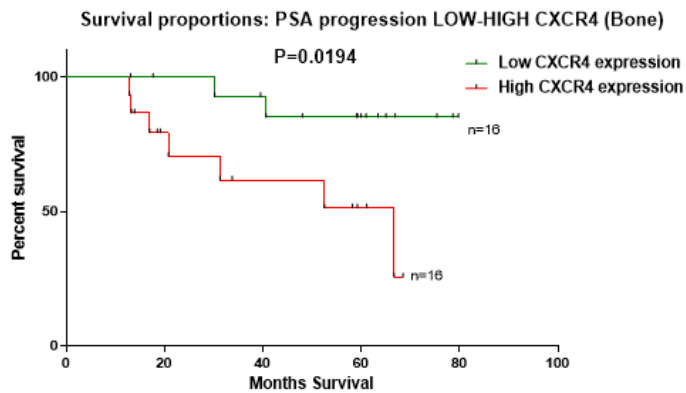
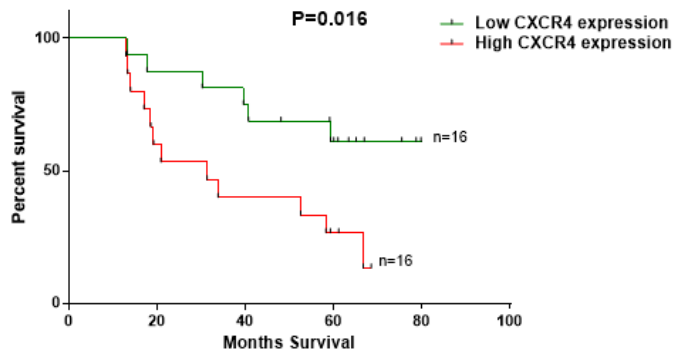
---

### A Survival proportions: Overall Survival LOW-HIGH PI4KA (Bone)



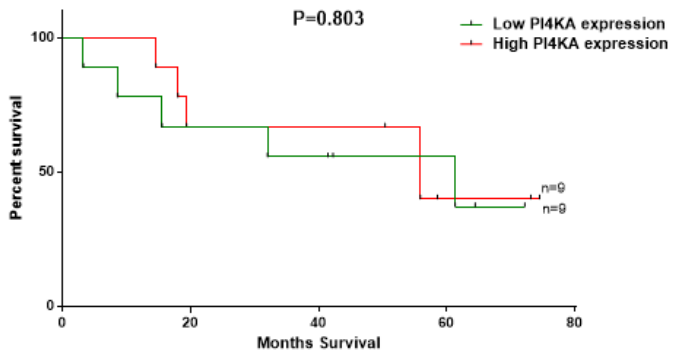
### B

#### Survival proportions: Overall Survival LOW-HIGH CXCR4 (Bone)

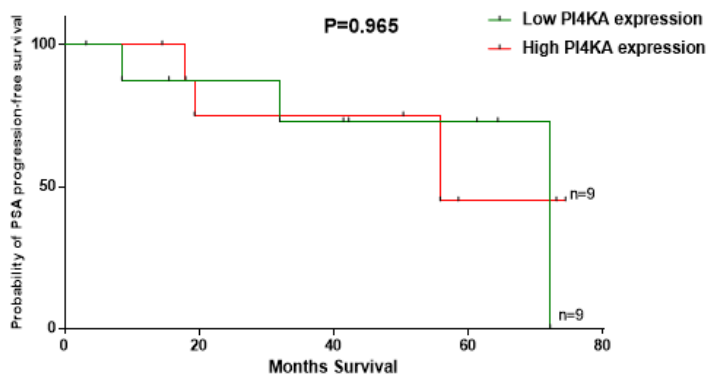


**C**

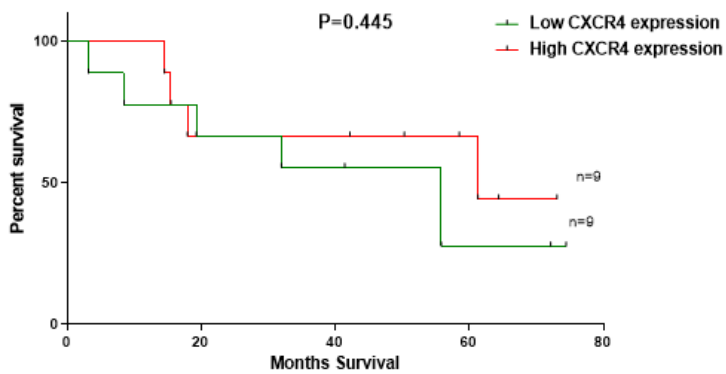
Survival proportions: Overall Survival LOW-HIGH PI4K (SoftTiss)



Survival proportions: PSA progression LOW-HIGH PI4K (SoftTiss)

**D**

Survival proportions: Overall Survival LOW-HIGH CXCR4 (SoftTiss)



Survival proportions: PSA progression LOW-HIGH CXCR4 (SoftTiss)

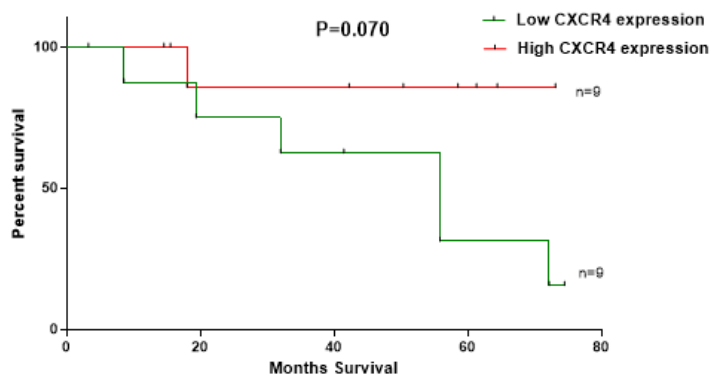


**Figure 30. Better OS and PSA progression is associated with low PI4KIII $\alpha$  and CXCR4 expression in bone biopsies.**

Kaplan-Meier analysis comparing OS and PSA progression in patients based on A) PI4KIII $\alpha$  levels in bone. B) CXCR4 levels in bone. C) PI4KIII $\alpha$  levels in soft-tissue. D) CXCR4 levels in soft-tissue.

Overall-Survival (OS) in bone biopsies

Genes	Hazard Ratio (95% CI)	P
	3.449 (1.286,9.251)	0.009
PI4KA	2.454 (0.946,6.365)	0.056
PI4KB	2.047 (0.791,5.300)	0.132
PI4K2A	3.000 (1.119,8.041)	0.022
PI4K2B	3.173 (1.181,8.525)	0.016
CXCR4	3.194 (1.189,8.579)	0.015
EFR3A	4.093 (1.446,11.588)	0.004
EFR3B	3.173 (1.181,8.525)	0.016
TTC7A	3.449 (1.286,9.251)	0.009
FAM126B	3.173 (1.181,8.525)	0.016
FAM126A		

**Table 6. Cox regression analysis of Overall Survival of bone metastasized PCa.**

Genes highlighted in yellow show a higher HR with  $p < 0.05$ , indicating poor OS in biopsies of bone metastasis.

## All tissues

	CXCR4	PI4KA	EFR3B	TTC7B
CXCR4		<b>R<sup>2</sup>=0.386</b> <b>P&lt;0.0001</b>	R <sup>2</sup> =0.001 P=0.795	R <sup>2</sup> =0.001 P=0.796
PI4KA	<b>R<sup>2</sup>=0.386</b> <b>P&lt;0.0001</b>		<b>R<sup>2</sup>=0.249</b> <b>P=0.0002</b>	<b>R<sup>2</sup>=0.283</b> <b>P&lt;0.0001</b>
EFR3B	R <sup>2</sup> =0.001 P=0.795	<b>R<sup>2</sup>=0.249</b> <b>P=0.0002</b>		<b>R<sup>2</sup>=0.124</b> <b>P=0.0123</b>
TTC7B	R <sup>2</sup> =0.001 P=0.796	<b>R<sup>2</sup>=0.283</b> <b>P&lt;0.0001</b>	<b>R<sup>2</sup>=0.124</b> <b>P=0.0123</b>	

## Bone

	CXCR4	PI4KA	EFR3B	TTC7B
CXCR4		<b>R<sup>2</sup>=0.415</b> <b>P&lt;0.0001</b>	R <sup>2</sup> =0.000 P=0.976	R <sup>2</sup> =0.002 P=0.812
PI4KA	<b>R<sup>2</sup>=0.415</b> <b>P&lt;0.0001</b>		<b>R<sup>2</sup>=0.327</b> <b>P=0.0006</b>	<b>R<sup>2</sup>=0.253</b> <b>P=0.0033</b>
EFR3B	R <sup>2</sup> =0.000 P=0.976	<b>R<sup>2</sup>=0.327</b> <b>P=0.0006</b>		<b>R<sup>2</sup>=0.288</b> <b>P=0.0015</b>
TTC7B	R <sup>2</sup> =0.002 P=0.812	<b>R<sup>2</sup>=0.253</b> <b>P=0.0033</b>	<b>R<sup>2</sup>=0.288</b> <b>P=0.0015</b>	

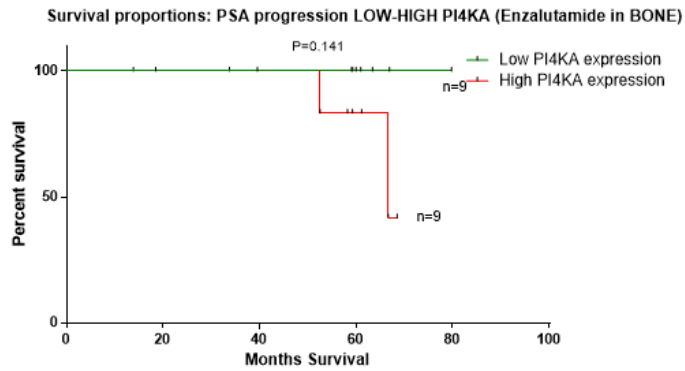
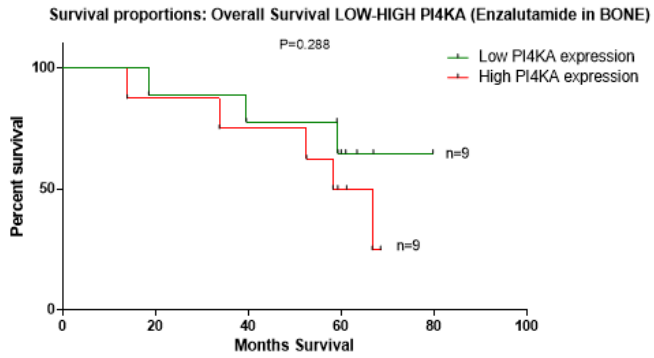
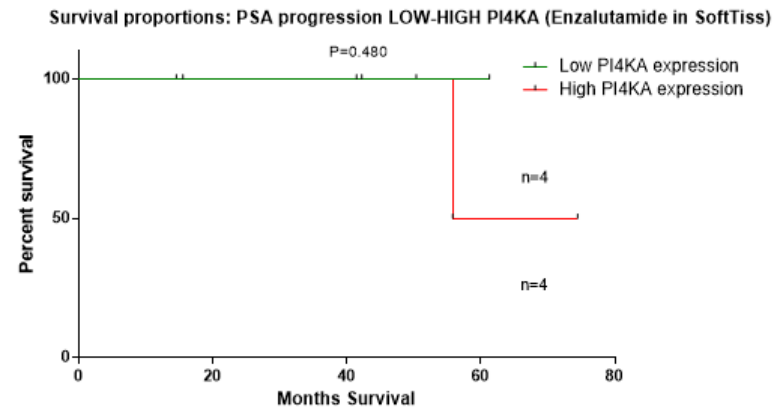
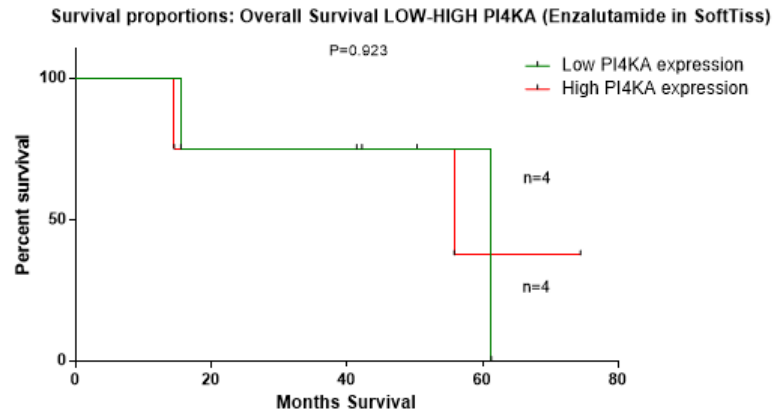
## Soft tissue

	CXCR4	PI4KA	EFR3B	TTC7B
CXCR4		<b>R<sup>2</sup>=0.346</b> <b>P=0.0102</b>	R <sup>2</sup> =0.021 P=0.566	R <sup>2</sup> =0.000 P=0.923
PI4KA	<b>R<sup>2</sup>=0.346</b> <b>P=0.0102</b>		R <sup>2</sup> =0.151 P=0.111	<b>R<sup>2</sup>=0.360</b> <b>P=0.0085</b>
EFR3B	R <sup>2</sup> =0.021 P=0.566	R <sup>2</sup> =0.151 P=0.111		R <sup>2</sup> =0.004 P=0.809
TTC7B	R <sup>2</sup> =0.000 P=0.923	<b>R<sup>2</sup>=0.360</b> <b>P=0.0085</b>	R <sup>2</sup> =0.004 P=0.809	

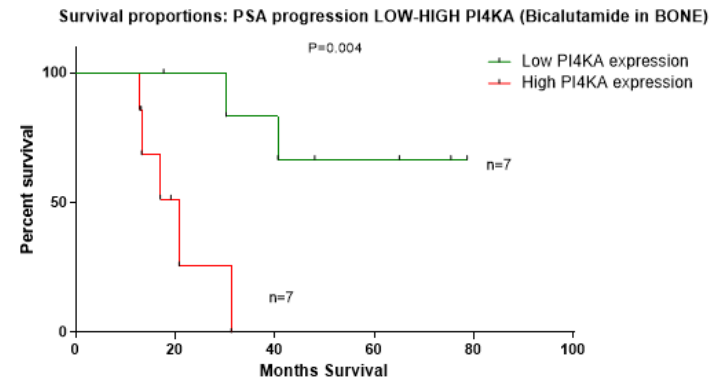
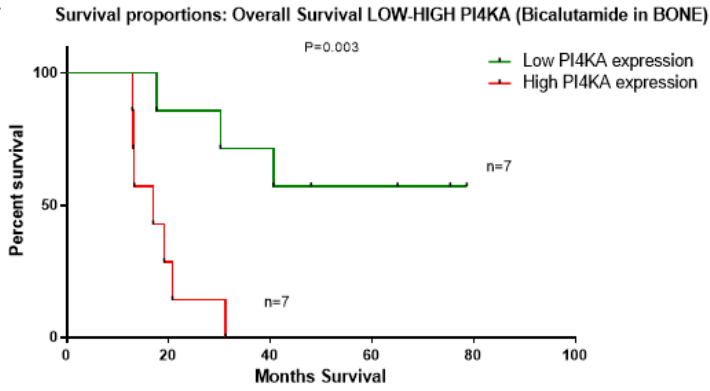
**Table 7. Pearson Correlation between the interacting proteins.**

The correlation showing significance between interacting proteins of tumor biopsies.

---

**A****B**

**C**



**D**

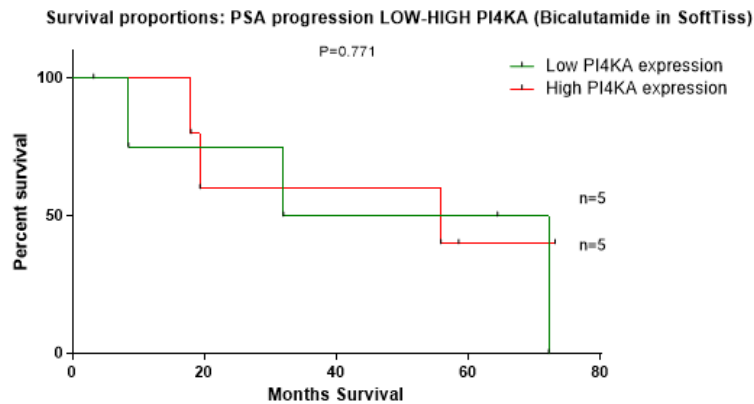
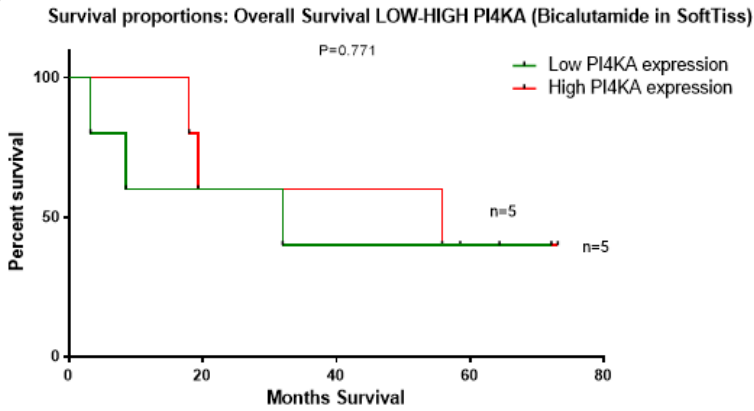


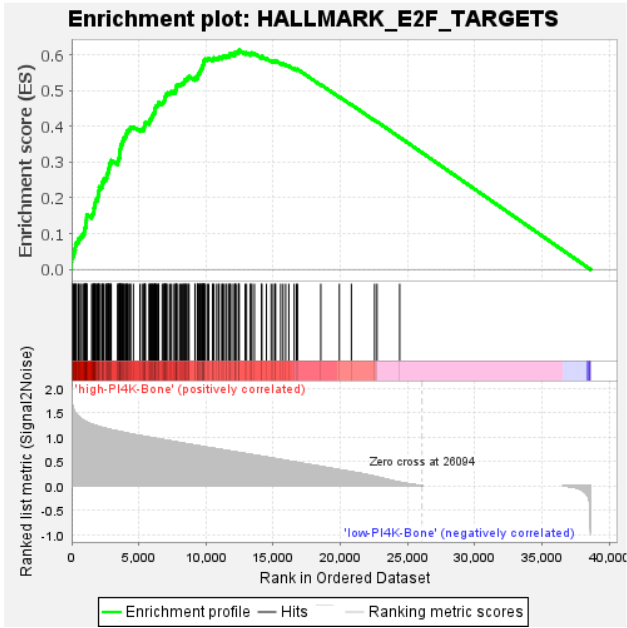
**Figure 31. Better OS and PSA progression is associated with low PI4KIII $\alpha$  in bone biopsies with Bicalutamide treatment in addition to ADT.**

Kaplan-Meier analysis comparing OS and PSA progression in patients based on PI4KIII $\alpha$  expression levels A) with enzalutamide treatment in bone biopsies B) with enzalutamide treatment in soft-tissue biopsies C) with bicalutamide treatment in bone biopsies D) with bicalutamide treatment in soft-tissue biopsies.

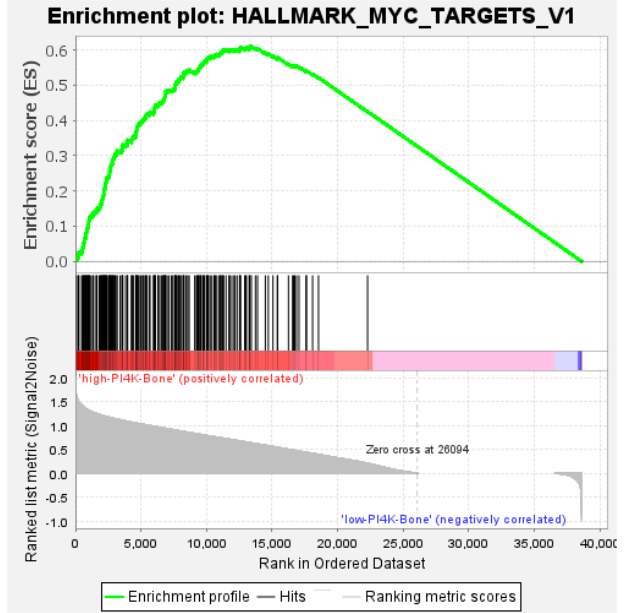
	GS follow link to MSigDB	GS DETAILS	SIZE	ES	NES	NOM p-val	FDR q-val	FWER p-val	RANK AT MAX	LEADING EDGE
1	<a href="#">HALLMARK_F2F_TARGETS</a>	<a href="#">Details...</a>	200	0.61	1.38	0.000	0.003	0.003	12466	tags=87%, list=32%, signal=128%
2	<a href="#">HALLMARK_MYC_TARGETS_V1</a>	<a href="#">Details...</a>	200	0.61	1.38	0.000	0.002	0.003	13420	tags=91%, list=35%, signal=139%
3	<a href="#">HALLMARK_OXIDATIVE_PHOSPHORYLATION</a>	<a href="#">Details...</a>	200	0.60	1.35	0.000	0.001	0.004	13408	tags=90%, list=35%, signal=136%
4	<a href="#">HALLMARK_MITOTIC_SPINDLE</a>	<a href="#">Details...</a>	199	0.60	1.35	0.000	0.001	0.004	13277	tags=88%, list=34%, signal=133%
5	<a href="#">HALLMARK_PROTEIN_SECRETION</a>	<a href="#">Details...</a>	96	0.60	1.33	0.000	0.002	0.011	12590	tags=85%, list=33%, signal=126%
6	<a href="#">HALLMARK_G2M_CHECKPOINT</a>	<a href="#">Details...</a>	199	0.59	1.32	0.000	0.002	0.011	13663	tags=87%, list=35%, signal=135%
7	<a href="#">HALLMARK_DNA_REPAIR</a>	<a href="#">Details...</a>	149	0.58	1.30	0.000	0.003	0.017	14534	tags=91%, list=38%, signal=146%
8	<a href="#">HALLMARK_PI3K_AKT_MTOR_SIGNALING</a>	<a href="#">Details...</a>	105	0.57	1.25	0.000	0.009	0.067	13776	tags=82%, list=36%, signal=127%
9	<a href="#">HALLMARK_MYC_TARGETS_V2</a>	<a href="#">Details...</a>	58	0.58	1.24	0.004	0.010	0.087	13420	tags=84%, list=35%, signal=129%
10	<a href="#">HALLMARK_UNFOLDED_PROTEIN_RESPONSE</a>	<a href="#">Details...</a>	113	0.54	1.20	0.000	0.026	0.232	13580	tags=77%, list=35%, signal=118%
11	<a href="#">HALLMARK_WNT_BETA_CATENIN_SIGNALING</a>	<a href="#">Details...</a>	42	0.56	1.19	0.022	0.027	0.263	13646	tags=81%, list=35%, signal=125%
12	<a href="#">HALLMARK_ADIPOGENESIS</a>	<a href="#">Details...</a>	200	0.52	1.17	0.001	0.040	0.389	16254	tags=85%, list=42%, signal=146%
13	<a href="#">HALLMARK_P53_PATHWAY</a>	<a href="#">Details...</a>	197	0.52	1.17	0.000	0.039	0.406	15267	tags=80%, list=40%, signal=132%
14	<a href="#">HALLMARK_MTORC1_SIGNALING</a>	<a href="#">Details...</a>	200	0.52	1.17	0.000	0.037	0.409	17811	tags=93%, list=46%, signal=171%
15	<a href="#">HALLMARK_PEROXISOME</a>	<a href="#">Details...</a>	104	0.52	1.15	0.015	0.056	0.577	16223	tags=83%, list=42%, signal=142%
16	<a href="#">HALLMARK_REACTIVE_OXYGEN_SPECIES_PATHWAY</a>	<a href="#">Details...</a>	48	0.53	1.14	0.077	0.069	0.678	14868	tags=85%, list=38%, signal=139%
17	<a href="#">HALLMARK_TGF_BETA_SIGNALING</a>	<a href="#">Details...</a>	54	0.53	1.13	0.067	0.075	0.731	16093	tags=87%, list=42%, signal=149%
18	<a href="#">HALLMARK_UV_RESPONSE_DN</a>	<a href="#">Details...</a>	144	0.50	1.13	0.018	0.075	0.749	15871	tags=81%, list=41%, signal=136%
19	<a href="#">HALLMARK_FATTY_ACID_METABOLISM</a>	<a href="#">Details...</a>	158	0.50	1.13	0.013	0.074	0.758	15000	tags=75%, list=39%, signal=123%
20	<a href="#">HALLMARK_INTERFERON_ALPHA_RESPONSE</a>	<a href="#">Details...</a>	97	0.51	1.13	0.029	0.070	0.761	17958	tags=94%, list=46%, signal=175%
21	<a href="#">HALLMARK_IL2_STAT5_SIGNALING</a>	<a href="#">Details...</a>	199	0.50	1.13	0.005	0.068	0.768	16924	tags=84%, list=44%, signal=149%
22	<a href="#">HALLMARK_INTERFERON_GAMMA_RESPONSE</a>	<a href="#">Details...</a>	199	0.50	1.12	0.007	0.075	0.820	18036	tags=89%, list=47%, signal=167%

**Table 8. Gene sets enriched in phenotype high-PI4K-Bone (n=13).**

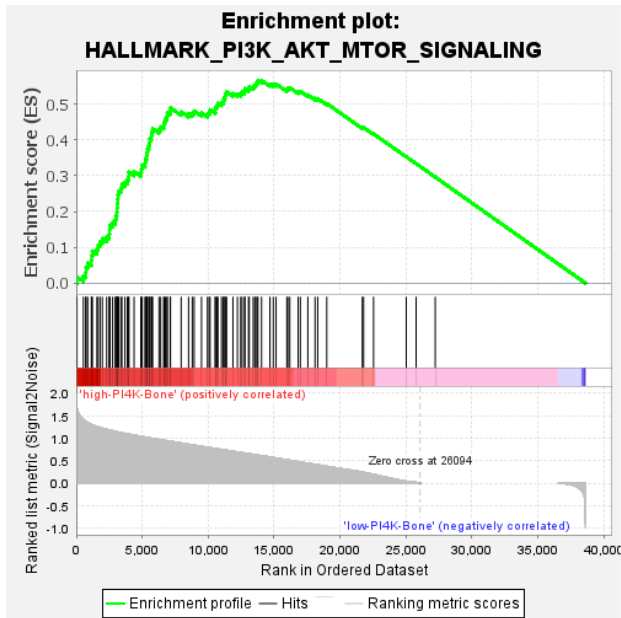
Gene sets enriched in this high PI4KIII $\alpha$  expressing bone biopsy cohort show enrichment in pathways involved in cell-proliferation ((FDR q-val < 0.05 and P<0.05)



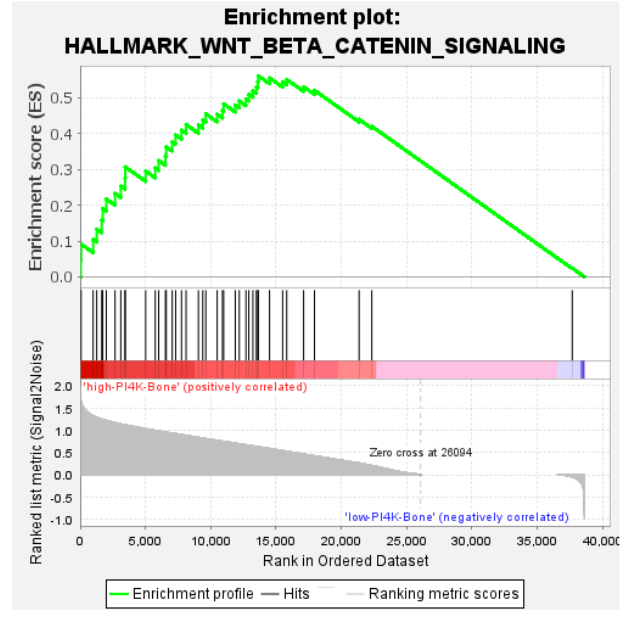
NES 1.38  
FDR q-value 0.003



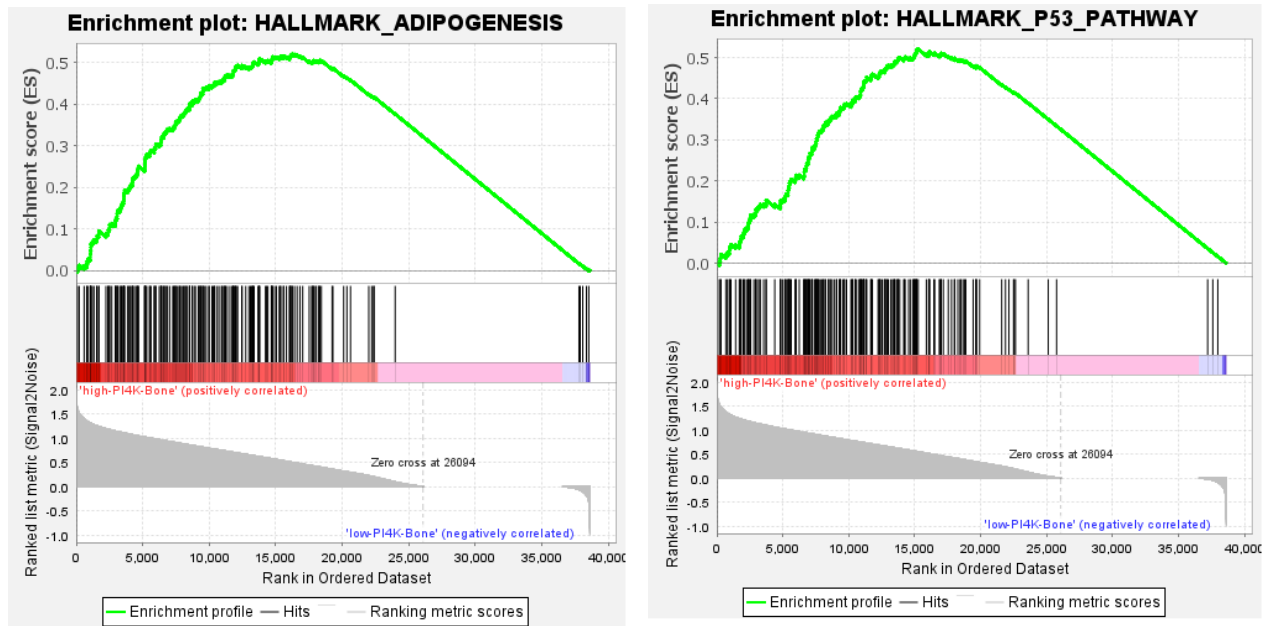
NES 1.38  
FDR q-value 0.003



NES 1.25  
FDR q-value 0.009



NES 1.19  
FDR q-value 0.027



NES 1.17  
FDR q-value 0.040

NES 1.17  
FDR q-value 0.039

**Figure 32. GSEA of proliferation-associated gene set in PI4KIII $\alpha$  high and low expressing bone biopsies.**

GSEA comparing pathways enriched in high PI4KIII $\alpha$  vs low PI4KIII $\alpha$  expressing human metastatic bone biopsy signature from bulk RNA-seq of hormone sensitive prostate cancer (mHSPC) patients. These are the top-most enriched pathways between the two cohorts, and are associated with the cell proliferative characteristics. The samples were classified into low (mRNA expression < 22.5) or high (mRNA expression > 22.5) based on the average.

High PI4KA  
expressing  
metastatic  
bone biopsies  
n=13

Low PI4KA  
expressing  
metastatic bone  
biopsies n=17

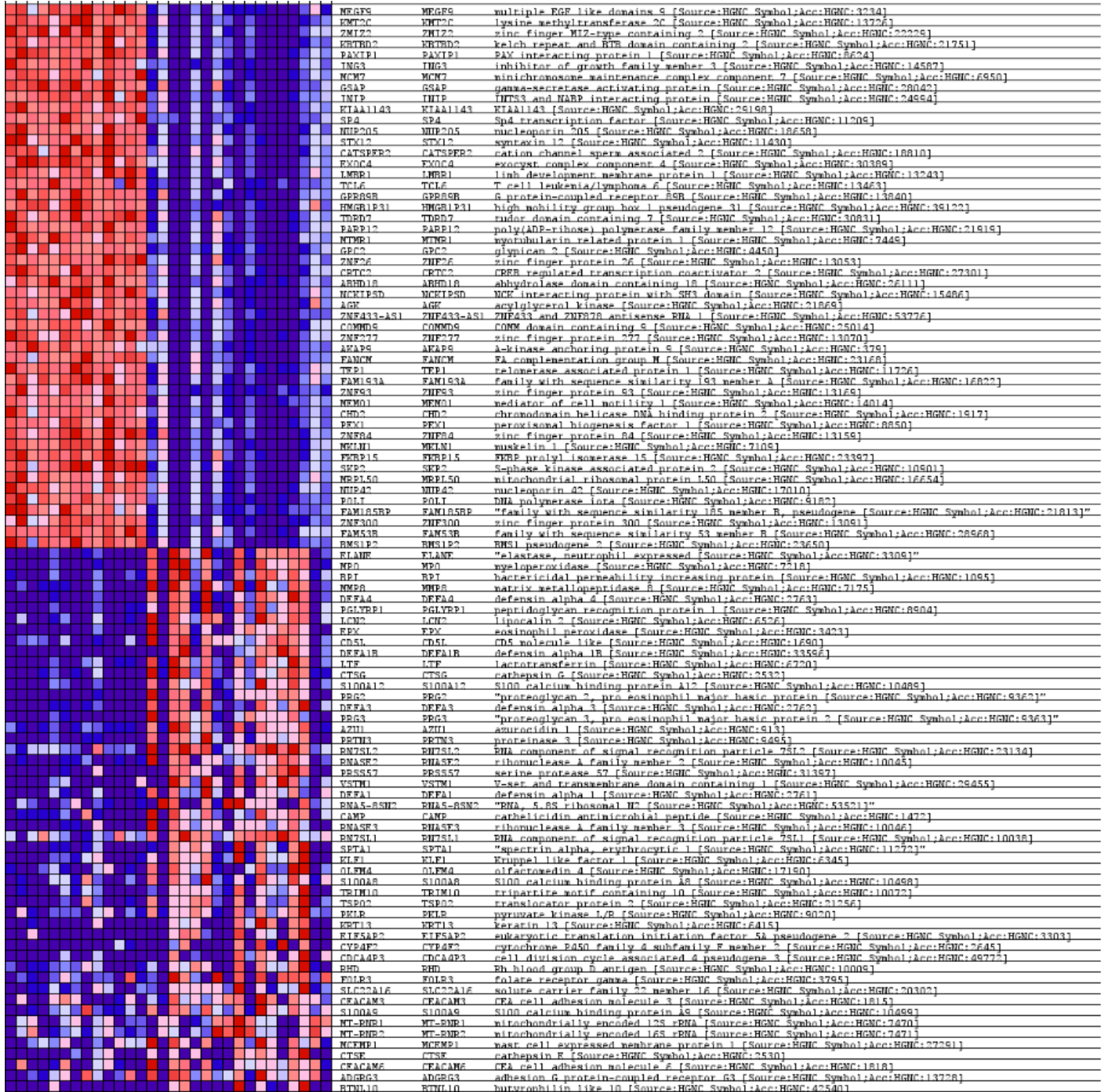
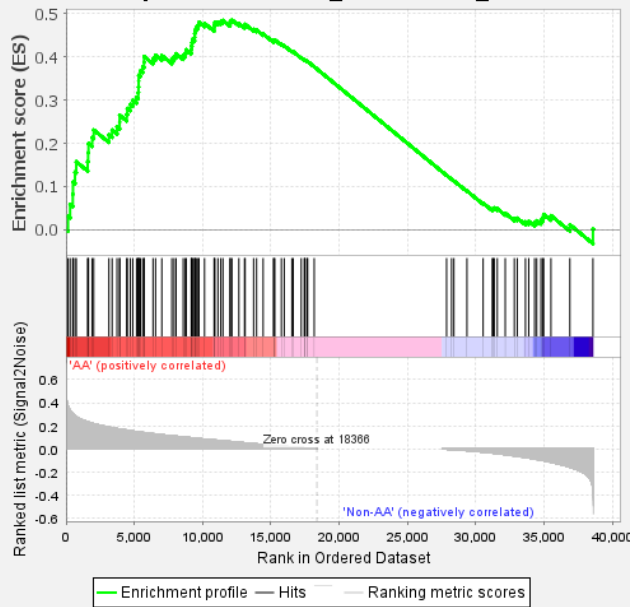


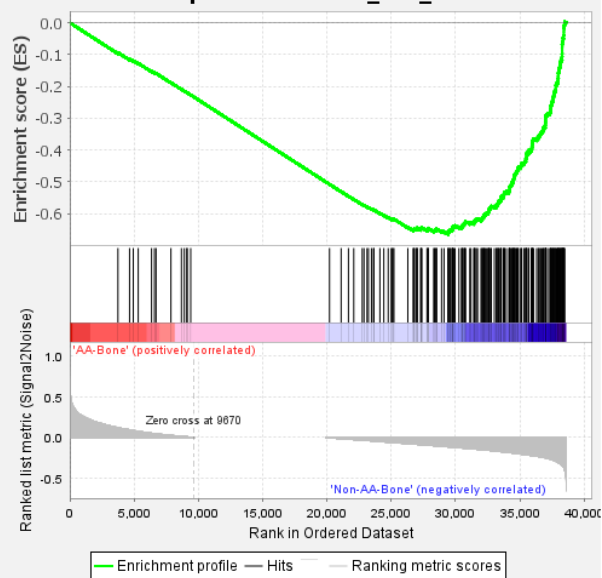
Figure 33. Heatmap representation of individual expression levels of top 50 features for each phenotype in Expression dataset in metastatic bone biopsies of mHSPC patient samples.

**Enrichment plot: HALLMARK\_ANDROGEN\_RESPONSE**

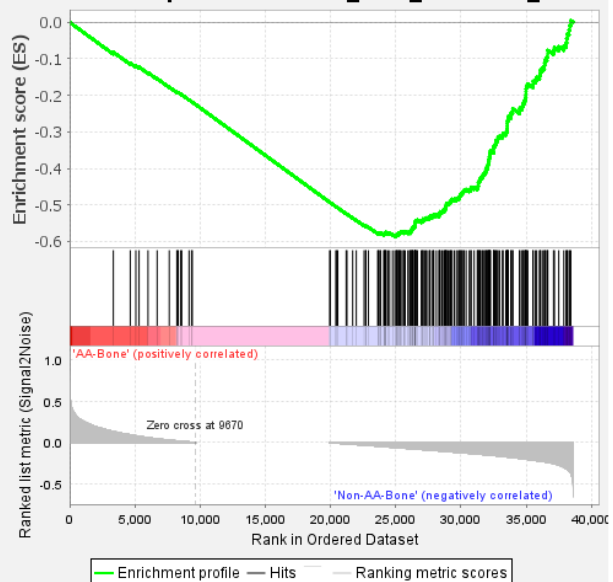
**Figure 34. GSEA of Hallmark Androgen Response in AA metastatic biopsies of all tissues.**

This pathway is enriched as one of the top-most molecular signatures with a NES= 1.40 and FDR q-value= 0.027.

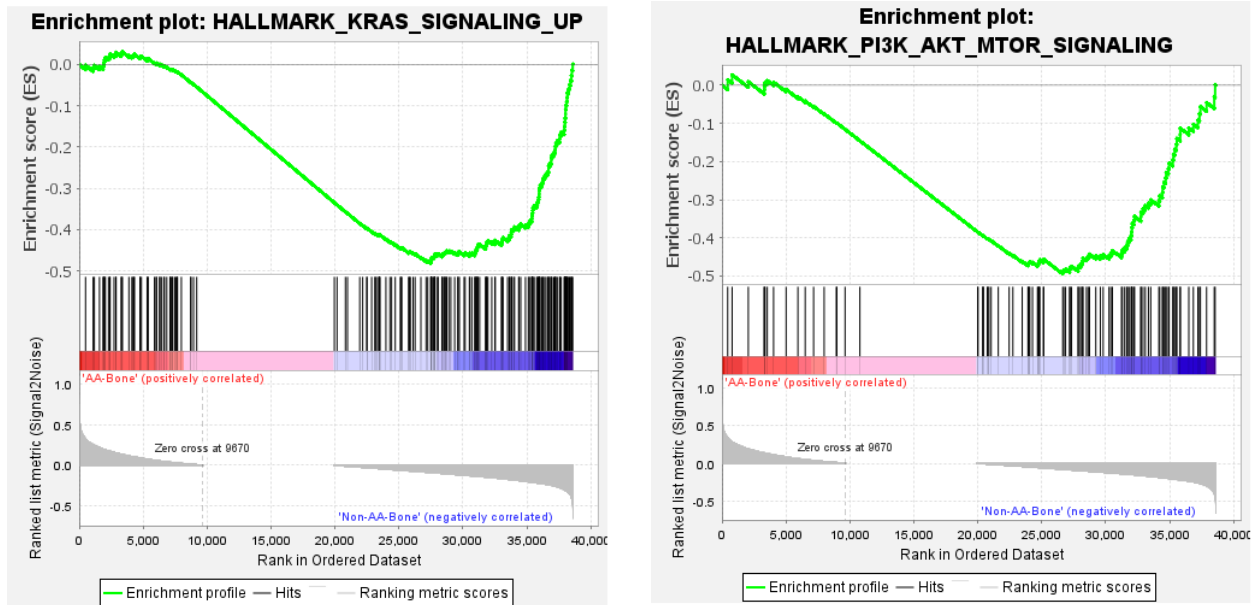
NES 1.40  
FDR q-value 0.027

**Enrichment plot: HALLMARK\_E2F\_TARGETS**

NES -2.15  
FDR q-value 0.0

**Enrichment plot: HALLMARK\_MYC\_TARGETS\_V1**

NES -1.89  
FDR q-value 0.0



NES -1.56  
FDR q-value 0.0

NES -0.49  
FDR q-value 0.0

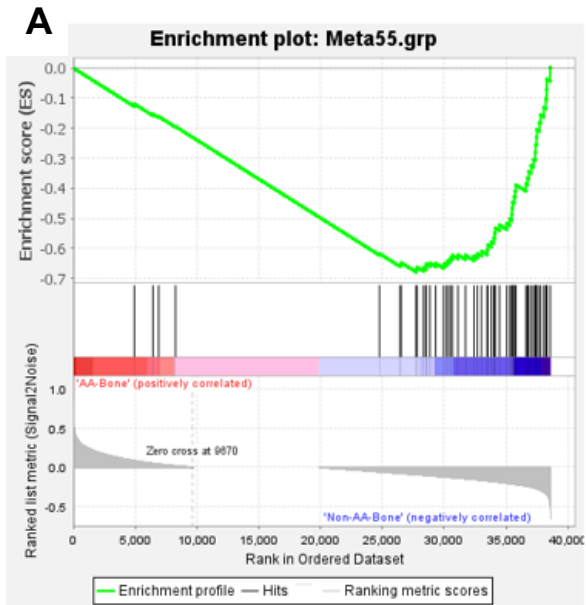
**Figure 35. GSEA of proliferation-associated gene set in Non-AA bone biopsies.**

GSEA comparing pathways enriched in AA vs Non-AA human metastatic bone biopsy signature from bulk RNA-seq of hormone sensitive prostate cancer (mHSPC) patients. These are the top-most pathways reciprocally enriched in Non-AA compared to AA cohorts, and are associated with the cell proliferative characteristics.

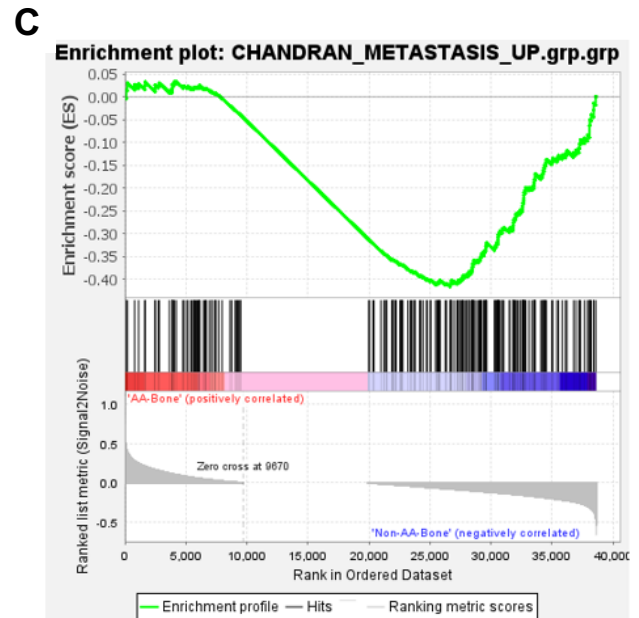
	GS follow link to MSigDB	GS DETAILS	SIZE	ES	NES	NOM p-val	FDR q-val	FWER p-val	RANK AT MAX	LEADING EDGE
1	<a href="#">HALLMARK_E2F_TARGETS</a>	<a href="#">Details ...</a>	200	-0.67	-2.15	0.000	0.000	0.000	9190	tags=73%, list=24%, signal=95%
2	<a href="#">HALLMARK_ALLOGRAFT_REJECTION</a>	<a href="#">Details ...</a>	200	-0.64	-2.07	0.000	0.000	0.000	8110	tags=64%, list=21%, signal=81%
3	<a href="#">HALLMARK_G2M_CHECKPOINT</a>	<a href="#">Details ...</a>	199	-0.63	-2.02	0.000	0.000	0.000	9051	tags=64%, list=23%, signal=84%
4	<a href="#">HALLMARK_INTERFERON_GAMMA_RESPONSE</a>	<a href="#">Details ...</a>	199	-0.61	-1.97	0.000	0.000	0.000	7959	tags=59%, list=21%, signal=74%
5	<a href="#">HALLMARK_MYC_TARGETS_V1</a>	<a href="#">Details ...</a>	200	-0.59	-1.89	0.000	0.000	0.000	13684	tags=79%, list=35%, signal=122%
6	<a href="#">HALLMARK_INTERFERON_ALPHA_RESPONSE</a>	<a href="#">Details ...</a>	97	-0.61	-1.84	0.000	0.000	0.000	7415	tags=54%, list=19%, signal=66%
7	<a href="#">HALLMARK_DNA_REPAIR</a>	<a href="#">Details ...</a>	149	-0.56	-1.74	0.000	0.000	0.003	14340	tags=72%, list=37%, signal=115%
8	<a href="#">HALLMARK_OXIDATIVE_PHOSPHORYLATION</a>	<a href="#">Details ...</a>	200	-0.54	-1.74	0.000	0.000	0.003	13095	tags=67%, list=34%, signal=101%
9	<a href="#">HALLMARK_IL2_STAT5_SIGNALING</a>	<a href="#">Details ...</a>	199	-0.53	-1.69	0.000	0.001	0.006	8237	tags=51%, list=21%, signal=65%
10	<a href="#">HALLMARK_MITOTIC_SPINDLE</a>	<a href="#">Details ...</a>	199	-0.52	-1.68	0.000	0.001	0.007	12184	tags=57%, list=32%, signal=83%
11	<a href="#">HALLMARK_IL6_JAK_STAT3_SIGNALING</a>	<a href="#">Details ...</a>	87	-0.55	-1.65	0.000	0.001	0.012	6968	tags=52%, list=18%, signal=63%
12	<a href="#">HALLMARK_INFLAMMATORY_RESPONSE</a>	<a href="#">Details ...</a>	200	-0.50	-1.64	0.000	0.002	0.019	9913	tags=56%, list=26%, signal=74%
13	<a href="#">HALLMARK_COMPLEMENT</a>	<a href="#">Details ...</a>	199	-0.50	-1.62	0.000	0.002	0.023	10918	tags=57%, list=28%, signal=79%
14	<a href="#">HALLMARK_TNFA_SIGNALING_VIA_NFKB</a>	<a href="#">Details ...</a>	200	-0.49	-1.59	0.000	0.003	0.035	9025	tags=49%, list=23%, signal=63%
15	<a href="#">HALLMARK_KRAS_SIGNALING_UP</a>	<a href="#">Details ...</a>	198	-0.48	-1.56	0.000	0.004	0.053	11140	tags=58%, list=29%, signal=81%
16	<a href="#">HALLMARK_MTORC1_SIGNALING</a>	<a href="#">Details ...</a>	200	-0.47	-1.53	0.000	0.006	0.087	12376	tags=61%, list=32%, signal=89%
17	<a href="#">HALLMARK_MYC_TARGETS_V2</a>	<a href="#">Details ...</a>	58	-0.54	-1.50	0.006	0.008	0.118	11909	tags=64%, list=31%, signal=92%
18	<a href="#">HALLMARK_PI3K_AKT_MTOR_SIGNALING</a>	<a href="#">Details ...</a>	105	-0.49	-1.49	0.002	0.008	0.129	11976	tags=60%, list=31%, signal=87%
19	<a href="#">HALLMARK_CHOLESTEROL_HOMEOSTASIS</a>	<a href="#">Details ...</a>	74	-0.50	-1.45	0.012	0.015	0.224	7857	tags=45%, list=20%, signal=56%
20	<a href="#">HALLMARK_PANCREAS_BETA_CELLS</a>	<a href="#">Details ...</a>	40	-0.53	-1.41	0.043	0.023	0.337	7135	tags=43%, list=18%, signal=52%
21	<a href="#">HALLMARK_UNFOLDED_PROTEIN_RESPONSE</a>	<a href="#">Details ...</a>	113	-0.43	-1.34	0.031	0.052	0.637	12593	tags=52%, list=33%, signal=77%

**Table 9. Gene sets enriched in phenotype Non-AA-Bone (n=19).**

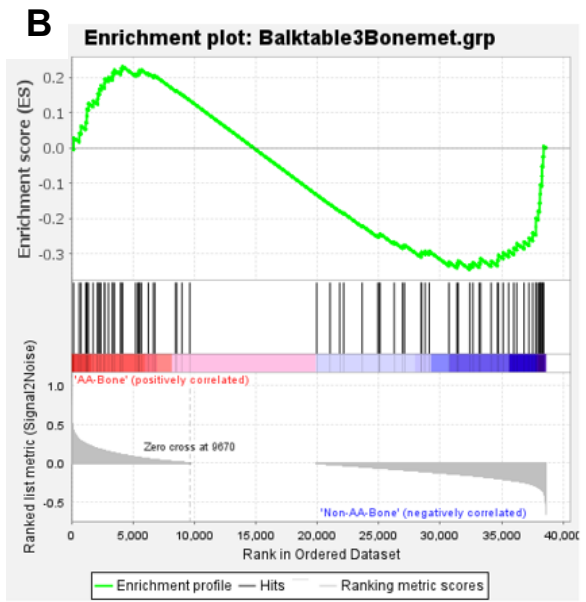
Gene sets enriched in the non-AA bone biopsy cohort show enrichment in pathways involved in cell-proliferation ((FDR q-val < 0.05 and P<0.05



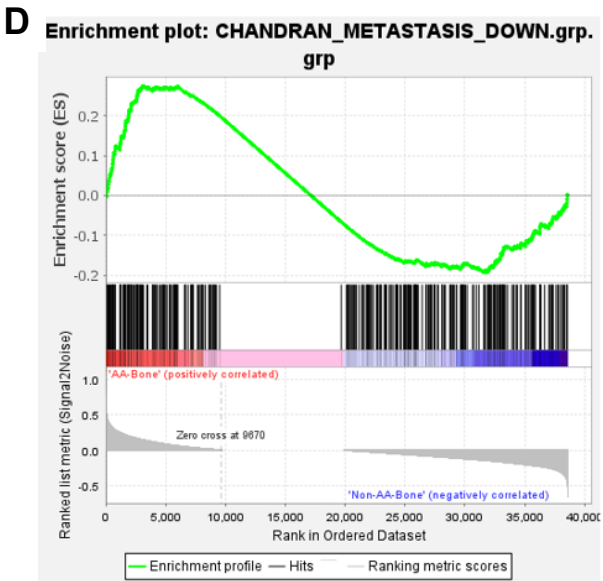
NES -1.88  
FDR q-value 0.0



NES -1.35  
FDR q-value 0.0



NES -0.99  
FDR q-value 0.49



NES 1.12  
FDR q-value 0.09

**Figure 36. GSEA using A) Meta-55, B) Balk et al, and C) Chandran et al- Metastasis-Up D) Chandran et al- Metastasis-Down-regulated gene signatures**

- showing reciprocally enriched metastatic gene signatures in non-AA bone biopsies, while Chandran et al, Metastasis-Down-regulated gene signatures showing enrichment in AA bone biopsies.

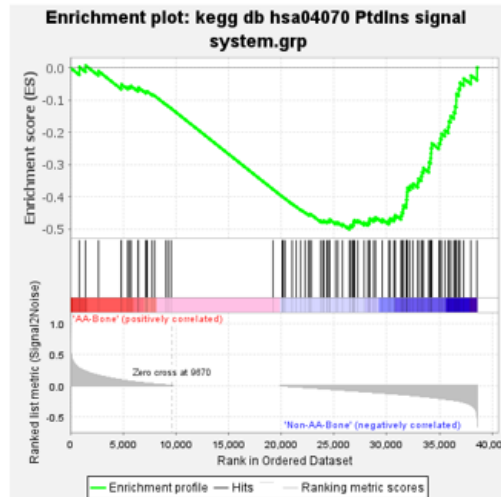
---

### Phosphatidylinositol Signaling system hsa04070

AA vs Non-AA Bone

NES = -1.51  
FDR = 0.001  
P = 0.001

*Enriched in Non-AA  
Bone samples*



### PI3K-AKT Signaling pathway hsa04151

NES = -1.21  
FDR = 0.048  
P = 0.048

*Enriched in Non-AA  
Bone samples*

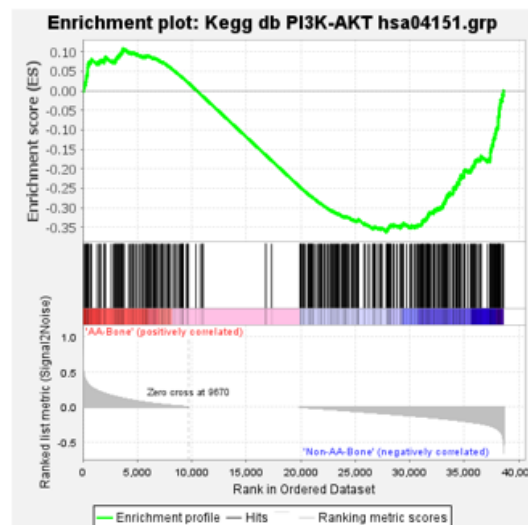
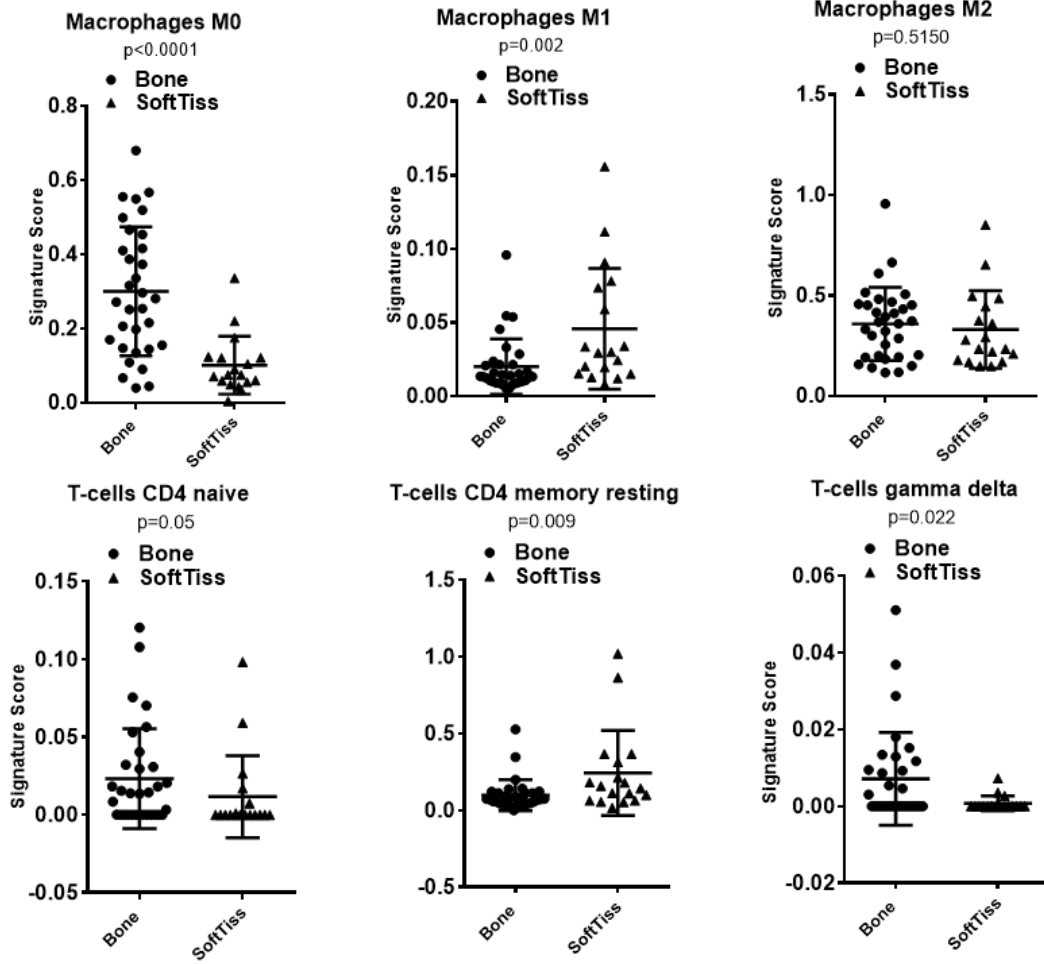


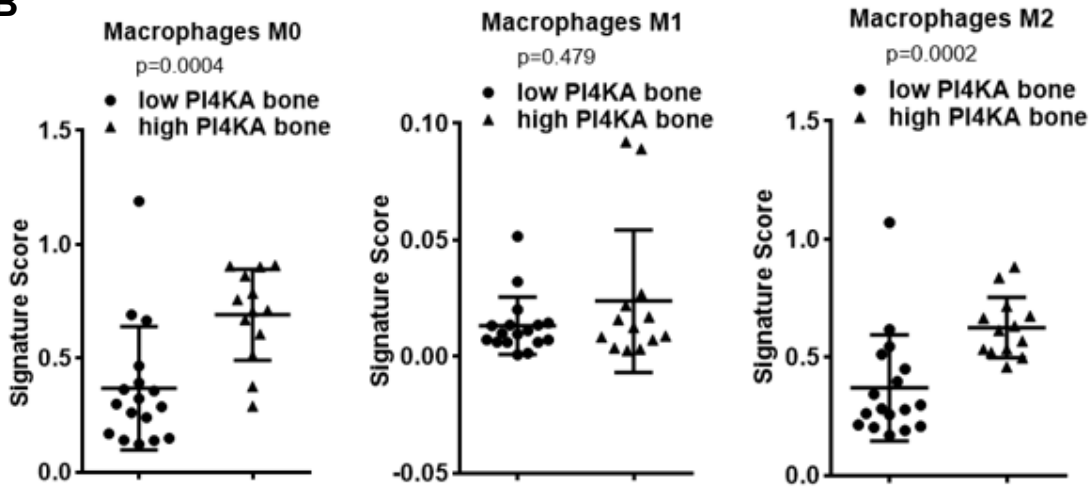
**Figure 37. GSEA using Kegg pathway database.**

showing reciprocal enrichment of both phosphatidylinositol signaling system (hsa04070) and PI3K-AKT signaling pathway (hsa04151) in Non-AA bone biopsies when compared to AA bone biopsies.

A



B



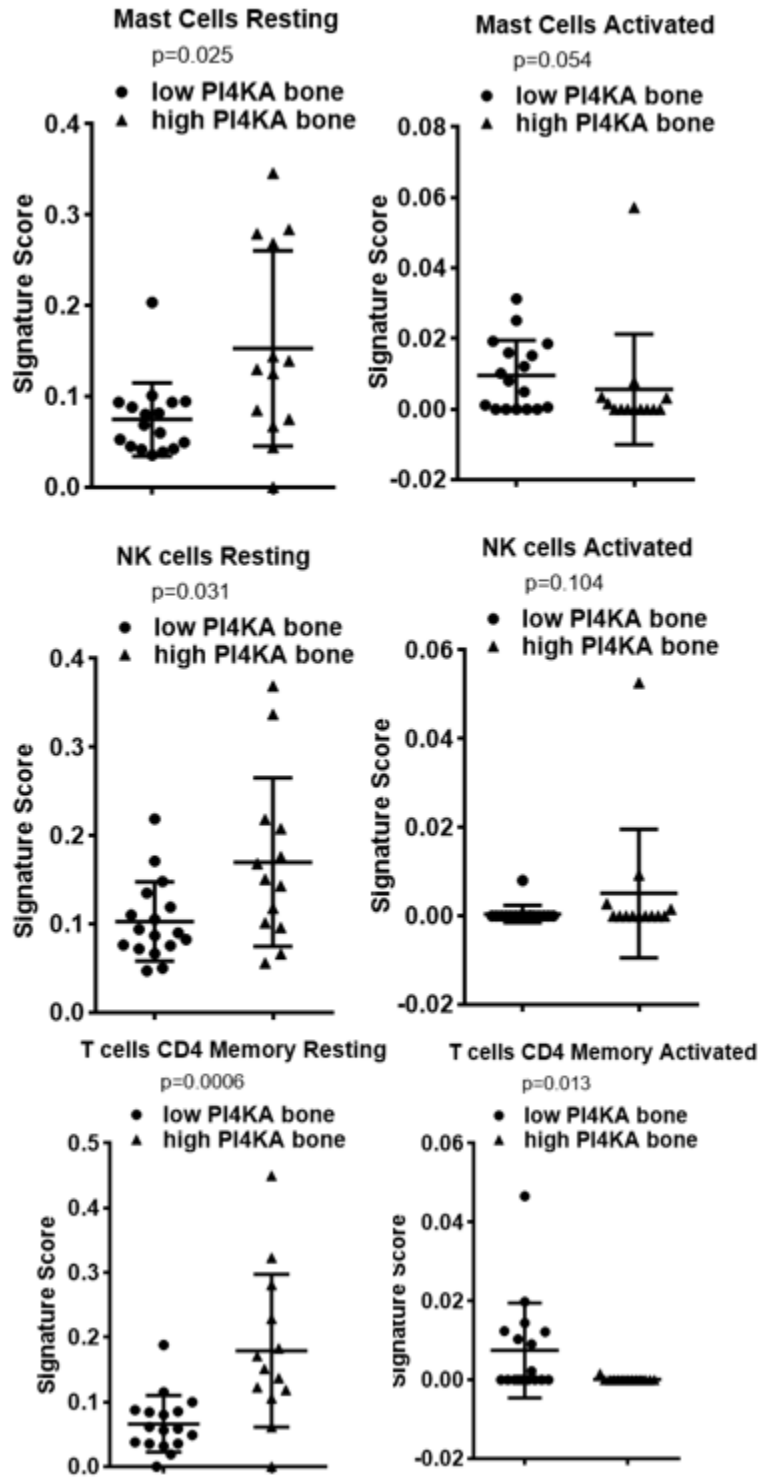


**Figure 38. Immune expression profile.**

A) between bone and soft-tissue: Soft-tissue biopsies show higher expression of immune-active macrophages (M1), and CD4 memory resting cells. While bone has a higher expression of resting macrophages (M0), immunosuppressive macrophages (M2), CD4 naïve and gamma-delta cells.

B) within the low and high PI4KIII $\alpha$  metastatic bone biopsies: low PI4KIII $\alpha$  expressing biopsies show almost similar expression of immune-active macrophages (M1) as high PI4KIII $\alpha$  biopsies, but high PI4KIII $\alpha$  expressing biopsies also shows higher expressions of resting macrophages (M0), and immunosuppressive macrophages (M2).

Other immune cells of significance such as mast cells, natural killer (NK) cells, and CD4 memory cells are of higher expression in their resting state in high PI4KIII $\alpha$  expressing biopsies, whereas they are of higher expression in their active state in low PI4KIII $\alpha$  expressing biopsies.

---

**6.2 Discussion.** The significance of PI4KIII $\alpha$  is evident in these metastatic samples from hormone sensitive PCa patient, on the basis of poor OS and PSA in bone biopsies with higher expression levels. The COX regression analysis also pointed towards significance in genes associated with PI4KIII $\alpha$  to be implicated in poor OS in bone biopsies. PI4KIII $\alpha$  seems to be of relevance in the hormone sensitive patients that underwent Bicalutamide treatment compared to Enzalutamide, this could underscore one of the limitations of the data availability of our patient cohort. PI4KIII $\alpha$  could potentially be of much importance in castrate-resistant patients when they are undergoing new generation androgen blockade therapies and this could only be verified if the OS and PSA data of patients are followed up for a longer time period, as resistance is known to be acquired overtime especially with the new generation drugs. This is evident from both PI4KIII $\alpha$  and EFR3B being significantly overexpressed in populations of neuro-endocrine differentiation (NED) (Fig

29B). NED is used as an identification marker for CRPC and is a characteristic of a more aggressive PCa with poor prognosis. The signaling transductions involved in this NED has been of interest for possible diagnostic and therapeutic targets. For example, 5-HT and PHTrP are associated with malignant growth and dysregulation through stimulation of GPCRs; neuropeptides also transduce messages through Src, PI3K/AKT, FAK kinases by activating transcription factors like NF $\kappa$ B<sup>170</sup>. Our Beltran analysis show PI4KIII $\alpha$  levels associate with a NE phenotype ( Fig 29B), so PI4KIII $\alpha$  inhibitors might prove useful in combination with other NED associated CRPC therapeutic strategies, such as somatostatin analogs that also couple to G proteins, bombesin antagonists, aurora kinase inhibitors, zoledronic acid et cetera<sup>170</sup>.

The patient tumor studies (GDS3289, GSE6919) show high PI4KIII $\alpha$  expression levels correlate with PCa metastatic tumor population. These findings support our DEG analysis that identified metastatic bone biopsies expressing high PI4KIII $\alpha$ , to be enriched in cell proliferative pathways, potentially contributing to the metastatic and invasive phenotype we observe in the public datasets.

When studying how race contributes to the development of PCa, it definitely seems to be one of the contributing factors in the proliferative and invasive capacity leading to metastasis, between AA and non-AA patients. Firstly, AA patients have the highest enrichment of androgen response pathways when compared to other races through GSEA analysis of metastatic biopsies (Fig 34). Interestingly in the clinical studies using our biopsies show, AA patients have better outcomes to PSA response with enzalutamide<sup>159</sup>. When AA patient were stratified based on the origin of biopsy, the GSEA analysis additionally showed enrichment of epithelial-mesenchymal-transition (EMT) pathways in bone biopsies, further contributing to the aggressive phenotype in the AA cohort.

PCa has a highly immuno-suppressive environment from a multi-factorial regulatory, pro-tumorigenic and immunosuppressive environment, contributing to broad mechanisms of resistance. The potential contribution or mere presence of PI4KIII $\alpha$  in more immunosuppressive profiles of metastatic bone biopsies, opens more potential areas of exploration on how PI4KIII $\alpha$  influences the TME of PCa. This is due to the Currently there are many ongoing trials that are testing immunotherapies with anti-CTLA-4, anti-PD-1/PD-L1, anti-CTLA-4 + anti-PD1/PD-L1, adenosine pathway inhibitors, bispecific antibodies and CART T cells, mostly in mCRPC and in some HSPC, mHSPC and CRPC cohorts. These are tested in combination with chemotherapy, anti-androgens, anti-CD73, antiangiogenics, PARP inhibitors, cytokine-targeted therapy, antitumor vaccines, immune checkpoint inhibitors, radiation et cetera. PI4KIII $\alpha$  could be potentially used as a tumor-intrinsic feature or a biomarker for optimizing patient selection, responsive to particular treatments.

In conclusion, we can assert the novel interaction of PI4KIII $\alpha$  and its adaptor protein-TTC7B with CXCR4, plays a role in CXCL12 induced invasion and proliferation, leading to metastasis in advanced PCa, resulting in poor overall OS and PSA progression. The attributes of EFR3B to the PI4KIII $\alpha$ - CXCR4 interaction requires further investigation, by confirmation through interaction studies. The limitations on performing these studies to detect endogenous interaction in cells relies on appropriate EFR3B antibodies, in my work we tried 2 different EFR3 antibodies in interaction studies but none of them are specific to EFR3B. Nonetheless EFR3B is shown to be an important protein in correlation (Table 7) and hazard studies (Table 6), contributing to the OS and PSA in bone. Thus PI4KIII $\alpha$  can be considered as another metastatic molecular feature and should be investigated for its role in resistance and possible immunosuppressive attributes.

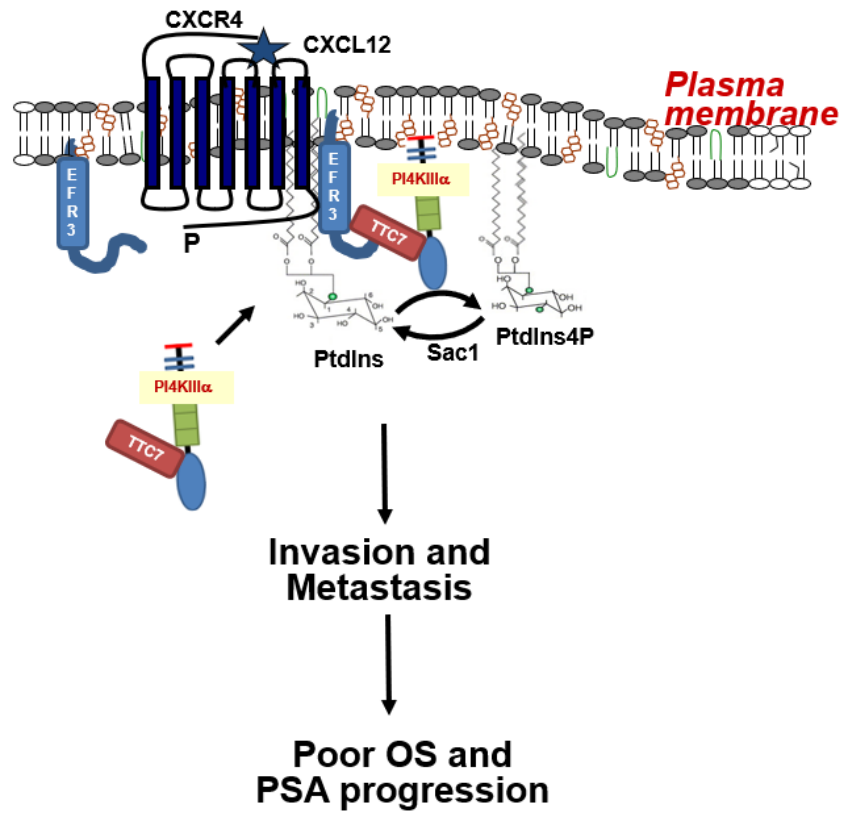


Figure 39. CXCR4 interacts with PI4KIII $\alpha$  leading to PCa invasion and metastasis.

## **MATERIALS AND METHODS**

**7.1 Cell Culture.** Prostate cancer cell lines PC3, C4-2B, VCaP were obtained from ATCC. PC3 and C4-2B were maintained in RPMI-1640 (Gibco-Invitrogen-Life Technologies), and supplemented with 10% heat-inactivated FBS (Hyclone, Fisher Scientific) and 1% P/S (50 units/ml penicillin, 50 ug/ml streptomycin, Gibco). VCaP cells were maintained in DMEM (ATCC), supplemented with 10% regular FBS (Cytiva, Hyclone, Fisher Scientific) and 1% P/S (50 units/ml penicillin, 50 ug/ml streptomycin, Gibco). C4-2B and PC3 stable, lentiviral generated cell lines were maintained in RPMI-1640 (Gibco-Invitrogen-Life Technologies) supplemented with 10% heat-inactivated FBS (Hyclone, Fisher Scientific), 1% P/S (50 units/ml penicillin, 50 ug/ml streptomycin, Gibco) and appropriate selection antibiotics (40ug/ml blasticidin S for PC3-RFP and PC3-CXCR4 overexpressing cells; puromycin at 2ug/ml for PC3 Scr-shRNA or 24ug/ml for PC3-CXCR4 shRNA knockdown cells; 40ug/ml blasticidin S and 0.35ug/ml puromycin for PC3-CXCR4 overexpressing and PI4K or Scr shRNA knockdown cells). All cell cultures were performed at 37°C with 5% CO<sub>2</sub>. All cell lines were authenticated with STR analysis (Genomics core at Michigan State University, East Lansing, MI) and shown to have markers respective for each cell line as established by ATCC, and were tested for mycoplasma contamination prior with Venor-GeM mycoplasma detection kit (Sigma Biochemicals, St. Louis, MO).

**7.2 Lentiviral generation of stable cell-lines.** Stably transduced PC3 cells with a knocked-down (GIPZ shRNA-CXCR4 lentiviral construct) or overexpressed (pLOC-CXCR4 lentiviral construct) CXCR4 gene were produced using a Trans-Lentiviral Packaging Kit (Thermo-Fisher Scientific) according to manufacturer's protocols. Briefly, pLOC-CXCR4 was generated by PCR cloning of CXCR4 gene from a pCDNA3-CXCR4 construct (30) as template. Transfection into HEK293T cells generated infectious, non-replicating pseudoviral particles used to stably transduce PC3 cells

and isolate stable clones selected with blasticidin S. GIPZshRNA-CXCR4 lentiviral construct targeting the 5'-UTR of CXCR4 mRNA (mature antisense sequence: 5'-ACAGCAACTAAGAACTTGG-3') was purchased/obtained through GE Dharmacon (Lafayette, CO 80026)/Wayne State University Biobank Core Facility and used in a similar manner to transduce PC3 cells with infectious, replication incompetent lentiviral particles to generate stable CXCR4-knockdown cells using puromycin for selection of stable clones. For selecting stable clones, lentivirus transduced cells were seeded in 96 well plates at single cell density, monitored for GFP/RFP fluorescence and treated with either blasticidin S or puromycin. Two clones were further characterized for CXCR4 overexpression and knockdown and used in subsequent experiments.

**7.3 Western Blot analysis.** Total cellular proteins were extracted using RIPA buffer with 1x Protease inhibitor cocktail (Roche, Indianapolis, IN). Protein was quantified using BCA protein assay (Pierce Biotechnology, Rockford, IL). Western blotting was performed using SDS-PAGE with gel transfer to a nitrocellulose membrane. Membranes were blocked in 5% BSA, probed with primary antibody in 5% BSA, and with secondary antibody linked with horseradish peroxidase, in 5%BSA. Enhanced chemiluminescence (ECL) substrate and autoradiography film was used to detect proteins. Primary and secondary antibodies are listed in Table . Densitometry was performed using image J software.

**7.4 Immunoprecipitation.** Prostate cancer cells were grown in their respective complete media till 70% confluency. Transient transfections were performed if showing native interactions with over-expressions using 15ug of plasmid and Lipofectamine2000 Transfection Reagent (Life Technologies, Invitrogen) in Opti-MEM media (Gibco). Cells were serum starved overnight, washed with PBS and treated with ligand CXCL12 (Peprotech, final [200ng/ml]) for 10 minutes

or left untreated. Cells were then lysed with 500ul/100mm-plate RIPA lysis buffer. Lysates were rotated in 4C for 15 minutes, and centrifuged at 15,000rpm for 15 minutes. The supernatants were used to determine protein concentration using BCA protein assay kit. (ThermoFisher Scientific). 400-600ug of protein lysate were rotated with 4ug of antibody (CXCR4 AB1846 Millipore) at 4C overnight., followed by rotation with 40ul of Pierce Protein A/G agarose (ThermoScientific) next day for 2 hours at 4C. The samples were centrifuged at 5000rpm for 30secs, and washed 3 times with RIPA bead wash-buffer and resuspended in denaturing sample buffer. The input samples along with the immunoprecipitation samples were heated at 100C for 5 minutes and immunoblotted as per Western blot analysis protocol.

**7.5 PI4KIII $\alpha$  lipid kinase assay.** In vitro PI4KIII $\alpha$  lipid kinase assays were performed as described earlier (22). Post kinase assay the chloroform-extracted PI(4)P product was separated by thin-layer chromatography (TLC) in n-propanol-2M acetic acid (65:35 v/v). PtdIns was visualized with I2 vapor following PI(4)P detection through autoradiography. PI4KIII $\alpha$  activity was set as one-fold in control PC3 cells (PC3 Scr and PC3-RFP) and compared with CXCR4 manipulated cells.

**7.6 Cell proliferation and invasion assays.** For cell proliferation, Prostate cancer cells were plated in 96-well by supplementing media with 10mM of HEPES buffer, with the appropriate drug treatments as applicable. Viable cells were measure using WST-1 (Roche) as per manufacturers protocol. For cell invasion 24-well 8uM transwells (Falcon) were coated with 37.5ug Matrigel per insert, cells were seeded on the top of the chamber in serum-free media, along with chemo - attractants in the lower chamber in serum-free media. After 24 hours cells were stained with 0.9% crystal violet, and imaged for quantitation.

**7.7 Fluorescence microscopy.** Cells were plated on coverslips coated with poly-L-lysine (Sigma) in a 6-well plate, and transfected with 2.5ug of respective plasmids with lipofectamine. Cells were serum starved overnight; treated with either 2uM GSK-F1 or 4ug/ml AMD-3100 for 2 hours and then ligand-induced with CXCL12 (200mg/ml, Peprotech). After treatment, cells were fixed with 4% PFA with 0.2% glutaraldehyde at room temperature for 15 minutes. After aspiration, cells were further incubated with 50mM NH<sub>4</sub>Cl in PBS and washed for 10 minutes, 3 times. Then cells were thoroughly washed with water, and mounted on slides using Vectashield with DAPI. Cells were imaged using Leica DMI3000 B fluorescence microscope.

**7.8 Proximity Ligation Assay.** Cells were plated on chamber slides and serum starved overnight. After ligand induction with CXCL12 (200ng/ml), cells were fixed with 4% PFA and permeabilized with mild buffer 0.01% tween-20 in PBS. The cells were further treated as per the Sigma Duolink DUO92101-1 kit. CXCR4-mouse and TTC7B-rabbit antibodies were used for primary incubation and observed for the presence of co-localization of CXCR4 and TTC7B using fluorescence microscope.

**7.9 Gene Expression Omnibus Database.** GDS3289 from the public database of GEO-NCBI was used to analyze the PI4KIII $\alpha$  expression from LCM-captured epithelial cell populations that represent prostate cancer progression from benign to metastatic disease. The total 104 epithelial and stromal samples from these different states were extracted, by downloading the platform and matrix files from the GDS3289 database. Data in the files were converted to log<sub>2</sub> scale and analyzed using GraphPad Prism 6.

**7.10 Patient and Clinical data.** Pre-biopsy samples from 50 patients with metastatic hormone-sensitive prostate cancer (mHSPC) were used for the clinical analysis in these studies. These patients participated in a multi-center trial conducted in 4 different centers in the US. These men

have no history of seizures, and have adequate marrow, renal and liver function, with a median age of 65. Clinical outcome data of the PSA response rate and Overall Survival statistics were obtained from this study for our analysis (Clinical trial: Identifier: NCT02058706). Total RNA was extracted using the RNeasy midi kits (Qiagen) along with ON-Column DNase digestion (Qiagen), as described below, and submitted to the core. A total of 32 bone biopsies and 18 soft-tissue biopsies were used in this study after RNA quality was confirmed, and RNA-sequencing (RNA-seq) was performed. The GSEA analysis was performed on the resulting RNA-seq TPM data, as described below. The upregulation and downregulation of genes in the pathways after this enrichment analysis was further verified by RT-PCR. Cibersortx machine-learning tool was also utilized to identify immune expression profile using the LM22 signature.

**7.11 RNA-sequencing analysis.** Transcriptomic analysis of PC3-CXCR4 Scr and 27-PI4KA shRNA cells were performed in quadruplicates. RNA was prepared from cultured cells using the Qiagen RNeasy mini kits (Qiagen) along with ON-Column DNase digestion (Qiagen), and submitted to the core. Poly-A pulldown was performed for total RNA enrichment with an acceptable RIN number above 7.

**7.12 Gene Set Enrichment Analysis.** Pathway enrichment was performed using GSEA software (version 4.1). The Hallmark pathway dataset was downloaded from the MsigDB database of the GSEA website. The Scr vs 27-PI4KA shRNA expression profile data and the attribute files were enriched and analyzed by default weighted enrichment statistics. The number of permutations was set to 1000. Similar methods were followed to analyze the metastatic biopsies of hormone-sensitive PCa patients.

**7.13 Pathway Analysis.** Pathway analysis was performed using iPathwayGuide (Advaita Bioinformatics) and DEGs with fold change  $\geq 1.5$  and FDR  $\leq 0.05$  was considered significant.

The software uses the DEG interactions as mapped by the Kyoto Encyclopedia of Genes and Genomes, (KEGG) database.

**7.14 Statistical Analysis.** GraphPad Prism 6 was used to assess statistical significance. Unpaired non-parametric t-test (Mann-Whitney) and one-way Anova followed by Tukey post-test were used to determine statistical significance ( $P < 0.05$ ) by comparing means of control and experimental groups. \*:  $P$  value  $< 0.05$ . \*\*:  $P$  value  $< 0.01$ . \*\*\*  $P$  value  $< 0.001$ . NS stands for “not significant”.

### **7.15 Antibody links.**

Anti-Rabbit HRP Linked CELL SIGNALING 7074S (1:5000) [DataSheet](#)

Mouse Anti-rabbit IgG (Conformation Specific) (L27A9) mAb (HRP Conjugate) CELL SIGNALING #5127 (1:5000) [DataSheet](#)

CXCR4 Millipore rabbit AB1846 (1:5000) [DataSheet](#)

CXCR4 R&D mouse MAB172 (for IF) [DataSheet](#)

TTC7B Invitrogen/ ThermoFisher PA5-63750 (1:1000) [DataSheet](#)

PI4KA Cell-signaling PA5-63750 #4902 (1:1000) [DataSheet](#)

Anti-mouse HRP linked CELL SIGNALING 7076S [DataSheet](#)

Protein A HRP conjugate CELL SIGNALING 12291S (1:1000) [DataSheet](#)

EFR3B LSBIO ab LS-C186976 [DataSheet](#)

EFR3B ABCAM ab-177971 [DataSheet](#)

Phospho-AKT rabbit CELL SIGNALING (1:1000) [DataSheet](#)

AKT-pan rabbit CELL SIGNALING (1:1000) [DataSheet](#)

AGXT2 mouse Proteintech (1:6000) [DataSheet](#)

GAPDH rabbit Proteintech (1:10,000) [DataSheet](#)

OTUD7A Novusbio rabbit Proteintech (1:1,000, but very strong so 1:2000 can try) [DataSheet](#)

EFHD1 Novusbio rabbit Proteintech (1:1,000) [DataSheet](#)

MMP1 R&D Biotechne mouse (powder reconstituted at 0.5mg/ml to 2ug/ml in 5%BSA)

[DataSheet](#)

**REFERENCES**

1. Sbrissa D, Semaan L, Govindarajan B, Li Y, Caruthers NJ, Stemmer PM, Cher ML, Sethi S, Vaishampayan U, Shisheva A, Chinni SR. A novel cross-talk between CXCR4 and PI4KIIIalpha in prostate cancer cells. *Oncogene*. 2019;38(3):332-44. Epub 20180815. doi: 10.1038/s41388-018-0448-0. PubMed PMID: 30111818; PMCID: PMC6336684.
2. van Zijl F, Krupitza G, Mikulits W. Initial steps of metastasis: cell invasion and endothelial transmigration. *Mutat Res*. 2011;728(1-2):23-34. Epub 20110512. doi: 10.1016/j.mrrev.2011.05.002. PubMed PMID: 21605699; PMCID: PMC4028085.
3. Hapach LA, Mosier JA, Wang W, Reinhart-King CA. Engineered models to parse apart the metastatic cascade. *NPJ Precis Oncol*. 2019;3:20. Epub 20190821. doi: 10.1038/s41698-019-0092-3. PubMed PMID: 31453371; PMCID: PMC6704099.
4. Pachmayr E, Treese C, Stein U. Underlying Mechanisms for Distant Metastasis - Molecular Biology. *Visc Med*. 2017;33(1):11-20. Epub 20170209. doi: 10.1159/000454696. PubMed PMID: 28785563; PMCID: PMC5520302.
5. Jiang WG, Sanders AJ, Katoh M, Ungefroren H, Gieseler F, Prince M, Thompson SK, Zollo M, Spano D, Dhawan P, Sliva D, Subbarayan PR, Sarkar M, Honoki K, Fujii H, Georgakilas AG, Amedei A, Niccolai E, Amin A, Ashraf SS, Ye L, Helferich WG, Yang X, Boosani CS, Guha G, Ciriolo MR, Aquilano K, Chen S, Azmi AS, Keith WN, Bilsland A, Bhakta D, Halicka D, Newsheer S, Pantano F, Santini D. Tissue invasion and metastasis: Molecular, biological and clinical perspectives. *Semin Cancer Biol*. 2015;35 Suppl:S244-S75. Epub 20150410. doi: 10.1016/j.semcancer.2015.03.008. PubMed PMID: 25865774.

6. Sznurkowska MK, Aceto N. The gate to metastasis: key players in cancer cell intravasation. *FEBS J.* 2021. Epub 20210602. doi: 10.1111/febs.16046. PubMed PMID: 34077633.
7. Nelson WG, De Marzo AM, Isaacs WB. Prostate cancer. *N Engl J Med.* 2003;349(4):366-81. doi: 10.1056/NEJMra021562. PubMed PMID: 12878745.
8. Gandaglia G, Abdollah F, Schifffmann J, Trudeau V, Shariat SF, Kim SP, Perrotte P, Montorsi F, Briganti A, Trinh QD, Karakiewicz PI, Sun M. Distribution of metastatic sites in patients with prostate cancer: A population-based analysis. *Prostate.* 2014;74(2):210-6. Epub 20131016. doi: 10.1002/pros.22742. PubMed PMID: 24132735.
9. Macedo F, Ladeira K, Pinho F, Saraiva N, Bonito N, Pinto L, Goncalves F. Bone Metastases: An Overview. *Oncol Rev.* 2017;11(1):321. Epub 20170509. doi: 10.4081/oncol.2017.321. PubMed PMID: 28584570; PMCID: PMC5444408.
10. Cackowski FC, Heath EI. Prostate cancer dormancy and recurrence. *Cancer Lett.* 2022;524:103-8. Epub 20211005. doi: 10.1016/j.canlet.2021.09.037. PubMed PMID: 34624433; PMCID: PMC8694498.
11. Litwin MS, Tan HJ. The Diagnosis and Treatment of Prostate Cancer: A Review. *JAMA.* 2017;317(24):2532-42. doi: 10.1001/jama.2017.7248. PubMed PMID: 28655021.
12. Aly M, Leval A, Schain F, Liwing J, Lawson J, Vago E, Nordstrom T, Andersson TM, Sjoland E, Wang C, Eloranta S, Akre O. Survival in patients diagnosed with castration-resistant prostate cancer: a population-based observational study in Sweden. *Scand J Urol.* 2020;54(2):115-21. Epub 20200408. doi: 10.1080/21681805.2020.1739139. PubMed PMID: 32266854.

13. Watson PA, Arora VK, Sawyers CL. Emerging mechanisms of resistance to androgen receptor inhibitors in prostate cancer. *Nat Rev Cancer*. 2015;15(12):701-11. Epub 20151113. doi: 10.1038/nrc4016. PubMed PMID: 26563462; PMCID: PMC4771416.
14. Formaggio N, Rubin MA, Theurillat JP. Loss and revival of androgen receptor signaling in advanced prostate cancer. *Oncogene*. 2021;40(7):1205-16. Epub 20210108. doi: 10.1038/s41388-020-01598-0. PubMed PMID: 33420371; PMCID: PMC7892335.
15. Gan L, Chen S, Wang Y, Watahiki A, Bohrer L, Sun Z, Wang Y, Huang H. Inhibition of the androgen receptor as a novel mechanism of taxol chemotherapy in prostate cancer. *Cancer Res*. 2009;69(21):8386-94. Epub 20091013. doi: 10.1158/0008-5472.CAN-09-1504. PubMed PMID: 19826044; PMCID: PMC2783542.
16. de Bono JS, Oudard S, Ozguroglu M, Hansen S, Machiels JP, Kocak I, Gravis G, Bodrogi I, Mackenzie MJ, Shen L, Roessner M, Gupta S, Sartor AO, Investigators T. Prednisone plus cabazitaxel or mitoxantrone for metastatic castration-resistant prostate cancer progressing after docetaxel treatment: a randomised open-label trial. *Lancet*. 2010;376(9747):1147-54. doi: 10.1016/S0140-6736(10)61389-X. PubMed PMID: 20888992.
17. McNevin CS, Baird AM, McDermott R, Finn SP. Diagnostic Strategies for Treatment Selection in Advanced Prostate Cancer. *Diagnostics (Basel)*. 2021;11(2). Epub 20210219. doi: 10.3390/diagnostics11020345. PubMed PMID: 33669657; PMCID: PMC7922176.
18. Parker C, Nilsson S, Heinrich D, Helle SI, O'Sullivan JM, Fossa SD, Chodacki A, Wiechno P, Logue J, Seke M, Widmark A, Johannessen DC, Hoskin P, Bottomley D, James ND, Solberg A, Syndikus I, Kliment J, Wedel S, Boehmer S, Dall'Oglio M, Franzen L, Coleman R, Vogelzang NJ, O'Bryan-Tear CG, Staudacher K, Garcia-Vargas J, Shan M, Bruland OS, Sartor O,

- Investigators A. Alpha emitter radium-223 and survival in metastatic prostate cancer. *N Engl J Med.* 2013;369(3):213-23. doi: 10.1056/NEJMoa1213755. PubMed PMID: 23863050.
19. Di Paolo G, De Camilli P. Phosphoinositides in cell regulation and membrane dynamics. *Nature.* 2006;443(7112):651-7. doi: 10.1038/nature05185. PubMed PMID: 17035995.
20. Burke JE. Structural Basis for Regulation of Phosphoinositide Kinases and Their Involvement in Human Disease. *Mol Cell.* 2018;71(5):653-73. doi: 10.1016/j.molcel.2018.08.005. PubMed PMID: 30193094.
21. Waugh MG. Phosphatidylinositol 4-kinases, phosphatidylinositol 4-phosphate and cancer. *Cancer Lett.* 2012;325(2):125-31. Epub 20120628. doi: 10.1016/j.canlet.2012.06.009. PubMed PMID: 22750097.
22. De Matteis MA, D'Angelo G. The role of the phosphoinositides at the Golgi complex. *Biochem Soc Symp.* 2007(74):107-16. doi: 10.1042/BSS0740107. PubMed PMID: 17233584.
23. Balla A, Balla T. Phosphatidylinositol 4-kinases: old enzymes with emerging functions. *Trends Cell Biol.* 2006;16(7):351-61. Epub 20060621. doi: 10.1016/j.tcb.2006.05.003. PubMed PMID: 16793271.
24. D'Angelo G, Vicinanza M, Di Campli A, De Matteis MA. The multiple roles of PtdIns(4)P -- not just the precursor of PtdIns(4,5)P<sub>2</sub>. *J Cell Sci.* 2008;121(Pt 12):1955-63. doi: 10.1242/jcs.023630. PubMed PMID: 18525025.
25. Sbrissa D, Ikonomov OC, Fu Z, Ijuin T, Gruenberg J, Takenawa T, Shisheva A. Core protein machinery for mammalian phosphatidylinositol 3,5-bisphosphate synthesis and turnover that regulates the progression of endosomal transport. Novel Sac phosphatase joins the ArPIKfyve-PIKfyve complex. *J Biol Chem.* 2007;282(33):23878-91. Epub 20070607. doi: 10.1074/jbc.M611678200. PubMed PMID: 17556371.

26. Gehrmann T, Heilmeyer LM, Jr. Phosphatidylinositol 4-kinases. *Eur J Biochem.* 1998;253(2):357-70. doi: 10.1046/j.1432-1327.1998.2530357.x. PubMed PMID: 9654085.
27. Clayton EL, Minogue S, Waugh MG. Mammalian phosphatidylinositol 4-kinases as modulators of membrane trafficking and lipid signaling networks. *Prog Lipid Res.* 2013;52(3):294-304. Epub 20130419. doi: 10.1016/j.plipres.2013.04.002. PubMed PMID: 23608234; PMCID: PMC3989048.
28. Nakatsu F, Baskin JM, Chung J, Tanner LB, Shui G, Lee SY, Pirruccello M, Hao M, Ingolia NT, Wenk MR, De Camilli P. PtdIns4P synthesis by PI4KIIIalpha at the plasma membrane and its impact on plasma membrane identity. *J Cell Biol.* 2012;199(6):1003-16. doi: 10.1083/jcb.201206095. PubMed PMID: 23229899; PMCID: PMC3518224.
29. Boura E, Nencka R. Phosphatidylinositol 4-kinases: Function, structure, and inhibition. *Exp Cell Res.* 2015;337(2):136-45. Epub 20150714. doi: 10.1016/j.yexcr.2015.03.028. PubMed PMID: 26183104.
30. Bojjireddy N, Botyanszki J, Hammond G, Creech D, Peterson R, Kemp DC, Snead M, Brown R, Morrison A, Wilson S, Harrison S, Moore C, Balla T. Pharmacological and genetic targeting of the PI4KA enzyme reveals its important role in maintaining plasma membrane phosphatidylinositol 4-phosphate and phosphatidylinositol 4,5-bisphosphate levels. *J Biol Chem.* 2014;289(9):6120-32. Epub 20140110. doi: 10.1074/jbc.M113.531426. PubMed PMID: 24415756; PMCID: PMC3937678.
31. Berger KL, Cooper JD, Heaton NS, Yoon R, Oakland TE, Jordan TX, Mateu G, Grakoui A, Randall G. Roles for endocytic trafficking and phosphatidylinositol 4-kinase III alpha in hepatitis C virus replication. *Proc Natl Acad Sci U S A.* 2009;106(18):7577-82. Epub 20090417. doi: 10.1073/pnas.0902693106. PubMed PMID: 19376974; PMCID: PMC2678598.

32. Borawski J, Troke P, Puyang X, Gibaja V, Zhao S, Mickanin C, Leighton-Davies J, Wilson CJ, Myer V, Cornellataracido I, Baryza J, Tallarico J, Joberty G, Bantscheff M, Schirle M, Bouwmeester T, Mathy JE, Lin K, Compton T, Labow M, Wiedmann B, Gaither LA. Class III phosphatidylinositol 4-kinase alpha and beta are novel host factor regulators of hepatitis C virus replication. *J Virol*. 2009;83(19):10058-74. Epub 20090715. doi: 10.1128/JVI.02418-08. PubMed PMID: 19605471; PMCID: PMC2748049.
33. Reiss S, Rebhan I, Backes P, Romero-Brey I, Erfle H, Matula P, Kaderali L, Poenisch M, Blankenburg H, Hiet MS, Longereich T, Diehl S, Ramirez F, Balla T, Rohr K, Kaul A, Buhler S, Pepperkok R, Lengauer T, Albrecht M, Eils R, Schirmacher P, Lohmann V, Bartenschlager R. Recruitment and activation of a lipid kinase by hepatitis C virus NS5A is essential for integrity of the membranous replication compartment. *Cell Host Microbe*. 2011;9(1):32-45. doi: 10.1016/j.chom.2010.12.002. PubMed PMID: 21238945; PMCID: PMC3433060.
34. Altan-Bonnet N, Balla T. Phosphatidylinositol 4-kinases: hostages harnessed to build panviral replication platforms. *Trends Biochem Sci*. 2012;37(7):293-302. Epub 20120525. doi: 10.1016/j.tibs.2012.03.004. PubMed PMID: 22633842; PMCID: PMC3389303.
35. Akimana C, Al-Khodor S, Abu Kwaik Y. Host factors required for modulation of phagosome biogenesis and proliferation of *Francisella tularensis* within the cytosol. *PLoS One*. 2010;5(6):e11025. Epub 20100611. doi: 10.1371/journal.pone.0011025. PubMed PMID: 20552012; PMCID: PMC2883998.
36. Baskin JM, Wu X, Christiano R, Oh MS, Schauder CM, Gazzo E, Messa M, Baldassari S, Assereto S, Biancheri R, Zara F, Minetti C, Raimondi A, Simons M, Walther TC, Reinisch KM, De Camilli P. The leukodystrophy protein FAM126A (hyccin) regulates PtdIns(4)P synthesis at

the plasma membrane. *Nat Cell Biol.* 2016;18(1):132-8. Epub 20151116. doi: 10.1038/ncb3271. PubMed PMID: 26571211; PMCID: PMC4689616.

37. Lees JA, Zhang Y, Oh MS, Schauder CM, Yu X, Baskin JM, Dobbs K, Notarangelo LD, De Camilli P, Walz T, Reinisch KM. Architecture of the human PI4KIIIalpha lipid kinase complex. *Proc Natl Acad Sci U S A.* 2017;114(52):13720-5. Epub 20171211. doi: 10.1073/pnas.1718471115. PubMed PMID: 29229838; PMCID: PMC5748228.

38. Wu X, Chi RJ, Baskin JM, Lucast L, Burd CG, De Camilli P, Reinisch KM. Structural insights into assembly and regulation of the plasma membrane phosphatidylinositol 4-kinase complex. *Dev Cell.* 2014;28(1):19-29. Epub 20131219. doi: 10.1016/j.devcel.2013.11.012. PubMed PMID: 24360784; PMCID: PMC4349574.

39. Baird D, Stefan C, Audhya A, Weys S, Emr SD. Assembly of the PtdIns 4-kinase Stt4 complex at the plasma membrane requires Ypp1 and Efr3. *J Cell Biol.* 2008;183(6):1061-74. doi: 10.1083/jcb.200804003. PubMed PMID: 19075114; PMCID: PMC2600738.

40. Burke JE, Inglis AJ, Perisic O, Masson GR, McLaughlin SH, Rutaganira F, Shokat KM, Williams RL. Structures of PI4KIIIbeta complexes show simultaneous recruitment of Rab11 and its effectors. *Science.* 2014;344(6187):1035-8. doi: 10.1126/science.1253397. PubMed PMID: 24876499; PMCID: PMC4046302.

41. Antonny B, Bigay J, Mesmin B. The Oxysterol-Binding Protein Cycle: Burning Off PI(4)P to Transport Cholesterol. *Annu Rev Biochem.* 2018;87:809-37. Epub 20180329. doi: 10.1146/annurev-biochem-061516-044924. PubMed PMID: 29596003.

42. Stefan CJ, Manford AG, Baird D, Yamada-Hanff J, Mao Y, Emr SD. Osh proteins regulate phosphoinositide metabolism at ER-plasma membrane contact sites. *Cell.* 2011;144(3):389-401. doi: 10.1016/j.cell.2010.12.034. PubMed PMID: 21295699.

43. Zewe JP, Wills RC, Sangappa S, Goulden BD, Hammond GR. SAC1 degrades its lipid substrate PtdIns4P in the endoplasmic reticulum to maintain a steep chemical gradient with donor membranes. *Elife*. 2018;7. Epub 20180220. doi: 10.7554/eLife.35588. PubMed PMID: 29461204; PMCID: PMC5829913.
44. Balla T. Rushing to maintain plasma membrane phosphoinositide levels. *J Gen Physiol*. 2020;152(12). doi: 10.1085/jgp.202012793. PubMed PMID: 33186443; PMCID: PMC7671492.
45. Nakatsu F, Kawasaki A. Functions of Oxysterol-Binding Proteins at Membrane Contact Sites and Their Control by Phosphoinositide Metabolism. *Front Cell Dev Biol*. 2021;9:664788. Epub 20210624. doi: 10.3389/fcell.2021.664788. PubMed PMID: 34249917; PMCID: PMC8264513.
46. Hammond GR, Fischer MJ, Anderson KE, Holdich J, Koteci A, Balla T, Irvine RF. PI4P and PI(4,5)P<sub>2</sub> are essential but independent lipid determinants of membrane identity. *Science*. 2012;337(6095):727-30. Epub 20120621. doi: 10.1126/science.1222483. PubMed PMID: 22722250; PMCID: PMC3646512.
47. Hammond GR, Schiavo G, Irvine RF. Immunocytochemical techniques reveal multiple, distinct cellular pools of PtdIns4P and PtdIns(4,5)P<sub>2</sub>. *Biochem J*. 2009;422(1):23-35. Epub 20090729. doi: 10.1042/BJ20090428. PubMed PMID: 19508231; PMCID: PMC2722159.
48. Balla A, Kim YJ, Varnai P, Szentpetery Z, Knight Z, Shokat KM, Balla T. Maintenance of hormone-sensitive phosphoinositide pools in the plasma membrane requires phosphatidylinositol 4-kinase III $\alpha$ . *Mol Biol Cell*. 2008;19(2):711-21. Epub 20071212. doi: 10.1091/mbc.e07-07-0713. PubMed PMID: 18077555; PMCID: PMC2230591.
49. Balla A, Tuymetova G, Tsiomenko A, Varnai P, Balla T. A plasma membrane pool of phosphatidylinositol 4-phosphate is generated by phosphatidylinositol 4-kinase type-III  $\alpha$ :

studies with the PH domains of the oxysterol binding protein and FAPP1. *Mol Biol Cell*. 2005;16(3):1282-95. Epub 20050105. doi: 10.1091/mbc.e04-07-0578. PubMed PMID: 15635101; PMCID: PMC551492.

50. Korzeniowski MK, Popovic MA, Szentpetery Z, Varnai P, Stojilkovic SS, Balla T. Dependence of STIM1/Orai1-mediated calcium entry on plasma membrane phosphoinositides. *J Biol Chem*. 2009;284(31):21027-35. Epub 20090529. doi: 10.1074/jbc.M109.012252. PubMed PMID: 19483082; PMCID: PMC2742867.

51. Bunney TD, Katan M. Phosphoinositide signalling in cancer: beyond PI3K and PTEN. *Nat Rev Cancer*. 2010;10(5):342-52. doi: 10.1038/nrc2842. PubMed PMID: 20414202.

52. Yuan TL, Cantley LC. PI3K pathway alterations in cancer: variations on a theme. *Oncogene*. 2008;27(41):5497-510. doi: 10.1038/onc.2008.245. PubMed PMID: 18794884; PMCID: PMC3398461.

53. Samuels Y, Wang Z, Bardelli A, Silliman N, Ptak J, Szabo S, Yan H, Gazdar A, Powell SM, Riggins GJ, Willson JK, Markowitz S, Kinzler KW, Vogelstein B, Velculescu VE. High frequency of mutations of the PIK3CA gene in human cancers. *Science*. 2004;304(5670):554. Epub 20040311. doi: 10.1126/science.1096502. PubMed PMID: 15016963.

54. Jia S, Liu Z, Zhang S, Liu P, Zhang L, Lee SH, Zhang J, Signoretti S, Loda M, Roberts TM, Zhao JJ. Essential roles of PI(3)K-p110beta in cell growth, metabolism and tumorigenesis. *Nature*. 2008;454(7205):776-9. Epub 20080625. doi: 10.1038/nature07091. PubMed PMID: 18594509; PMCID: PMC2750091.

55. Wee S, Wiederschain D, Maira SM, Loo A, Miller C, deBeaumont R, Stegmeier F, Yao YM, Lengauer C. PTEN-deficient cancers depend on PIK3CB. *Proc Natl Acad Sci U S A*.

2008;105(35):13057-62. Epub 20080828. doi: 10.1073/pnas.0802655105. PubMed PMID: 18755892; PMCID: PMC2529105.

56. Urick ME, Rudd ML, Godwin AK, Sgroi D, Merino M, Bell DW. PIK3R1 (p85alpha) is somatically mutated at high frequency in primary endometrial cancer. *Cancer Res.* 2011;71(12):4061-7. Epub 20110408. doi: 10.1158/0008-5472.CAN-11-0549. PubMed PMID: 21478295; PMCID: PMC3117071.

57. Jaiswal BS, Janakiraman V, Kljavin NM, Chaudhuri S, Stern HM, Wang W, Kan Z, Dbouk HA, Peters BA, Waring P, Dela Vega T, Kenski DM, Bowman KK, Lorenzo M, Li H, Wu J, Modrusan Z, Stinson J, Eby M, Yue P, Kaminker JS, de Sauvage FJ, Backer JM, Seshagiri S. Somatic mutations in p85alpha promote tumorigenesis through class IA PI3K activation. *Cancer Cell.* 2009;16(6):463-74. doi: 10.1016/j.ccr.2009.10.016. PubMed PMID: 19962665; PMCID: PMC2804903.

58. Meng D, He W, Zhang Y, Liang Z, Zheng J, Zhang X, Zheng X, Zhan P, Chen H, Li W, Cai L. Development of PI3K inhibitors: Advances in clinical trials and new strategies (Review). *Pharmacol Res.* 2021;173:105900. Epub 20210920. doi: 10.1016/j.phrs.2021.105900. PubMed PMID: 34547385.

59. Chu KM, Minogue S, Hsuan JJ, Waugh MG. Differential effects of the phosphatidylinositol 4-kinases, PI4KIIalpha and PI4KIIIbeta, on Akt activation and apoptosis. *Cell Death Dis.* 2010;1:e106. doi: 10.1038/cddis.2010.84. PubMed PMID: 21218173; PMCID: PMC3015391.

60. Li J, Lu Y, Zhang J, Kang H, Qin Z, Chen C. PI4KIIalpha is a novel regulator of tumor growth by its action on angiogenesis and HIF-1alpha regulation. *Oncogene.* 2010;29(17):2550-9. Epub 20100215. doi: 10.1038/onc.2010.14. PubMed PMID: 20154717.

61. Minogue S, Waugh MG, De Matteis MA, Stephens DJ, Berditchevski F, Hsuan JJ. Phosphatidylinositol 4-kinase is required for endosomal trafficking and degradation of the EGF receptor. *J Cell Sci.* 2006;119(Pt 3):571-81. doi: 10.1242/jcs.02752. PubMed PMID: 16443754.
62. Qin Y, Li L, Pan W, Wu D. Regulation of phosphatidylinositol kinases and metabolism by Wnt3a and Dvl. *J Biol Chem.* 2009;284(34):22544-8. Epub 20090626. doi: 10.1074/jbc.M109.014399. PubMed PMID: 19561074; PMCID: PMC2755661.
63. Mossinger J, Wieffer M, Krause E, Freund C, Gerth F, Krauss M, Haucke V. Phosphatidylinositol 4-kinase IIalpha function at endosomes is regulated by the ubiquitin ligase Itch. *EMBO Rep.* 2012;13(12):1087-94. Epub 20121113. doi: 10.1038/embor.2012.164. PubMed PMID: 23146885; PMCID: PMC3512407.
64. Wei YJ, Sun HQ, Yamamoto M, Wlodarski P, Kunii K, Martinez M, Barylko B, Albanesi JP, Yin HL. Type II phosphatidylinositol 4-kinase beta is a cytosolic and peripheral membrane protein that is recruited to the plasma membrane and activated by Rac-GTP. *J Biol Chem.* 2002;277(48):46586-93. Epub 20020924. doi: 10.1074/jbc.M206860200. PubMed PMID: 12324459.
65. Mazzocca A, Liotta F, Carloni V. Tetraspanin CD81-regulated cell motility plays a critical role in intrahepatic metastasis of hepatocellular carcinoma. *Gastroenterology.* 2008;135(1):244-56 e1. Epub 20080321. doi: 10.1053/j.gastro.2008.03.024. PubMed PMID: 18466772.
66. Jeganathan S, Morrow A, Amiri A, Lee JM. Eukaryotic elongation factor 1A2 cooperates with phosphatidylinositol-4 kinase III beta to stimulate production of filopodia through increased phosphatidylinositol-4,5 bisphosphate generation. *Mol Cell Biol.* 2008;28(14):4549-61. Epub 20080512. doi: 10.1128/MCB.00150-08. PubMed PMID: 18474610; PMCID: PMC2447124.

67. Pinke DE, Lee JM. The lipid kinase PI4KIIIbeta and the eEF1A2 oncogene co-operate to disrupt three-dimensional in vitro acinar morphogenesis. *Exp Cell Res.* 2011;317(17):2503-11. Epub 20110807. doi: 10.1016/j.yexcr.2011.08.002. PubMed PMID: 21851817.
68. Ishikawa S, Egami H, Kurizaki T, Akagi J, Tamori Y, Yoshida N, Tan X, Hayashi N, Ogawa M. Identification of genes related to invasion and metastasis in pancreatic cancer by cDNA representational difference analysis. *J Exp Clin Cancer Res.* 2003;22(2):299-306. PubMed PMID: 12866581.
69. Guerreiro AS, Fattet S, Kulesza DW, Atamer A, Elsing AN, Shalaby T, Jackson SP, Schoenwaelder SM, Grotzer MA, Delattre O, Arcaro A. A sensitized RNA interference screen identifies a novel role for the PI3K p110gamma isoform in medulloblastoma cell proliferation and chemoresistance. *Mol Cancer Res.* 2011;9(7):925-35. Epub 20110607. doi: 10.1158/1541-7786.MCR-10-0200. PubMed PMID: 21652733.
70. Giroux V, Iovanna J, Dagorn JC. Probing the human kinome for kinases involved in pancreatic cancer cell survival and gemcitabine resistance. *FASEB J.* 2006;20(12):1982-91. doi: 10.1096/fj.06-6239com. PubMed PMID: 17012250.
71. Adhikari H, Kattan WE, Kumar S, Zhou P, Hancock JF, Counter CM. Oncogenic KRAS is dependent upon an EFR3A-PI4KA signaling axis for potent tumorigenic activity. *Nat Commun.* 2021;12(1):5248. Epub 20210909. doi: 10.1038/s41467-021-25523-5. PubMed PMID: 34504076; PMCID: PMC8429657.
72. Kattan WE, Liu J, Montufar-Solis D, Liang H, Brahmendra Barathi B, van der Hoeven R, Zhou Y, Hancock JF. Components of the phosphatidylserine endoplasmic reticulum to plasma membrane transport mechanism as targets for KRAS inhibition in pancreatic cancer. *Proc Natl*

Acad Sci U S A. 2021;118(51). doi: 10.1073/pnas.2114126118. PubMed PMID: 34903667; PMCID: PMC8713765.

73. Ma H, Blake T, Chitnis A, Liu P, Balla T. Crucial role of phosphatidylinositol 4-kinase IIIalpha in development of zebrafish pectoral fin is linked to phosphoinositide 3-kinase and FGF signaling. *J Cell Sci.* 2009;122(Pt 23):4303-10. Epub 20091103. doi: 10.1242/jcs.057646. PubMed PMID: 19887586; PMCID: PMC2779132.

74. Furuta Y, Uehara T, Nomura Y. Correlation between delayed neuronal cell death and selective decrease in phosphatidylinositol 4-kinase expression in the CA1 subfield of the hippocampus after transient forebrain ischemia. *J Cereb Blood Flow Metab.* 2003;23(8):962-71. doi: 10.1097/01.WCB.0000073948.29308.F8. PubMed PMID: 12902840.

75. Jungerius BJ, Hoogendoorn ML, Bakker SC, Van't Slot R, Bardoel AF, Ophoff RA, Wijmenga C, Kahn RS, Sinke RJ. An association screen of myelin-related genes implicates the chromosome 22q11 PIK4CA gene in schizophrenia. *Mol Psychiatry.* 2008;13(11):1060-8. Epub 20070925. doi: 10.1038/sj.mp.4002080. PubMed PMID: 17893707.

76. Saito T, Stopkova P, Diaz L, Papolos DF, Boussemart L, Lachman HM. Polymorphism screening of PIK4CA: possible candidate gene for chromosome 22q11-linked psychiatric disorders. *Am J Med Genet B Neuropsychiatr Genet.* 2003;116B(1):77-83. doi: 10.1002/ajmg.b.10042. PubMed PMID: 12497619.

77. Rubin JB. Chemokine signaling in cancer: one hump or two? *Semin Cancer Biol.* 2009;19(2):116-22. Epub 20081017. doi: 10.1016/j.semcancer.2008.10.001. PubMed PMID: 18992347; PMCID: PMC2694237.

78. Gahbauer S, Pluhackova K, Bockmann RA. Closely related, yet unique: Distinct homo- and heterodimerization patterns of G protein coupled chemokine receptors and their fine-tuning

- by cholesterol. *PLoS Comput Biol.* 2018;14(3):e1006062. Epub 20180312. doi: 10.1371/journal.pcbi.1006062. PubMed PMID: 29529028; PMCID: PMC5864085.
79. Poltavets V, Faulkner JW, Dhattrak D, Whitfield RJ, McColl SR, Kochetkova M. CXCR4-CCR7 Heterodimerization Is a Driver of Breast Cancer Progression. *Life (Basel).* 2021;11(10). Epub 20211007. doi: 10.3390/life11101049. PubMed PMID: 34685420; PMCID: PMC8538406.
80. Bleul CC, Farzan M, Choe H, Parolin C, Clark-Lewis I, Sodroski J, Springer TA. The lymphocyte chemoattractant SDF-1 is a ligand for LESTR/fusin and blocks HIV-1 entry. *Nature.* 1996;382(6594):829-33. doi: 10.1038/382829a0. PubMed PMID: 8752280.
81. Bleul CC, Fuhlbrigge RC, Casasnovas JM, Aiuti A, Springer TA. A highly efficacious lymphocyte chemoattractant, stromal cell-derived factor 1 (SDF-1). *J Exp Med.* 1996;184(3):1101-9. doi: 10.1084/jem.184.3.1101. PubMed PMID: 9064327; PMCID: PMC2192798.
82. Rot A, von Andrian UH. Chemokines in innate and adaptive host defense: basic chemokines grammar for immune cells. *Annu Rev Immunol.* 2004;22:891-928. doi: 10.1146/annurev.immunol.22.012703.104543. PubMed PMID: 15032599.
83. Peled A, Petit I, Kollet O, Magid M, Ponomaryov T, Byk T, Nagler A, Ben-Hur H, Many A, Shultz L, Lider O, Alon R, Zipori D, Lapidot T. Dependence of human stem cell engraftment and repopulation of NOD/SCID mice on CXCR4. *Science.* 1999;283(5403):845-8. doi: 10.1126/science.283.5403.845. PubMed PMID: 9933168.
84. Ratajczak MZ, Zuba-Surma E, Kucia M, Reza R, Wojakowski W, Ratajczak J. The pleiotropic effects of the SDF-1-CXCR4 axis in organogenesis, regeneration and tumorigenesis. *Leukemia.* 2006;20(11):1915-24. Epub 20060810. doi: 10.1038/sj.leu.2404357. PubMed PMID: 16900209.

85. Popple A, Durrant LG, Spendlove I, Rolland P, Scott IV, Deen S, Ramage JM. The chemokine, CXCL12, is an independent predictor of poor survival in ovarian cancer. *Br J Cancer*. 2012;106(7):1306-13. Epub 20120313. doi: 10.1038/bjc.2012.49. PubMed PMID: 22415233; PMCID: PMC3314783.
86. Jiang YP, Wu XH, Shi B, Wu WX, Yin GR. Expression of chemokine CXCL12 and its receptor CXCR4 in human epithelial ovarian cancer: an independent prognostic factor for tumor progression. *Gynecol Oncol*. 2006;103(1):226-33. Epub 20060502. doi: 10.1016/j.ygyno.2006.02.036. PubMed PMID: 16631235.
87. Zhou W, Jiang Z, Liu N, Xu F, Wen P, Liu Y, Zhong W, Song X, Chang X, Zhang X, Wei G, Yu J. Down-regulation of CXCL12 mRNA expression by promoter hypermethylation and its association with metastatic progression in human breast carcinomas. *J Cancer Res Clin Oncol*. 2009;135(1):91-102. Epub 20080801. doi: 10.1007/s00432-008-0435-x. PubMed PMID: 18670789.
88. Liu G, Yuan X, Zeng Z, Tunici P, Ng H, Abdulkadir IR, Lu L, Irvin D, Black KL, Yu JS. Analysis of gene expression and chemoresistance of CD133+ cancer stem cells in glioblastoma. *Mol Cancer*. 2006;5:67. Epub 20061202. doi: 10.1186/1476-4598-5-67. PubMed PMID: 17140455; PMCID: PMC1697823.
89. Zheng X, Xie Q, Li S, Zhang W. CXCR4-positive subset of glioma is enriched for cancer stem cells. *Oncol Res*. 2011;19(12):555-61. doi: 10.3727/096504012x13340632812631. PubMed PMID: 22812188.
90. Barbieri F, Bajetto A, Florio T. Role of chemokine network in the development and progression of ovarian cancer: a potential novel pharmacological target. *J Oncol*.

2010;2010:426956. Epub 20091214. doi: 10.1155/2010/426956. PubMed PMID: 20049170; PMCID: PMC2798669.

91. Scotton CJ, Wilson JL, Scott K, Stamp G, Wilbanks GD, Fricker S, Bridger G, Balkwill FR. Multiple actions of the chemokine CXCL12 on epithelial tumor cells in human ovarian cancer. *Cancer Res.* 2002;62(20):5930-8. PubMed PMID: 12384559.

92. Kang H, Watkins G, Parr C, Douglas-Jones A, Mansel RE, Jiang WG. Stromal cell derived factor-1: its influence on invasiveness and migration of breast cancer cells in vitro, and its association with prognosis and survival in human breast cancer. *Breast Cancer Res.* 2005;7(4):R402-10. Epub 20050404. doi: 10.1186/bcr1022. PubMed PMID: 15987445; PMCID: PMC1175055.

93. Yang P, Wang G, Huo H, Li Q, Zhao Y, Liu Y. SDF-1/CXCR4 signaling up-regulates survivin to regulate human sacral chondrosarcoma cell cycle and epithelial-mesenchymal transition via ERK and PI3K/AKT pathway. *Med Oncol.* 2015;32(1):377. Epub 20141127. doi: 10.1007/s12032-014-0377-x. PubMed PMID: 25428386.

94. Yang DL, Xin MM, Wang JS, Xu HY, Huo Q, Tang ZR, Wang HF. Chemokine receptor CXCR4 and its ligand CXCL12 expressions and clinical significance in bladder cancer. *Genet Mol Res.* 2015;14(4):17699-707. Epub 20151222. doi: 10.4238/2015.December.21.43. PubMed PMID: 26782415.

95. Ishigami S, Natsugoe S, Okumura H, Matsumoto M, Nakajo A, Uenosono Y, Arigami T, Uchikado Y, Setoyama T, Arima H, Hokita S, Aikou T. Clinical implication of CXCL12 expression in gastric cancer. *Ann Surg Oncol.* 2007;14(11):3154-8. Epub 20070726. doi: 10.1245/s10434-007-9521-6. PubMed PMID: 17653799.

96. Ghanem I, Riveiro ME, Paradis V, Faivre S, de Parga PM, Raymond E. Insights on the CXCL12-CXCR4 axis in hepatocellular carcinoma carcinogenesis. *Am J Transl Res.* 2014;6(4):340-52. Epub 20140718. PubMed PMID: 25075251; PMCID: PMC4113496.
97. Zhang S, Qi L, Li M, Zhang D, Xu S, Wang N, Sun B. Chemokine CXCL12 and its receptor CXCR4 expression are associated with perineural invasion of prostate cancer. *J Exp Clin Cancer Res.* 2008;27:62. Epub 20081104. doi: 10.1186/1756-9966-27-62. PubMed PMID: 18983683; PMCID: PMC2596092.
98. Imai H, Sunaga N, Shimizu Y, Kakegawa S, Shimizu K, Sano T, Ishizuka T, Oyama T, Saito R, Minna JD, Mori M. Clinicopathological and therapeutic significance of CXCL12 expression in lung cancer. *Int J Immunopathol Pharmacol.* 2010;23(1):153-64. doi: 10.1177/039463201002300114. PubMed PMID: 20378003; PMCID: PMC3368436.
99. Sakai N, Yoshidome H, Shida T, Kimura F, Shimizu H, Ohtsuka M, Takeuchi D, Sakakibara M, Miyazaki M. CXCR4/CXCL12 expression profile is associated with tumor microenvironment and clinical outcome of liver metastases of colorectal cancer. *Clin Exp Metastasis.* 2012;29(2):101-10. Epub 20111111. doi: 10.1007/s10585-011-9433-5. PubMed PMID: 22075627.
100. Teng F, Tian WY, Wang YM, Zhang YF, Guo F, Zhao J, Gao C, Xue FX. Cancer-associated fibroblasts promote the progression of endometrial cancer via the SDF-1/CXCR4 axis. *J Hematol Oncol.* 2016;9:8. Epub 20160206. doi: 10.1186/s13045-015-0231-4. PubMed PMID: 26851944; PMCID: PMC4744391.
101. Duda DG, Kozin SV, Kirkpatrick ND, Xu L, Fukumura D, Jain RK. CXCL12 (SDF1alpha)-CXCR4/CXCR7 pathway inhibition: an emerging sensitizer for anticancer

therapies? Clin Cancer Res. 2011;17(8):2074-80. Epub 20110224. doi: 10.1158/1078-0432.CCR-10-2636. PubMed PMID: 21349998; PMCID: PMC3079023.

102. Hirata H, Hinoda Y, Kikuno N, Kawamoto K, Dahiya AV, Suehiro Y, Tanaka Y, Dahiya R. CXCL12 G801A polymorphism is a risk factor for sporadic prostate cancer susceptibility. Clin Cancer Res. 2007;13(17):5056-62. doi: 10.1158/1078-0432.CCR-07-0859. PubMed PMID: 17785557.

103. Tomlins SA, Laxman B, Varambally S, Cao X, Yu J, Helgeson BE, Cao Q, Prensner JR, Rubin MA, Shah RB, Mehra R, Chinnaiyan AM. Role of the TMPRSS2-ERG gene fusion in prostate cancer. Neoplasia. 2008;10(2):177-88. doi: 10.1593/neo.07822. PubMed PMID: 18283340; PMCID: PMC2244693.

104. Singareddy R, Semaan L, Conley-Lacomb MK, St John J, Powell K, Iyer M, Smith D, Heilbrun LK, Shi D, Sakr W, Cher ML, Chinni SR. Transcriptional regulation of CXCR4 in prostate cancer: significance of TMPRSS2-ERG fusions. Mol Cancer Res. 2013;11(11):1349-61. Epub 20130805. doi: 10.1158/1541-7786.MCR-12-0705. PubMed PMID: 23918819; PMCID: PMC3901058.

105. Cai J, Kandagatla P, Singareddy R, Kropinski A, Sheng S, Cher ML, Chinni SR. Androgens Induce Functional CXCR4 through ERG Factor Expression in TMPRSS2-ERG Fusion-Positive Prostate Cancer Cells. Transl Oncol. 2010;3(3):195-203. Epub 20100601. doi: 10.1593/tlo.09328. PubMed PMID: 20563261; PMCID: PMC2887649.

106. Thomas RM, Kim J, Revelo-Penafiel MP, Angel R, Dawson DW, Lowy AM. The chemokine receptor CXCR4 is expressed in pancreatic intraepithelial neoplasia. Gut. 2008;57(11):1555-60. Epub 20080729. doi: 10.1136/gut.2007.143941. PubMed PMID: 18664506; PMCID: PMC8634735.

107. Weekes CD, Song D, Arcaroli J, Wilson LA, Rubio-Viqueira B, Cusatis G, Garrett-Mayer E, Messersmith WA, Winn RA, Hidalgo M. Stromal cell-derived factor 1alpha mediates resistance to mTOR-directed therapy in pancreatic cancer. *Neoplasia*. 2012;14(8):690-701. doi: 10.1593/neo.111810. PubMed PMID: 22952422; PMCID: PMC3432475.
108. Wang Z, Ma Q, Liu Q, Yu H, Zhao L, Shen S, Yao J. Blockade of SDF-1/CXCR4 signalling inhibits pancreatic cancer progression in vitro via inactivation of canonical Wnt pathway. *Br J Cancer*. 2008;99(10):1695-703. Epub 20081028. doi: 10.1038/sj.bjc.6604745. PubMed PMID: 19002187; PMCID: PMC2584946.
109. Singh AP, Arora S, Bhardwaj A, Srivastava SK, Kadakia MP, Wang B, Grizzle WE, Owen LB, Singh S. CXCL12/CXCR4 protein signaling axis induces sonic hedgehog expression in pancreatic cancer cells via extracellular regulated kinase- and Akt kinase-mediated activation of nuclear factor kappaB: implications for bidirectional tumor-stromal interactions. *J Biol Chem*. 2012;287(46):39115-24. Epub 20120920. doi: 10.1074/jbc.M112.409581. PubMed PMID: 22995914; PMCID: PMC3493952.
110. McCubrey JA, Steelman LS, Chappell WH, Abrams SL, Wong EW, Chang F, Lehmann B, Terrian DM, Milella M, Tafuri A, Stivala F, Libra M, Basecke J, Evangelisti C, Martelli AM, Franklin RA. Roles of the Raf/MEK/ERK pathway in cell growth, malignant transformation and drug resistance. *Biochim Biophys Acta*. 2007;1773(8):1263-84. Epub 20061007. doi: 10.1016/j.bbamcr.2006.10.001. PubMed PMID: 17126425; PMCID: PMC2696318.
111. Hayashi H, Kume T. Forkhead transcription factors regulate expression of the chemokine receptor CXCR4 in endothelial cells and CXCL12-induced cell migration. *Biochem Biophys Res Commun*. 2008;367(3):584-9. Epub 20080108. doi: 10.1016/j.bbrc.2007.12.183. PubMed PMID: 18187037; PMCID: PMC2265419.

112. Carmeliet P. VEGF as a key mediator of angiogenesis in cancer. *Oncology*. 2005;69 Suppl 3:4-10. Epub 20051121. doi: 10.1159/000088478. PubMed PMID: 16301830.
113. Jee SH, Chu CY, Chiu HC, Huang YL, Tsai WL, Liao YH, Kuo ML. Interleukin-6 induced basic fibroblast growth factor-dependent angiogenesis in basal cell carcinoma cell line via JAK/STAT3 and PI3-kinase/Akt pathways. *J Invest Dermatol*. 2004;123(6):1169-75. doi: 10.1111/j.0022-202X.2004.23497.x. PubMed PMID: 15610530.
114. Chu CY, Cha ST, Lin WC, Lu PH, Tan CT, Chang CC, Lin BR, Jee SH, Kuo ML. Stromal cell-derived factor-1alpha (SDF-1alpha/CXCL12)-enhanced angiogenesis of human basal cell carcinoma cells involves ERK1/2-NF-kappaB/interleukin-6 pathway. *Carcinogenesis*. 2009;30(2):205-13. Epub 20081009. doi: 10.1093/carcin/bgn228. PubMed PMID: 18849299.
115. Kim J, Mori T, Chen SL, Amersi FF, Martinez SR, Kuo C, Turner RR, Ye X, Bilchik AJ, Morton DL, Hoon DS. Chemokine receptor CXCR4 expression in patients with melanoma and colorectal cancer liver metastases and the association with disease outcome. *Ann Surg*. 2006;244(1):113-20. doi: 10.1097/01.sla.0000217690.65909.9c. PubMed PMID: 16794396; PMCID: PMC1570598.
116. Muller A, Homey B, Soto H, Ge N, Catron D, Buchanan ME, McClanahan T, Murphy E, Yuan W, Wagner SN, Barrera JL, Mohar A, Verastegui E, Zlotnik A. Involvement of chemokine receptors in breast cancer metastasis. *Nature*. 2001;410(6824):50-6. doi: 10.1038/35065016. PubMed PMID: 11242036.
117. Shiozawa Y, Pedersen EA, Havens AM, Jung Y, Mishra A, Joseph J, Kim JK, Patel LR, Ying C, Ziegler AM, Pienta MJ, Song J, Wang J, Loberg RD, Krebsbach PH, Pienta KJ, Taichman RS. Human prostate cancer metastases target the hematopoietic stem cell niche to establish

footholds in mouse bone marrow. *J Clin Invest.* 2011;121(4):1298-312. Epub 20110323. doi: 10.1172/JCI43414. PubMed PMID: 21436587; PMCID: PMC3069764.

118. Sun YX, Schneider A, Jung Y, Wang J, Dai J, Wang J, Cook K, Osman NI, Koh-Paige AJ, Shim H, Pienta KJ, Keller ET, McCauley LK, Taichman RS. Skeletal localization and neutralization of the SDF-1(CXCL12)/CXCR4 axis blocks prostate cancer metastasis and growth in osseous sites in vivo. *J Bone Miner Res.* 2005;20(2):318-29. Epub 20041116. doi: 10.1359/JBMR.041109. PubMed PMID: 15647826.

119. Chinni SR, Sivalogan S, Dong Z, Filho JC, Deng X, Bonfil RD, Cher ML. CXCL12/CXCR4 signaling activates Akt-1 and MMP-9 expression in prostate cancer cells: the role of bone microenvironment-associated CXCL12. *Prostate.* 2006;66(1):32-48. doi: 10.1002/pros.20318. PubMed PMID: 16114056.

120. Chinni SR, Yamamoto H, Dong Z, Sabbota A, Bonfil RD, Cher ML. CXCL12/CXCR4 transactivates HER2 in lipid rafts of prostate cancer cells and promotes growth of metastatic deposits in bone. *Mol Cancer Res.* 2008;6(3):446-57. doi: 10.1158/1541-7786.MCR-07-0117. PubMed PMID: 18337451; PMCID: PMC3842603.

121. Conley-LaComb MK, Semaan L, Singareddy R, Li Y, Heath EI, Kim S, Cher ML, Chinni SR. Pharmacological targeting of CXCL12/CXCR4 signaling in prostate cancer bone metastasis. *Mol Cancer.* 2016;15(1):68. Epub 20161103. doi: 10.1186/s12943-016-0552-0. PubMed PMID: 27809841; PMCID: PMC5093938.

122. Li X, Ma Q, Xu Q, Liu H, Lei J, Duan W, Bhat K, Wang F, Wu E, Wang Z. SDF-1/CXCR4 signaling induces pancreatic cancer cell invasion and epithelial-mesenchymal transition in vitro through non-canonical activation of Hedgehog pathway. *Cancer Lett.* 2012;322(2):169-76. Epub 20120323. doi: 10.1016/j.canlet.2012.02.035. PubMed PMID: 22450749; PMCID: PMC3408048.

123. Hu TH, Yao Y, Yu S, Han LL, Wang WJ, Guo H, Tian T, Ruan ZP, Kang XM, Wang J, Wang SH, Nan KJ. SDF-1/CXCR4 promotes epithelial-mesenchymal transition and progression of colorectal cancer by activation of the Wnt/beta-catenin signaling pathway. *Cancer Lett.* 2014;354(2):417-26. Epub 20140820. doi: 10.1016/j.canlet.2014.08.012. PubMed PMID: 25150783.
124. Yu T, Wu Y, Helman JI, Wen Y, Wang C, Li L. CXCR4 promotes oral squamous cell carcinoma migration and invasion through inducing expression of MMP-9 and MMP-13 via the ERK signaling pathway. *Mol Cancer Res.* 2011;9(2):161-72. Epub 20110104. doi: 10.1158/1541-7786.MCR-10-0386. PubMed PMID: 21205837.
125. Engl T, Relja B, Marian D, Blumenberg C, Muller I, Beecken WD, Jones J, Ringel EM, Bereiter-Hahn J, Jonas D, Blaheta RA. CXCR4 chemokine receptor mediates prostate tumor cell adhesion through alpha5 and beta3 integrins. *Neoplasia.* 2006;8(4):290-301. doi: 10.1593/neo.05694. PubMed PMID: 16756721; PMCID: PMC1600676.
126. Weilbaecher KN, Guise TA, McCauley LK. Cancer to bone: a fatal attraction. *Nat Rev Cancer.* 2011;11(6):411-25. Epub 20110519. doi: 10.1038/nrc3055. PubMed PMID: 21593787; PMCID: PMC3666847.
127. Kukreja P, Abdel-Mageed AB, Mondal D, Liu K, Agrawal KC. Up-regulation of CXCR4 expression in PC-3 cells by stromal-derived factor-1alpha (CXCL12) increases endothelial adhesion and transendothelial migration: role of MEK/ERK signaling pathway-dependent NF-kappaB activation. *Cancer Res.* 2005;65(21):9891-8. doi: 10.1158/0008-5472.CAN-05-1293. PubMed PMID: 16267013.

128. Burger JA, Kipps TJ. CXCR4: a key receptor in the crosstalk between tumor cells and their microenvironment. *Blood*. 2006;107(5):1761-7. Epub 20051103. doi: 10.1182/blood-2005-08-3182. PubMed PMID: 16269611.
129. Orimo A, Gupta PB, SgROI DC, Arenzana-Seisdedos F, Delaunay T, Naeem R, Carey VJ, Richardson AL, Weinberg RA. Stromal fibroblasts present in invasive human breast carcinomas promote tumor growth and angiogenesis through elevated SDF-1/CXCL12 secretion. *Cell*. 2005;121(3):335-48. doi: 10.1016/j.cell.2005.02.034. PubMed PMID: 15882617.
130. Ao M, Franco OE, Park D, Raman D, Williams K, Hayward SW. Cross-talk between paracrine-acting cytokine and chemokine pathways promotes malignancy in benign human prostatic epithelium. *Cancer Res*. 2007;67(9):4244-53. doi: 10.1158/0008-5472.CAN-06-3946. PubMed PMID: 17483336.
131. Konopleva MY, Jordan CT. Leukemia stem cells and microenvironment: biology and therapeutic targeting. *J Clin Oncol*. 2011;29(5):591-9. Epub 20110110. doi: 10.1200/JCO.2010.31.0904. PubMed PMID: 21220598; PMCID: PMC4874213.
132. Deng Y, Cheng J, Fu B, Liu W, Chen G, Zhang Q, Yang Y. Hepatic carcinoma-associated fibroblasts enhance immune suppression by facilitating the generation of myeloid-derived suppressor cells. *Oncogene*. 2017;36(8):1090-101. Epub 20160905. doi: 10.1038/onc.2016.273. PubMed PMID: 27593937.
133. Schmidt A, Zhang XM, Joshi RN, Iqbal S, Wahlund C, Gabrielsson S, Harris RA, Tegner J. Human macrophages induce CD4(+)Foxp3(+) regulatory T cells via binding and re-release of TGF-beta. *Immunol Cell Biol*. 2016;94(8):747-62. Epub 20160510. doi: 10.1038/icb.2016.34. PubMed PMID: 27075967.

134. Kioi M, Vogel H, Schultz G, Hoffman RM, Harsh GR, Brown JM. Inhibition of vasculogenesis, but not angiogenesis, prevents the recurrence of glioblastoma after irradiation in mice. *J Clin Invest.* 2010;120(3):694-705. Epub 20100222. doi: 10.1172/JCI40283. PubMed PMID: 20179352; PMCID: PMC2827954.
135. Yin H, Wang Y, Chen W, Zhong S, Liu Z, Zhao J. Drug-resistant CXCR4-positive cells have the molecular characteristics of EMT in NSCLC. *Gene.* 2016;594(1):23-9. Epub 20160828. doi: 10.1016/j.gene.2016.08.043. PubMed PMID: 27581786.
136. Saigusa S, Toiyama Y, Tanaka K, Yokoe T, Okugawa Y, Kawamoto A, Yasuda H, Inoue Y, Miki C, Kusunoki M. Stromal CXCR4 and CXCL12 expression is associated with distant recurrence and poor prognosis in rectal cancer after chemoradiotherapy. *Ann Surg Oncol.* 2010;17(8):2051-8. Epub 20100223. doi: 10.1245/s10434-010-0970-y. PubMed PMID: 20177796.
137. Dubrovskaja A, Hartung A, Bouchez LC, Walker JR, Reddy VA, Cho CY, Schultz PG. CXCR4 activation maintains a stem cell population in tamoxifen-resistant breast cancer cells through AhR signalling. *Br J Cancer.* 2012;107(1):43-52. Epub 20120529. doi: 10.1038/bjc.2012.105. PubMed PMID: 22644306; PMCID: PMC3389396.
138. Wang Y, Miao H, Li W, Yao J, Sun Y, Li Z, Zhao L, Guo Q. CXCL12/CXCR4 axis confers adriamycin resistance to human chronic myelogenous leukemia and oroxylin A improves the sensitivity of K562/ADM cells. *Biochem Pharmacol.* 2014;90(3):212-25. Epub 20140523. doi: 10.1016/j.bcp.2014.05.007. PubMed PMID: 24858801.
139. Kim SY, Lee CH, Midura BV, Yeung C, Mendoza A, Hong SH, Ren L, Wong D, Korz W, Merzouk A, Salari H, Zhang H, Hwang ST, Khanna C, Helman LJ. Inhibition of the CXCR4/CXCL12 chemokine pathway reduces the development of murine pulmonary metastases.

Clin Exp Metastasis. 2008;25(3):201-11. Epub 20071211. doi: 10.1007/s10585-007-9133-3. PubMed PMID: 18071913; PMCID: PMC2730112.

140. Hassan S, Buchanan M, Jahan K, Aguilar-Mahecha A, Gaboury L, Muller WJ, Alsawafi Y, Mourskaia AA, Siegel PM, Salvucci O, Basik M. CXCR4 peptide antagonist inhibits primary breast tumor growth, metastasis and enhances the efficacy of anti-VEGF treatment or docetaxel in a transgenic mouse model. *Int J Cancer*. 2011;129(1):225-32. Epub 20101112. doi: 10.1002/ijc.25665. PubMed PMID: 20830712.

141. Wong D, Kandagatla P, Korz W, Chinni SR. Targeting CXCR4 with CTCE-9908 inhibits prostate tumor metastasis. *BMC Urol*. 2014;14:12. Epub 20140128. doi: 10.1186/1471-2490-14-12. PubMed PMID: 24472670; PMCID: PMC3912255.

142. Roccaro AM, Sacco A, Purschke WG, Moschetta M, Buchner K, Maasch C, Zboralski D, Zollner S, Vonhoff S, Mishima Y, Maiso P, Reagan MR, Lonardi S, Ungari M, Facchetti F, Eulberg D, Kruschinski A, Vater A, Rossi G, Klusmann S, Ghobrial IM. SDF-1 inhibition targets the bone marrow niche for cancer therapy. *Cell Rep*. 2014;9(1):118-28. Epub 20140925. doi: 10.1016/j.celrep.2014.08.042. PubMed PMID: 25263552; PMCID: PMC4194173.

143. Zeng Z, Shi YX, Samudio IJ, Wang RY, Ling X, Frolova O, Levis M, Rubin JB, Negrin RR, Estey EH, Konoplev S, Andreeff M, Konopleva M. Targeting the leukemia microenvironment by CXCR4 inhibition overcomes resistance to kinase inhibitors and chemotherapy in AML. *Blood*. 2009;113(24):6215-24. Epub 20081027. doi: 10.1182/blood-2008-05-158311. PubMed PMID: 18955566; PMCID: PMC2699240.

144. Beider K, Begin M, Abraham M, Wald H, Weiss ID, Wald O, Pikarsky E, Zeira E, Eizenberg O, Galun E, Hardan I, Engelhard D, Nagler A, Peled A. CXCR4 antagonist 4F-benzoyl-

- TN14003 inhibits leukemia and multiple myeloma tumor growth. *Exp Hematol.* 2011;39(3):282-92. Epub 20101205. doi: 10.1016/j.exphem.2010.11.010. PubMed PMID: 21138752.
145. Gagner JP, Sarfraz Y, Ortenzi V, Alotaibi FM, Chiriboga LA, Tayyib AT, Douglas GJ, Chevalier E, Romagnoli B, Tuffin G, Schmitt M, Lemercier G, Dembowsky K, Zagzag D. Multifaceted C-X-C Chemokine Receptor 4 (CXCR4) Inhibition Interferes with Anti-Vascular Endothelial Growth Factor Therapy-Induced Glioma Dissemination. *Am J Pathol.* 2017;187(9):2080-94. Epub 20170720. doi: 10.1016/j.ajpath.2017.04.020. PubMed PMID: 28734730; PMCID: PMC5809520.
146. De Clercq E. Mozobil(R) (Plerixafor, AMD3100), 10 years after its approval by the US Food and Drug Administration. *Antivir Chem Chemother.* 2019;27:2040206619829382. doi: 10.1177/2040206619829382. PubMed PMID: 30776910; PMCID: PMC6379795.
147. Uy GL, Rettig MP, Motabi IH, McFarland K, Trinkaus KM, Hladnik LM, Kulkarni S, Abboud CN, Cashen AF, Stockerl-Goldstein KE, Vij R, Westervelt P, DiPersio JF. A phase 1/2 study of chemosensitization with the CXCR4 antagonist plerixafor in relapsed or refractory acute myeloid leukemia. *Blood.* 2012;119(17):3917-24. Epub 20120202. doi: 10.1182/blood-2011-10-383406. PubMed PMID: 22308295; PMCID: PMC3350358.
148. Ghobrial IM, Liu CJ, Zavidij O, Azab AK, Baz R, Laubach JP, Mishima Y, Armand P, Munshi NC, Basile F, Constantine M, Vredenburgh J, Boruchov A, Crilley P, Henrick PM, Hornburg KTV, Leblebjian H, Chuma S, Reyes K, Noonan K, Warren D, Schlossman R, Paba-Prada C, Anderson KC, Weller E, Trippa L, Shain K, Richardson PG. Phase I/II trial of the CXCR4 inhibitor plerixafor in combination with bortezomib as a chemosensitization strategy in relapsed/refractory multiple myeloma. *Am J Hematol.* 2019;94(11):1244-53. Epub 20191004. doi: 10.1002/ajh.25627. PubMed PMID: 31456261.

149. Chaudary N, Pintilie M, Jelveh S, Lindsay P, Hill RP, Milosevic M. Plerixafor Improves Primary Tumor Response and Reduces Metastases in Cervical Cancer Treated with Radio-Chemotherapy. *Clin Cancer Res.* 2017;23(5):1242-9. Epub 20161003. doi: 10.1158/1078-0432.CCR-16-1730. PubMed PMID: 27697997.
150. Feig C, Jones JO, Kraman M, Wells RJ, Deonarine A, Chan DS, Connell CM, Roberts EW, Zhao Q, Caballero OL, Teichmann SA, Janowitz T, Jodrell DI, Tuveson DA, Fearon DT. Targeting CXCL12 from FAP-expressing carcinoma-associated fibroblasts synergizes with anti-PD-L1 immunotherapy in pancreatic cancer. *Proc Natl Acad Sci U S A.* 2013;110(50):20212-7. Epub 20131125. doi: 10.1073/pnas.1320318110. PubMed PMID: 24277834; PMCID: PMC3864274.
151. Righi E, Kashiwagi S, Yuan J, Santosuosso M, Leblanc P, Ingraham R, Forbes B, Edelblute B, Collette B, Xing D, Kowalski M, Mingari MC, Vianello F, Birrer M, Orsulic S, Dranoff G, Poznansky MC. CXCL12/CXCR4 blockade induces multimodal antitumor effects that prolong survival in an immunocompetent mouse model of ovarian cancer. *Cancer Res.* 2011;71(16):5522-34. Epub 20110708. doi: 10.1158/0008-5472.CAN-10-3143. PubMed PMID: 21742774; PMCID: PMC3959864.
152. Geng F, Guo J, Guo QQ, Xie Y, Dong L, Zhou Y, Liu CL, Yu B, Wu H, Wu JX, Zhang HH, Kong W, Yu XH. A DNA vaccine expressing an optimized secreted FAPalpha induces enhanced anti-tumor activity by altering the tumor microenvironment in a murine model of breast cancer. *Vaccine.* 2019;37(31):4382-91. Epub 20190612. doi: 10.1016/j.vaccine.2019.06.012. PubMed PMID: 31202521.
153. Komorowski MP, McGray AR, Kolakowska A, Eng K, Gil M, Opyrchal M, Litwinska B, Nemeth MJ, Odunsi KO, Kozbor D. Reprogramming antitumor immunity against chemoresistant ovarian cancer by a CXCR4 antagonist-armed viral oncotherapy. *Mol Ther Oncolytics.*

2016;3:16034. Epub 20161214. doi: 10.1038/mto.2016.34. PubMed PMID: 28035333; PMCID: PMC5155641.

154. Fumagalli A, Zarca A, Neves M, Caspar B, Hill SJ, Mayor F, Jr., Smit MJ, Marin P. CXCR4/ACKR3 Phosphorylation and Recruitment of Interacting Proteins: Key Mechanisms Regulating Their Functional Status. *Mol Pharmacol.* 2019;96(6):794-808. Epub 20190305. doi: 10.1124/mol.118.115360. PubMed PMID: 30837297.

155. Hammond GR, Machner MP, Balla T. A novel probe for phosphatidylinositol 4-phosphate reveals multiple pools beyond the Golgi. *J Cell Biol.* 2014;205(1):113-26. Epub 20140407. doi: 10.1083/jcb.201312072. PubMed PMID: 24711504; PMCID: PMC3987136.

156. Balla T, Varnai P. Visualization of cellular phosphoinositide pools with GFP-fused protein-domains. *Curr Protoc Cell Biol.* 2009;Chapter 24:Unit 24 4. doi: 10.1002/0471143030.cb2404s42. PubMed PMID: 19283730; PMCID: PMC3125592.

157. Tomlins SA, Mehra R, Rhodes DR, Cao X, Wang L, Dhanasekaran SM, Kalyana-Sundaram S, Wei JT, Rubin MA, Pienta KJ, Shah RB, Chinnaiyan AM. Integrative molecular concept modeling of prostate cancer progression. *Nat Genet.* 2007;39(1):41-51. Epub 20061217. doi: 10.1038/ng1935. PubMed PMID: 17173048.

158. Beltran H, Prandi D, Mosquera JM, Benelli M, Puca L, Cyrta J, Marotz C, Giannopoulou E, Chakravarthi BV, Varambally S, Tomlins SA, Nanus DM, Tagawa ST, Van Allen EM, Elemento O, Sboner A, Garraway LA, Rubin MA, Demichelis F. Divergent clonal evolution of castration-resistant neuroendocrine prostate cancer. *Nat Med.* 2016;22(3):298-305. Epub 20160208. doi: 10.1038/nm.4045. PubMed PMID: 26855148; PMCID: PMC4777652.

159. Vaishampayan UN, Heilbrun LK, Monk P, 3rd, Tejwani S, Sonpavde G, Hwang C, Smith D, Jasti P, Dobson K, Dickow B, Heath EI, Semaan L, Cher ML, Fontana JA, Chinni S. Clinical

Efficacy of Enzalutamide vs Bicalutamide Combined With Androgen Deprivation Therapy in Men With Metastatic Hormone-Sensitive Prostate Cancer: A Randomized Clinical Trial. *JAMA Netw Open*. 2021;4(1):e2034633. Epub 20210104. doi: 10.1001/jamanetworkopen.2020.34633. PubMed PMID: 33496795; PMCID: PMC7838941.

160. Arriaga JM, Panja S, Alshalalfa M, Zhao J, Zou M, Giacobbe A, Madubata CJ, Kim JY, Rodriguez A, Coleman I, Virk RK, Hibshoosh H, Ertunc O, Ozbek B, Fountain J, Jeffrey Karnes R, Luo J, Antonarakis ES, Nelson PS, Feng FY, Rubin MA, De Marzo AM, Rabadan R, Sims PA, Mitrofanova A, Abate-Shen C. A MYC and RAS co-activation signature in localized prostate cancer drives bone metastasis and castration resistance. *Nat Cancer*. 2020;1(11):1082-96. Epub 20201019. doi: 10.1038/s43018-020-00125-0. PubMed PMID: 34085047; PMCID: PMC8171279.

161. Stanbrough M, Bubley GJ, Ross K, Golub TR, Rubin MA, Penning TM, Febbo PG, Balk SP. Increased expression of genes converting adrenal androgens to testosterone in androgen-independent prostate cancer. *Cancer Res*. 2006;66(5):2815-25. doi: 10.1158/0008-5472.CAN-05-4000. PubMed PMID: 16510604.

162. Zhao E, Wang L, Dai J, Kryczek I, Wei S, Vatan L, Altuwaijri S, Sparwasser T, Wang G, Keller ET, Zou W. Regulatory T cells in the bone marrow microenvironment in patients with prostate cancer. *Oncoimmunology*. 2012;1(2):152-61. doi: 10.4161/onci.1.2.18480. PubMed PMID: 22720236; PMCID: PMC3376984.

163. Zou L, Barnett B, Safah H, Larussa VF, Evdemon-Hogan M, Mottram P, Wei S, David O, Curiel TJ, Zou W. Bone marrow is a reservoir for CD4<sup>+</sup>CD25<sup>+</sup> regulatory T cells that traffic through CXCL12/CXCR4 signals. *Cancer Res*. 2004;64(22):8451-5. doi: 10.1158/0008-5472.CAN-04-1987. PubMed PMID: 15548717.

164. Arwert EN, Harney AS, Entenberg D, Wang Y, Sahai E, Pollard JW, Condeelis JS. A Unidirectional Transition from Migratory to Perivascular Macrophage Is Required for Tumor Cell Intravasation. *Cell Rep.* 2018;23(5):1239-48. doi: 10.1016/j.celrep.2018.04.007. PubMed PMID: 29719241; PMCID: PMC5946803.
165. Hughes R, Qian BZ, Rowan C, Muthana M, Keklikoglou I, Olson OC, Tazzyman S, Danson S, Addison C, Clemons M, Gonzalez-Angulo AM, Joyce JA, De Palma M, Pollard JW, Lewis CE. Perivascular M2 Macrophages Stimulate Tumor Relapse after Chemotherapy. *Cancer Res.* 2015;75(17):3479-91. Epub 20150812. doi: 10.1158/0008-5472.CAN-14-3587. PubMed PMID: 26269531; PMCID: PMC5024531.
166. Sanchez-Martin L, Estechea A, Samaniego R, Sanchez-Ramon S, Vega MA, Sanchez-Mateos P. The chemokine CXCL12 regulates monocyte-macrophage differentiation and RUNX3 expression. *Blood.* 2011;117(1):88-97. Epub 20101007. doi: 10.1182/blood-2009-12-258186. PubMed PMID: 20930067.
167. Levesque JP, Hendy J, Takamatsu Y, Simmons PJ, Bendall LJ. Disruption of the CXCR4/CXCL12 chemotactic interaction during hematopoietic stem cell mobilization induced by GCSF or cyclophosphamide. *J Clin Invest.* 2003;111(2):187-96. doi: 10.1172/JCI15994. PubMed PMID: 12531874; PMCID: PMC151860.
168. Stultz J, Fong L. How to turn up the heat on the cold immune microenvironment of metastatic prostate cancer. *Prostate Cancer Prostatic Dis.* 2021;24(3):697-717. Epub 20210405. doi: 10.1038/s41391-021-00340-5. PubMed PMID: 33820953; PMCID: PMC8384622.
169. Zhao Y, Niu C, Cui J. Gamma-delta (gammadelta) T cells: friend or foe in cancer development? *J Transl Med.* 2018;16(1):3. Epub 20180110. doi: 10.1186/s12967-017-1378-2. PubMed PMID: 29316940; PMCID: PMC5761189.

170. Conteduca V, Aieta M, Amadori D, De Giorgi U. Neuroendocrine differentiation in prostate cancer: current and emerging therapy strategies. *Crit Rev Oncol Hematol*. 2014;92(1):11-24. Epub 20140527. doi: 10.1016/j.critrevonc.2014.05.008. PubMed PMID: 24952997.

**ABSTRACT****ROLE OF PHOSPHATIDYLINOSITOL 4-KINASE III $\alpha$  IN CHEMOKINE SIGNALING**

by

**BARANI GOVINDARJAN****August 2022****Advisor:** Dr. Sreenivasa Chinni**Major:** Pathology**Degree:** Doctor of Philosophy

The CXCR4-CXCL12 chemokine signaling axis plays a key role in migration and bone metastasis in prostate cancer (PC). Androgens regulate CXCR4 expression and its receptor activation in lipid-raft micro domains of PC cells, resulting in higher protease expression and invasion. In order to identify some novel CXCR4 co-regulators associated within the lipid-raft, a SILAC (Stable isotope labeling using amino acid in cell culture)-based proteomic analysis was performed with PC3 stable cell-lines over-expressing or knocking-down CXCR4. Phosphatidylinositol 4-kinase III alpha (PI4KIII $\alpha$  or PI4KA) and SAC1 lipid phosphatase were identified as candidate proteins enriched in CXCR4 expressing cells. PI4KA is an evolutionarily conserved mammalian kinase that converts PI to PI4P; and SAC1 dephosphorylates PI4P to PI. PI4K is required for the maintenance and functioning of the plasma-membrane and vesicular trafficking in the Golgi apparatus. PI4KA is also needed to maintain a steady pool of PI(4,5)P<sub>2</sub> in the plasma-membrane, to be utilized in various signaling pathways.

We show that CXCR4 interacts with PI4KA through its adaptor proteins EFR3B and TTC7B, recruiting it to the plasma-membrane for PI4P generation. Similarly, PI4KA was closely linked to CXCR4 induced PC cell invasion, and knockdown of PI4KA in CXCR4 over-expressing

PC3 cell lines reduced cell invasion. Also, localized productions of PI4P was evident in invasive projections of CXCR4 over-expressing cell lines through immunofluorescence microscopy. PC tumor microarray data show increased PI4K expression in metastatic PC tissue vs localized or normal adjacent tissue. These data suggest a novel interaction between PI4KA and CXCR4, promoting tumor cell invasion and metastasis. Pharmacological targeting of PI4KA, its adaptor proteins or its signaling-related proteins might prove therapeutically beneficial and enhance survival in PC patients.

## **AUTOBIOGRAPHICAL STATEMENT**

Barani Govindarajan was born in Chennai, India; and finished high schooling in Ohio. She graduated from The Ohio State University, with a Bachelors in Microbiology. She further continued her education, by obtaining a Masters in Biotechnology. Under the guidance of Dr. Sreenivasa Chinni, she started pursuing her Ph.D. at Wayne State University School of Medicine in the Pathology department. This work is a result of 6 years of knowledge gained through the many learnings and failures in the process.

It has been an incredible journey, learning how to be an intuitive critic and complex problem solver. She has gained much hands-on training on molecular biology, protein interactions, and cellular assays with a focus in Prostate cancer. She has also had the opportunity to gain knowledge in translational research from patient biopsies and efficiently utilize them for bioinformatic analysis. This training has provided a well-rounded knowledge on both molecular and translational aspects of oncology.

Barani has been invited to give oral talks in international conferences and participated in many symposiums. She is currently working on submitting her first-author manuscripts and looking forward to more fruitful writings and publications in her future works.